OBSERVING ZAMBEZI BASIN
FROM SPACE

SATELLITE RAINFALL BIAS ERROR CORRECTION AND
PROPAGATION ANALYSIS FOR HYDROLOGICAL MODELLING

Webster Gumindoga

Promotion committee:

dr. ir. C. Van der Tol	Universiteit Twente, Promoter
dr. ing. T.H.M. Rientjes	Universiteit Twente, co-Promoter
prof. dr. H. Makurira	University of Zimbabwe, co-Promoter
prof. dr. C.J. van Westen	Universiteit Twente
prof. A.D. Nelson	Universiteit Twente
prof. P. Bauer-Gottwein	Technical University of Denmark
prof. M. van der Ploeg	Wageningen University & Research
prof. N.C. van de Giesen	Technische Universiteit Delft

This research was funded by WaterNet, a regional network of university departments, research and training institutes with the aim to build capacity for water resources management in Southern and East Africa. The research was also funded by the University of Twente's Faculty of Geo-Information Science and Earth Observation (ITC). The University of Zimbabwe supported this research.

ITC Dissertation Number: 429

ISBN: 978-90-365-5627-9

DOI: 10.3990/1.9789036556286

URL: https://doi.org/10.3990/1.9789036556286

OBSERVING ZAMBEZI BASIN
FROM SPACE

SATELLITE RAINFALL BIAS ERROR CORRECTION AND PROPAGATION ANALYSIS FOR HYDROLOGICAL MODELLING

DISSERTATION

to obtain
the degree of doctor at the University of Twente,
on the authority of the rector magnificus,
Prof. dr. ir. A. Veldkamp,
on account of the decision of the graduation committee,
to be publicly defended
on 10 May 2023 at 10.45 hrs

by

Webster Gumindoga
born on 04 March 1984
in Gutu District, Zimbabwe

This dissertation has been approved by

Dr. ir. C. Van der Tol	(Promoter)
Dr. ing. T.H.M. Rientjes	(Co-Supervisor)
Dr. A.T. Haile	(Co-Supervisor)
Prof. dr. ing. H. Makurira	(Co-Supervisor)

Table of Contents

Acknowledgements

First of all, I would like to thank the University of Twente's Faculty of Geoinformation Science and Earth Observation (ITC) for giving me a platform to carry out my studies as an extramural PhD student. This means that I was based in Harare, Zimbabwe for most of my PhD time.

To my promoter, Dr. ir. C. Van der Tol, thank you so much for allowing me to carry out this study under your guidance according to the Dutch Law. I cherish your commitment especially in the last phases of this PhD journey to see me complete the studies. To my co-promotor dr. ir. Tom Rientjes, words cannot express how much you have shaped me to become a better scientist, spatial hydrologist and sound researcher. Our journey started in 2009 when I was carrying out my MSc research in the Lake Tana basin in Ethiopia. I cherish the thought provoking physical and virtual meetings we have had over the MSc-PhD journey. I recall the fruitful meetings we have had in the Zambezi Basin as well as the meetings in Harare (Zimbabwe) and the meetings in Enschede (The Netherlands). All these fantastic meetings not only shaped the research ideas in this thesis, but also provided a platform for me to think critically and be an independent researcher. I will forever cherish this 'long' research journey because it provided me with a capacity to be a confident expert in hydrological modelling, water resources management and geoinformation science. I could not have accomplished all this without your relentless support, constructive advice, guidance and scientific intuitive solutions, for which I am truly thankful. Indeed, it has really been a pleasure working with you.

I would also like to extent my appreciation to my other co-supervisor Dr. Alemseged Tamiru Haile. Your input into the manuscripts made the work lighter. Your knowledge on satellite rainfall estimation and hydrological modelling was very valuable to this PhD work. I also cherish the input and knowledge you imparted to me since the days I was carrying out my MSc research in the lake Tana Basin.

To my local supervisor Prof. Hodson Makurira thank you for not only being available as an academic supervisor but also as a mentor in my early career and research journey. I also cherish the trips to Mushumbi, Chidodo and Masoka in Middle Zambezi Basin to set up the weather stations whose data we continue to use for various applications in the post PhD phase.

Special thanks also go to Prof. dr. Paolo Reggiani for providing useful comments and suggestions to this work as well as providing the REW model code.

My acknowledgement also goes to the ITC staff in the Department of Water Resources particularly Ir. Arno van Lieshout and Ms. Tina Butt-Castro, Ceciel Wolters and Ellen Hemmink. Also, to all the administrative staff in the Twente Graduate School (TGS) who made sure that I finish my studies successfully.

I would also like to thank WaterNet that supported the PhD studies through the *DANIDA Transboundary PhD Research Fund* in the Zambezi Basin. Specifically, I would like to thank Prof Jean-Kileshe Onema for giving me the chance to be one of the beneficiaries of the DANIDA supported scholarships in tranboundary research. His constant checking on the progress of this PhD made sure that I don't sleep on the job. I am also thankful to the meteorological and hydrological departments in Botswana, Malawi, Mozambique, Zambia and Zimbabwe for providing time series of hydrometeorological data.

I am also grateful to the University of Zimbabwe's Construction and Civil Engineering Department as well as Geography and Environmental Science chairpersons particularly Hon. Prof. Amon Murwira, Prof. Hodson Makurira, Dr. James Tumbare, Dr. Alexander Mhizha and Eng. Samson Shumba who granted me leave to travel to Enschede, The Netherlands during the period of the PhD studies. Together with the ever-supporting work colleagues (lecturers) in the department, particularly Eng. Z. Hoko and Prof. I. Nhapi, I would like to thank you all for the opportunity to advance my academic life whilst working at the university.

I would like to thank the various MSc Integrated Water Resources Management (IWRM) and Water Resources Engineering (WREM) students who carried out research in the Zambezi basin and whose work contributed directly and indirectly to this PhD study. I would not forget my fellow PhD mates who encouraged me during this journey: Donald Rwasoka, Calisto Omondi, Dr. Moitela Lekula and Dr. Tawanda Gara.

Let me take this special opportunity to thank my lovely wife Belona Gumindoga for the prayers, encouragement and emotional support during the period time as well as taking care of the boys (Paolo, Johannes and David) during my physical absence while pursuing these studies. My siblings support during the PhD period cannot go unmentioned. To my parents Mr. Tadios Everton and Mrs. Vongai Gumindoga, I honor you for being the first Professors of my life. The early educational foundations you gave all of us as siblings made it easy for me to sail through and go past any potential discouragements and hindrances in attaining this higher-level qualification.

To my seniors at church particularly Snr. Rev. CST and Rev. N. Tuturu, thank you so much for the encouragement and granting me leave from church at

critical moments to travel abroad for my studies. Special mention goes to my special brethren: Wisdom Manaka, Emmanuel Hweru and Ernest Maswera for their prayers as well as encouragement to finish the race.

Last but not least, I would like to thank the Lord Almighty who makes everything beautiful in its time. At the point when it looked like the journey would not come to an end, I always had that trust that he who began a good work in me would bring it to completion.

Webster Gumindoga

Enschede May 2023

Summary

Comprehensive scientific understanding and quantitative estimates of water balance components of the Zambezi River Basin are limited. Furthermore, water balance estimation using hydrologic models in this largest basin of Southern Africa often is rendered ineffective by the unavailability of land surface and meteorological data. With the advent of remote sensing technology over the past decades, the quality, quantity and resolution of remote sensing data has significantly improved and nowadays offers opportunities to integrate remote sensing data into hydrological models. Satellite-based rainfall estimates (SREs) have emerged as a viable alternative or supplement to rain gauge observations due to their availability over vast ungauged parts of the world. In addition, SREs allow construction of time series since observations are consistently repeated over time. In hydrological modeling, rainfall represents meteorological forcing. Therefore, once preprocessed and adequately bias corrected, SREs can serve hydrological and water resource modelling. Products, however, only are representations of reality with specific spatial (i.e., the pixel foot print) and temporal resolutions (revisit time) and thus representations by the various SRE product developers are dissimilar. The use of SREs in hydrological modelling therefore requires understanding of how effects of satellite rainfall errors propagate to effect streamflow simulation mismatch.

This research aims to access such propagation effects for the Climate Prediction Center-MORPHing (CMORPH) satellite rainfall product. A comprehensive dataset that includes CMORPH rainfall images, in situ weather gauges as well as streamflow measurements is developed for the selected study domain (see Chapter 2). The study narrows down to Kabompo Basin, a headwater catchment of the Zambezi River and applies a state-of-the-art, integrated and mass conservative Representative Elementary Watershed (REW) model (see Chapter 3). Principal to the (entire) research methodology is to evaluate how the performance of the data driven REW model used for streamflow simulation is affected when bias corrected satellite data, instead of gauged data, is used to drive the model. A number of bias correction schemes as combined with streamflow model performance indicators serve SRE propagation assessment to cause streamflow simulation mismatch. The study demonstrates how systematic errors (i.e., bias errors) in CMORPH SREs affect streamflow outcomes and mismatch of the physically based REW rainfall-runoff model. This study further shows how uncorrected and bias corrected CMORPH SREs affect actual evapotranspiration

(ET_a) and streamflow, and therefore closure of the water balance. A further contribution of this study is the development of a methodology for assessing rainfall to streamflow error propagation in a multi-objective model calibration framework with analysis that encompass the use of a suite of performance indicators and objective functions. The findings provide new insights on use of SREs for hydrologic modelling with emphasis on satellite rainfall error propagation assessments.

In Chapter 4, SRE evaluations for occurrence and rain rate are carried out at sub-basin scale and at daily, weekly, and seasonal time scale by means of probability of detection *(POD)*, false alarm ratio *(FAR)*, critical success index *(CSI)* and frequency bias *(FBS)*. CMORPH predicts 60 % of the rainfall occurrences. Results show improved rainfall detection for the wet season as compared to the dry season. Improved detection is also shown for rainfall rates smaller than 2.5 mm/day. Findings on SRE error decomposition revealed sources of Hit, Missed and False rainfall bias. CMORPH performance (detection of rainfall occurrences and estimations for rainfall depth) at sub-basin scale increases when daily estimates are accumulated to weekly estimates. Findings suggest that for the Zambezi Basin, errors in CMORPH rainfall should be corrected before the product can serve applications such as in hydrological modelling that largely rely on reliable and accurate rainfall inputs.

SREs are prone to bias as they are indirect derivatives of the visible, infrared, and/or microwave cloud properties, hence SREs need correction. Chapter 5 shows the influence of elevation and distance from large scale open water bodies on bias for CMORPH rainfall estimates in the Zambezi Basin. The effectiveness of five linear/non-linear and time-space variant/invariant bias correction schemes was evaluated for daily rainfall estimates and climatic seasonality. Schemes used are: Spatio-temporal Bias *(STB)*, Elevation zone bias *(EZ)*, Power transform (PT), Distribution transformation *(DT)* and the Quantile mapping based on an empirical distribution *(QME)*. To evaluate effectiveness of the bias correction techniques, spatial and temporal cross-validation was applied based on 8 rain gauge stations for the period 1998-1999. For correction of CMORPH estimates, *STB* and *EZ* schemes proved to be more effective in removing bias. *STB* improved the correlation coefficient and Nash Sutcliffe efficiency by 50 % and 53 % respectively and reduced the root mean squared difference and relative bias *(Rel. Bias (%))* by 25 % and 33 % respectively. Paired t-tests showed that there is no significant difference ($p < 0.05$) in the daily means of CMORPH against gauge rainfall after bias correction. ANOVA post-hoc tests revealed that the *STB* and

EZ bias correction schemes are preferred. Bias is highest for very light rainfall (< 2.5 mm/day), for which most effective bias reduction is shown, in particular for the wet season. Similar findings are shown through quantile-quantile (q-q) plots. The spatial cross-validation approach revealed that the majority of the bias correction schemes removed bias by more than 28 %. The temporal cross-validation approach showed effectiveness of the bias correction schemes. Taylor diagrams show that station elevation has an influence on CMORPH performance. Effects of distance >10 km from large scale open water bodies are minimum whereas the effect at shorter distances are indicated but not conclusive by lack of rain gauges. Findings show the importance of applying bias correction to SREs.

Chapter 6 contains a hydrological evaluation (2008-2013) of gauge-based rainfall, uncorrected and bias corrected CMORPH satellite-based rainfall estimates in the Kabompo Basin, a headwater catchment of the Zambezi River. Results of REW modelling by use of rain gauge rainfall served as benchmark to the simulation results. The period 2004–2007 was selected for REW model calibration and the period 2008–2010 for model validation, using rain gauge rainfall. Results of streamflow simulation were evaluated by comparing observed and simulated streamflow by Nash Sutcliffe Efficiency *(NSE)* and Relative Volume Error *(RVE)* objective functions. Results showed that errors in uncorrected CMORPH rainfall estimates cause large mismatch between simulated and observed streamflow. The uncorrected CMORPH rainfall showed an overall overestimation of rainfall for the 2000-2015 period. A linear-multiplicative bias correction scheme was applied to remove the bias. The study further assessed how optimised model parameter values are affected by bias error in the rainfall input. As such the model was recalibrated when bias corrected and uncorrected rainfall replaced rain gauge-based inputs as rainfall forcing. When applied to the REW model, bias corrected CMORPH rainfall improved the match between observed and simulated streamflow. Improvements in streamflow simulation are reported for highest discharges and streamflow totals. Objective function values for *RVE* and for *NSE* improved significantly by the bias correction. Optimized REW parameter values (in particular, parameters that control the volume of the simulated hydrograph) by model recalibration changed by more than 50 % when gauge-based rainfall inputs are replaced by uncorrected CMORPH estimates. However, parameter values remained within physically plausible ranges for bias corrected CMORPH, for intermediate flows and for the wet season. This study shows that bias correction of CMORPH rainfall in the Kabompo Basin is critical for successful application in rainfall-runoff modelling.

For the REW model (2006–2012), Chapter 7 shows CMORPH error propagation assessments based on automated multi-objective calibration that was by means of the ε-NSGAII algorithm. A parameter set was optimized for the REW model using in situ-based point-to-pixel interpolated rainfall. This set served as a reference parameter set with optimum model parameter values for *Y*-objective function when the ε-NSGAII algorithm was rerun following the introduction of SRE. For uncorrected CMORPH, use of multi-objective functions targeting specific hydrograph characteristics resulted in overall augmentation of rainfall error to cause streamflow simulation mismatch whereas for bias corrected CMORPH, such resulted in attenuation of error. Analysis for water balance composition has great potential to improve application of satellite precipitation products in water management and decision making in the Zambezi basin. This study advises optimization of model parameters for each respective rainfall input data source so to identify unique outcomes and effects of respective rainfall data sources on the simulated water balance composition and closure.

The research presented in this thesis highlights the need for bias correction of satellite rainfall products before products are fit for use for streamflow modelling in the data scarce and water limited Zambezi Basin. Findings indicate that bias correction of rainfall is critical to improve capturing streamflow characteristics for effective water resources management in the basin. Statements and reports in the literature that SREs can be used directly in water resources applications are invalidated and deposed by this study. Results also show that no optimal bias correction can be prescribed for the basin's localized places (sub-catchments) in the Zambezi Basin. Even after application of the most effective bias correction scheme, errors are still relatively high to cause mismatch in streamflow simulation and errors in water balance simulation. This is evidenced by some underestimation of highest flows and overestimation of low flows. Sources of uncertainty and error that could contribute to the mismatch are rainfall representation, inaccurate representation of catchment characteristics such as land cover, stage-discharge relationship and the applied rainfall-runoff model structure. A detailed analysis of small spatial variability and spatial correlation analysis of in situ-based observations presumably is a prerequisite before satellite rainfall effects at short distances to a large-scale water body can be assessed.

Samenvatting

Het wetenschappelijk inzicht in de hydrologie van het grootste stroomgebied in Zuidelijk Afrika, de Zambezi, is beperkt. Exacte kennis van de hoeveelheden water zijn er niet, en het maken van schattingen met behulp van modellen is ontoereikend door het gebrek aan meteorologische gegevens en andere relevante data. Met de ontwikkeling van aardobservatietechnologie van de afgelopen tientallen jaren is de kwaliteit, kwantiteit en de resolutie sterk toegenomen. De huidige mogelijkheden om aardobservatiedata te integreren in hydrologische modellen zijn legio. Satellietwaarnemingen van regen (SWR) zijn tegenwoordig een geschikt alternatief voor of aanvulling op data van neerslagstations, dankzij de beschikbaarheid over gebieden zonder veldwaarnemingen overall op aarde. SWRs maken het bovendien mogelijk om tijdseries te construeren, aangezien de waarnemingen consequente en structureel worden uitgevoerd. In hydrologische modellen vormt de regen de voeding van het model. Daarom kunnen SWRs, na voorbewerking en correctie voor systematische afwijkingen (bias), gebruikt worden in hydrologische modellen en modellen voor de waterbeschikbaarheid.

Data producten zijn echter alleen representatief voor de werkelijkheid binnen een specifieke ruimtelijke schaal (de voetafdruk van de satellietmeting) en ruimtelijke resolutie (de herhalingstijd van de baan van de satelliet). De representativiteit van aangeboden SWR data verschilt per product. Het is daarom nodig om te begrijpen hoe fouten in neerslagdata uit satellieten gepropageerd worden in gesimuleerde rivierafvoeren.

Dit onderzoek heeft als doel om deze verspreiding van fouten in te schatten, en wel voor het CMORPH neerslagproduct (Climate Prediction Center-MORPHing). Een uitgebreide dataset van CMORPH neerslagbeelden, in-situ weerstation data en metingen van rivierafvoeren zijn ontwikkeld voor een afgebalend studiegebied (zie Hoofdstuk 2). De studie beperkt zich tot het stroomgebied van de Kabompo, een bovenstrooms deel van de Zambezi. Hiervoor is een nieuw concept, namelijk een massa-conservatief ‘Represenative Elementary Watershed (REW) model toegepast (Hoofdstuk 3). Het belangrijkste onderdeel van de onderzoeksmethodiek was het evalueren van de prestaties van een REW model voor rivierafvoer, wanneer deze gevoed wordt met gecorrigeerde satellietdata in plaats van data van neerslagstations. Een aantal schema’s voor correctie van de systematische afwijking en indicatoren voor de prestatie van het model dienen als instrumenten om de fout in de rivierafvoer door het gebruik van SWRs te onderzoeken. Het onderzoek laat zien hoe systematische

fouten in CMORPH data de gesimuleerde rivierafvoeren en het verschil tussen het REW model en de metingen beïnvloeden. Deze studie laat verder zien hoe ongecorrigeerde en bias-gecorrigeerde CMORPH SWRs de gesimuleerde actuele verdamping en afvoer beïnvloeden, en daarmee de sluiting van de waterbalans. Een verdere bijdrage van deze studie is de ontwikkeling van een methode om de vertaling van fouten in neerslag naar de rivierafvoer te onderzoeken, via modelkalibratie, met een reeks indicatoren voor de prestatie en doelstellingen. De bevindingen geven inzicht in het gebruik van SWR voor hydrologisch modelleren, vooral de propagatie van fouten van satellietdata.

In hoofdstuk 4 zijn de gevallen van het voorkomen van neerslag en neerslagintensiteiten in SWRs geëvalueerd op dagelijkse, wekelijkse en seizoens-schaal via een ‘kans op detectie-analyse (POD), ‘vals alarm ratio’ (FAR), succes index (CSI) en frequentie afwijking (FBS). SMORPH voorspelt 60% van de neerslaggevallen correct. De detectie was accurater in het natte seizoen dan in het droge seizoen. Verbeterde detectie was trad ook op bij neerslagintensiteiten kleiner dan 2.5 mm/dag. De fout kan worden onderverdeeld naargelang het type:, namelijk ‘Hit’, ‘Gemist’, ‘Loos alarm’, en ‘Verkeerde bias’. De detectie van gevallen van regen en de schattingen van de neerslaghoeveelheden van CMORPH voor sub-stroomgebieden verbeterde na aggregatie van dagelijkse wekelijkse schattingen. De bevindingen suggereren dat voor de Zambezi, de fouten in de CMORPH neerslag gecorrigeerd moeten worden voordat het product gebruikt kan worden in toepassingen zoals in hydrologisch modelleren, waarvoor betrouwbare en nauwkeurige invoer van gegevens vereist is.

SWR zijn gevoelig voor bias omdat ze indirect zijn afgeleid van de zichtbare en infrarode eigenschappen en microgolven van wolken. Daarom is correctie van SWRs nodig. Hoofdstuk 5 toont de invloed van hoogte en afstand tot grote wateroppervlakten op de bias van CMORPH neerslag in het stroomgebied van de Zambezi. De effectiviteit van vijf (niet)-lineaire bias correctie schema’s, zowel variërend als constant in tijd en ruimte, is geëvalueerd voor dagelijkse neerslagschattingen en voor de seizoenmatige patroon. De gebruikte schema’s waren: ruimte-tijd bias (RTB), topografische hoogte zone bias (HZ), machtstransformatie (MT), verdelingstransformatie (VT), en het kwantiel projecteren op basis van een empirische verdeling (KPE). Om de effectiviteit van de bias-correctie te evalueren, is ruimtelijke en temporele projectie kruiselings gevalideerd voor acht neerslagstations voor de periode 1998-1999. De correctie RTB en HZ bleken het meest effectief in het corrigeren van de bias. RTB verbeterde de correlatie coëfficiënt en de Nash-Sutcliffe efficiëntie met

respectievelijk 50% en 53%, en beperkten de kwadratisch gemiddelde afwijking (RMSE) en relatieve bias (%) met respectievelijk 25% en 33%. Gekoppelde t-testen lieten zien dat er na bias correctie geen significant verschil is ($p<0.05$) in de dagelijkse gemiddelden van CMORPH tegen data van neerslagstations. ANOVA post-hoc testen toonden aan dat de RTB en HZ bias correctie schema's de voorkeur hebben. De bias is het hoogste voor zeer lichte neerslag (<2.5 mm/dag), waarvoor de grootste effectieve bias vermindering optreedt, vooral voor het natte seizoen. De bevindingen verkregen via kwantiel-kwantiel (q-q) diagrammen waren vergelijkbaar. De ruimtelijke kruisvalidatiebenadering liet zien dat de meerderheid van de bias correctieschema's meer dan 28 % van de bias verwijderden. De kruisvalidatie in de tijd liet zien hoe effectief de bias correctie is. Tayler diagrammen lieten zien dat de topografische hoogte van het weerstation de prestaties van CMORPH beïnvloedt. De effecten van open water zijn op afstanden van meer dan 10 km zijn minimaal, maar op kortere afstand lijken ze wel op te treden. Een heldere conclusie kan echter niet worden getrokken bij gebrek aan data van neerstagstations. De bevindingen laten zien hoe belangrijk het is om bias correctie op SWR's uit te voeren.

Hoofdstuk 6 behandelt een hydrologische studie (2008-2013) van neerslag van stations, en schattingen van ongecorrigeerde en bias gecorrigeerde CMORPH satellietneerslag in het stroomgebied van de Kabompo, een bovenstroomse tak van de Zambezi. De resultaten van REW modellering met behulp van stationsdata vormde de referentie voor de simulaties. De periode van 2004-2007 is uitgekozen voor REW modelkalibratie en de periode 200802010 voor modelvalidatie, met gebruik van neerslag gemeten bij stations. De resultaten van de afvoersimulatie zijn geëvalueerd door gemeten en gesimuleerde afvoer te vergelijken met Nash Sutcliffe efficiëntie (NSE) en relatieve volume fout (RVE) als doelfuncties. De resultaten laten zien dat fouten in ongecorrigeerde CMORPH neerslagschattingen leiden tot een groot verschil in gesimuleerde en gemeten afvoer. De ongecorrigeerde CMORPH neerslag zorgde voor een overschatting van de neerslag voor de periode 2000-2015. Een lineaire correctiefactor was toegepast om de bias te verwijderen. Verder is onderzocht hoe geoptimaliseerde waardes van parameters beïnvloed worden door de bias in de neerslag invoer. Met dit doel is et model dus opnieuw gekalibreerd na het vervangen van de stationsdata door bias gecorrigeerde en ongecorrigeerde CMORPH neerslag. De bias gecorrigeerde CMORPH neerslag verbeterde de overeenstemming tussen gemeten en gesimuleerde afvoertotalen. De doelfuncties RVE en NSE verbeterden significant door de bias correctie. De geoptimaliseerde REW parameter waardes, en dan

vooral de parameters die het volume van de gesimuleerde hydrograaf bepalen, veranderden met meer dan 50% nadat de stationswaarnemingen zijn vervangen door ongecorrigeerde CMORPH schattingen. De waardes van de parameters bleven wel binnen de grenzen die fysisch geloofwaardig zijn, voor bias gecorrigeerde CMORPH, voor mediane rivierafvoeren, en voor het natte seizoen. De studie toont aan dat bias correctie van CMORPH neerslag in het stroomgebied van de Kabombo noodzakelijk is voor een succesvolle toepassing van neerslag-afvoer modellen.

Hoofdstuk 7 laat voor het REW model (2006-2012) de propagatie van de fout in CMORPH zien, op basis van een automatische multi-doel kalibratie en met behulp van het ε-NSGAII algoritme. Een set van parameters is geoptimaliseerd voor het RWE model met behulp van in-situ punt-tot-pixel interpolaties van neerslag. Deze set dient als referentie parameter set met voor optimale modelparameter waardes voor een Y-doelfunctie wanneer het ε-NSGAII algoritme opnieuw wordt gedraaid na de introductie van SWR. De fout in de simulaties in rivierafvoer neemt toe bij gebruik van niet-gecorrigeerde CMORPH neerslag, maar juist af bij gebruik van gecorrigeerde CMORPH data, gemeten naar de multi-doelfuncties. Een analyse van de samenstelling van de waterbalans kan de toepassing van satelliet gebaseerde neerslagproducten voor watermanagement en besluitvorming verbeteren. Het advies is om modelparameters te optimaliseren voor elke databron van neerslag invoer, om zo de invloed van de data bron op de gesimuleerde waterbalans en de sluiting van de waterbalans te begrijpen.

Het onderzoek in dit proefschrift belicht de noodzaak voor bias correctie van data producten van satellieten, voordat deze geschikt zijn voor de simulatie van rivierafvoer in de Zambezi, een stroomgebied waarin data schaars zijn en de waterbeschikbaarheid beperkt. De bevindingen tonen dat bias correctie van neerslag een essentiële stap is naar beter begrip van de rivierafvoer en effectief management van de beschikbare waterbronnen in het stroomgebied. Claims in rapporten en in de wetenschappelijke literatuur dat SWR direct gebruikt kan worden in toepassingen op het gebied van waterbeschikbaarheid zijn onjuist. De resultaten laten ook zien dat geen enkele bias correctie optimaal is voor deelgebieden van de Zambezi. Zelfs na toepassing van de meest effectieve bias correctie, zijn de fouten nog relatief groot, en dit veroorzaakt een fout in de gesimuleerde rivierafvoer en in de water balans. De onderschatting van de piekafvoeren en overschatting van de lage afvoeren zijn hier bewijs van. De bronnen van onzekerheid en fouten die kunnen bijdragen aan het verschil zijn de

representativiteit van de neerslag, de onnauwkeurige beschrijving van eigenschappen van het stroomgebied zoals landbedekking, de relaties tussen peil en debiet, en de toegepaste neerslag-afvoer modelstructuur. Een gedetailleerde analyse van kleinschalige ruimtelijke variabiliteit en ruimtelijke correlatieanalyse van veldmetingen lijkt een vereiste in onderzoek naar de invloed van satelliet neerslag van korte afstand tot grootschalige toepassing.

Chapter 1: Introduction

1.1. Background.

The Zambezi River basin which is the biggest river basin in Southern Africa has over 47 million inhabitants (Hoel, 2015). The basin shows indications that its hydrological cycle is undergoing changes by increased climate variability and unsustainable landuse activities (Hughes and Farinosi, 2020; Chisanga *et al.*, 2022). These changes threaten the functions and services by the river such as providing water to riparian countries (Bisselink *et al.,* 2016; Petersen-Perlman, 2016). With an area of 1.39 million km^2 (4 % of the African continent) and serving 8 countries, a clear scientific understanding of all major variables affecting its hydrological cycle is lacking (Spalding-Fecher *et al.,* 2017, 2016). The unavailability of adequate landsurface and meteorological data hinders quantitative estimates of the water balance (Paparrizos *et al.,* 2016; Piniewski *et al.,* 2017). In cases where data is available, the data represents point scale characteristics, is often of short duration and in many cases incomplete. Remote sensing allows observation of time invariant catchment properties and time variant hydrological cycle variables (Brocca *et al.,* 2017; McCabe *et al.,* 2017) and properties in respective time and space domains and is the premise for application in such data poor catchments (Najmaddin *et al.,* 2017; Zhou and Han, 2017). Improvements of the products can substantially improve the predictive capabilities and quantitative estimates of hydrological models (Talib and Randhir, 2017; Welde and Gebremariam 2017). Therefore, remote sensing observations have a potentially important role in providing spatial information for hydrological parameterization of rainfall-runoff models (Alazzy *et al.,* 2017; Liu *et al.,* 2017). It should however be noted that remote sensing in most cases does not directly observe hydrological processes but only variables of those processes.

Precipitation is one of the key hydrologic variables and its accurate and up-to-date measurement is key for dependable hydrologic predictions (Maidment *et al.,* 2017; Meyer *et al.,* 2017). For the purpose of improving precipitation estimation techniques in space and time, satellite rainfall estimates (SREs) are available. Nowadays satellite rainfall products are produced at a spatial resolution of 8 km × 8 km, but often at smaller resolution, such as; Climate Prediction Centre Morphing technique (CMORPH), Tropical Rainfall Measuring Mission (TRMM), Precipitation Estimation from Remotely Sensed Information using

Artificial Neural Networks (PERSIANN) and Integrated Multi-satellitE Retrievals for GPM (IMERG).

Several multi-satellite precipitation products such as CMORPH, PERSIANN, IMERG and TRMM have been developed with the objective to improve satellite rainfall estimates to serve hydrological applications. Although quality of products advanced, products are affected by errors which affect water resources applications, hence the need for error assessment and correction studies.

1.2. Errors in satellite rainfall estimates

SREs rely on use of different satellite sensors that are infra-red (IR) and Passive Microwave (PMW) (Habib *et al.,* 2012a). The IR sensor measures the temperature of a cloud top that serves to estimate ground rainfall. The major weakness of the IR technique is detection of rainfall, bearing in mind that the relation between cloud top temperature and ground rainfall only is weakly defined. For PMW, rainfall at the surface is related to microwave emission from rain drops (low frequency channels) and microwave scattering from ice (high frequency channels). The IR has relatively high temporal resolution and the PMW has a better estimation quality (Asadullah *et al.,* 2010).

Several studies indicate that satellite rainfall products contain errors which manifest as systematic and random (Ringard *et al.,* 2015; Romilly and Gebremichael, 2011). Errors result from the use of satellite sensors that provide indirect estimate of ground rainfall (Pereira Filho *et al.*, 2010; Romano *et al.*, 2017). Random errors depend on the sensor sampling design and is influenced by surface features on the earth surface, distance to large scale water bodies, topography (Jury, 2017) and how well the average ambient atmospheric conditions are represented (Cattani *et al.* 2016; Manz *et al.* 2016; Moazami *et al.* 2014).

Systematic errors can occur because of problems with tuning the satellite algorithm, or from limitations in what the satellite instrument is able to detect (Maggioni *et al.,* 2022; Song *et al.*, 2019). Systematic errors in SREs commonly are referred to as bias, that indicates the accumulated systematic difference between rain gauge observations and SRE based counter parts. Bias in SREs is expressed for rainfall depth (Habib *et al.,* 2014), rain rate (Haile *et al.,* 2013a) and frequency at which rain rates occur (Khan *et al.*, 2014). Bias may be negative or positive where negative bias indicates underestimation whereas positive bias indicates overestimation (Liu, 2015; Moazami *et al.*, 2013). Bias correction of

satellite rainfall estimates is important before application in water resources management (Habib *et al.,* 2014). Random errors cannot be corrected unequivocally but systematic errors can be corrected (Kimani *et al.,* 2017; Wehbe *et al.,* 2017).

The quality of SREs differs per location and region but also differs in the time domain (Parida *et al.* 2017; Serrat-Capdevila *et al.* 2016; Zambrano-Bigiarini *et al.* 2017). The relationships between SRE performance and distance to large scale water bodies at different temporal and spatial scales is also an area of research interest because of the presence of water bodies and rugged terrains in the Zambezi basin. Haile *et al.* (2009) showed that for the Nile Basin, there are indications that the presence of Lake Tana (≈ 3050 km^2, Ethiopia) affects rainfall at short distances to the lake (< 10 km). In many African basins, errors in rainfall estimates are reported for rainfall depth (Cattani *et al.* 2016; Kimani *et al.* 2017), rainfall occurrence (Haile *et al.* 2014 and Mashingia *et al.,* 2014) and rainfall rate (Dezfuli *et al.* 2017; Nicholson, 2013). In the Zambezi Basin in Southern Africa, Cohen Liechti *et al.* (2012) found that CMORPH overestimates rainfall depth by nearly 50 % with large spatial variation. However, for the Upper Zambezi Basin, Valdés-Pineda *et al.* (2016) observed that CMORPH showed fair agreement with gauge-based estimates for daily rainfall depth, with correlation coefficient that ranged from 0.52 to 0.83. The above studies show that the CMORPH product is used for hydro-meteorological studies in the Zambezi Basin but performance of CMORPH and estimation of errors associated with rainfall depth, occurrence and rainfall rate is not comprehensively established. In Mozambique in the Lower Zambezi, CMORPH often shows better performance in the rainy season (Toté *et al.,* 2015) than in the dry season. Several studies in Africa also show that low rainfall rates are overestimated and high rainfall rates are underestimated (Thiemig *et al.* 2012; Toté *et al.* 2015). Thiemig *et al.* (2012) further shows that the average annual precipitation is being overestimated by more than 500 mm/annum in 30 % of the Zambezi basin's area. As such, findings on CMORPH performance cannot be generalized upon and this indicates the need for localized assessments in the Zambezi Basin.

Performance evaluation of SRE as a methodological step is by statistical as well as hydrological modelling evaluation. Statistical evaluation is normally through indicators which show how well rainfall is detected by a satellite, the estimation of volumetric error in the SRE, as well as error decomposition analysis. Time series of SREs for rainfall depths and occurrence of specific rainfall rates also are evaluated by decomposing the estimation error that result from wrongly detected

and estimated rainfall. Error analysis aims at estimating missed and false rainfall by the satellite and erroneous estimates when both gauge and satellite indicate rainfall. Respective errors are referred to as Missed bias (missed rainfall), False bias (false rainfall) and Hit bias (Yong *et al.* 2016). Error components for Hit, Missed and False bias [mm/day] make up the total bias, and all these terms can be converted to a percentage to make them comparable to other values obtained in other hydrological catchments. Error or bias decomposition aims to identify the error components and thus all errors must be jointly interpreted in satellite rainfall retrieval studies (Xu *et al.,* 2016). Hydrological evaluation shows how error in satellite rainfall propagate to cause mismatch in runoff simulation.

Studies (Cohen Liechti *et al.,* 2012; Meier *et al.,* 2011) on use of SREs in the Zambezi River Basin mainly focused on accuracy assessment of the SREs using standard statistical indicators with little or no effort to perform bias correction despite the evidence of errors in these products. The use of uncorrected SREs is reported for hydrological modelling in the Nile Basin (Bitew and Gebremichael, 2011) and Zambezi Basin (Cohen Liechti *et al.,* 2012), respectively, and for drought monitoring in Mozambique (Toté *et al.,* 2015). The poor performance of SREs in above studies urges for bias correction to result in more accurate rainfall representation.

1.3. SRE bias error propagation in hydrological modeling

The effectiveness of bias correction schemes often is assessed by means of hydrological modelling. Different models are available which can be used for rainfall-runoff predictions. Whereas Gumindoga *et al.* (2020); Shanhu *et al.* (2016); Wehbe *et al.* (2017) provide information on use of SRE's for hydrological applications, aspects of error propagation to streamflow mismatch are not commonly explored. Studies by Artan *et al.* (2007); Du *et al.* (2012) and Nikolopoulos *et al.* (2012) on application of SREs in hydrologic modelling studies discuss patterns of error propagation and highlight the nonlinear error transformation process, i.e. the hydrologic models transform and propagate relatively small error without distinctly affecting model performance, but may augment this error at higher rainfall magnitudes.

The field of error propagation and water balance closure error assessments are topics of continuing interest in data scarce regions (Sheffield *et al.,* 2009). However, research on SRE error propagation is unknown in the Zambezi River

Basin. Propagation of rainfall error to streamflow error by hydrological modelling commonly is evaluated by analysing mismatches between observed streamflow and simulated counterparts subject to respective rainfall input data sources. For that purpose, objective functions may be combined and optimized by use of automated single or multi-objective model calibration algorithms (see De Vos and Rientjes, 2007). Yapo *et al.* (1998) identified a set of optimal solutions (model parameter sets) based on a trade-off between different objective functions. De Vos and Rientjes (2007) showed that not all differences between modelled and observed hydrograph characteristics (e.g., peak flows or low flows) can be expressed adequately by single objective functions and optimized model parameter set. Rientjes *et al*. (2013a), Monteil *et al.* (2020) and Shahed Behrouz *et al.* (2020) show that multi-objective calibration allows the simultaneous evaluation of multiple outputs from the model. These applications have been on knowledge-driven or parametric hydrological model approaches and thus, it is likely that aspects of satellite rainfall error propagation can be assessed from such a calibration approach.

A model selected for this study is the Representative Elementary Watershed (REW). REW is a hydrological model that simulates runoff and streamflow at the subwatershed scale (Reggiani *et al.,* 2000, 1999, 1998; Reggiani and Rientjes, 2005; Reggiani and Schellekens, 2003). The REW approach has a number of successful and innovative applications in water resources modeling as demonstrated by a number of recent scientific publications (Reggiani, Todini and Meißner, 2014; Reggiani and Majid Hassanizadeh, 2016; Elgamal, Reggiani and Jonoski, 2017). Example catchments where the model has been successfully applied are the Donga catchment in Benin, Geer River Basin in Belgium, Can Le catchment in Vietnam, Collie River Basin in Western Australia and Weiherbach Catchment in Germany. However, there are no reported applications of bias corrected CMORPH estimates in African basins for REW hydrological modelling. Unlike conventional conceptual watershed models (Abbott *et al.,* 1986) such as the Soil and Water Assessment Tool (SWAT), the Topographic-driven hydrologic model (TOPMODEL), the Hydrologic Modeling System (HEC-HMS) and the *Hydrologiska Byråns Vattenbalansavdelning* model (HBV), REW is a physically based model and applies differential equations for movement of water. REW can also generate distributed predictions of state variables and water fluxes in a research catchment, and because it is physically based, can potentially predict the effects of changes in climate and in landscape properties such as soil type, vegetation and land use, on the catchment's responses (Lee *et al.*, 2005). As such,

hydrological responses can be simulated over extensive time periods allowing assessment of impacts related to bias corrected satellite-based rainfall products. For this study the model was tested for use of satellite remote sensing data that represent the meteorological forcing terms. Multi-objective approaches are tested for rainfall error propagation to cause mismatch in streamflow hydrograph shape, combinations of specific hydrograph characteristics, streamflow mismatch and assessments of water balance closure.

In rainfall-runoff model calibration, most approaches rely on single-objective functions (Yang *et al.*, 2014). Optimisation via single-objective calibration reduces model performance to represent streamflow characteristics other than the one considered in the objective function values. Optimality in the context of multi-objective global optimization is named after Vilfredo Pareto (Moore, 1897). A solution is classified as Pareto optimal when there is no feasible solution that will improve some objective values without degrading performance in at least one other objective (Deb *et al.*, 2002; Kollat and Reed, 2006). The case for two solutions (Tang *et al.*, 2006), are incommensurable, i.e. one solution simulates the peaks better and simulates the base flow poorer, while the other solution simulates the peaks poorer and simulates the base flow effectively (Reichert and Schuwirth, 2012; Yang *et al.*, 2014; Forootan, 2018).

In this study, to obtain the Pareto solutions, the Non-dominated Sorting Genetic Algorithm II (NSGAII) algorithm (Deb *et al.*, 2002), which was later modified by Yang *et al.* (2014), is adopted. The modified algorithm, is efficient, reliable, and easy to use (Yang *et al.*, 2014) owing to its dynamic population sizing and archiving which lead to rapid conjunction to very high-quality solutions with minimal user input. The study took advantage of the inherent characteristics of NSGAII to assess error propagation from rainfall to REW streamflow mismatch. Note that it is crucial that approaches of optimization be the same when findings of rainfall error propagation by different rainfall input sources are to be compared. Otherwise, the optimization approach impacts results of rainfall error propagation as different optimization principles affect optimized model parameter values. In this study, ε-NSGAII was applied to multi-objective calibration to enable assessment of CMORPH performance. The emphasis is on indicating the impact of selected objective functions on hydrograph characteristics and simulation errors rather than on further development of the optimization algorithm as several studies have already investigated this aspect (Johnsen *et al.*, 2005; Tang *et al.*, 2006).

1.4. Problem statement

In the Zambezi River basin, simulations using hydrologic models often is rendered ineffective by the unavailability of climatic data. In most of Zambezi sub-basins, there is scarcity of climatic data but in cases where data is available, the data only is available at point scale. In addition to poor basin accessibility, the rain gauge network in the Zambezi River Basin is sparse which hampers to quantify water balance components. To overcome rainfall data scarcity, SREs are a solution since observations cover large geographical areas, have a larger and more consistent spatial coverage compared to rain gauges, as well as the fact that observations are repeated over constant time intervals. The observation of rainfall by satellites in respective time and space domains is the premise for application in data poor catchments. The additional advantage is that observations are available free of charge. Such advantages have triggered researchers to develop algorithms and methodology of using satellite-based rainfall estimates for hydrological modelling. In hydrological modeling, these variables represent meteorological forcing (i.e., rainfall or evapotranspiration) and storages (soil moisture and groundwater).

Satellite rainfall however has errors that manifest in the volume, distribution, frequency and intensity domain to cause mismatch in runoff simulation. The low number of rainfall stations in the Zambezi basin and lack of time series at respective time interval often is considered as argument to deny performance assessments and bias correction of SREs. This study considers the poor density of network stations in the Zambezi Basin as a reason to evaluate whether SREs are sufficiently accurate to serve as an alternative or supplementary data source. As such, the Zambezi Basin offers an opportunity to explore bias correction schemes which are appropriate for the vast basin, to motivate use of SREs for future applications such as in water resources studies.

Recent publications on CMORPH (a gridded precipitation product) applications in African basins exist (Gumindoga *et al.*, 2019; Haile *et al.*, 2015; Koutsouris *et al.*, 2016; Shanhu *et al.*, 2016; Wehbe *et al.*, 2017) but studies on SRE error propagation to streamflow mismatch are limited. For the proposed research it is hypothesized that observing (or knowing) the time-space patterns of a high-quality rainfall data set, and product in particular, allows for more accurate error propagation analysis and water balance simulation in the water limited southern African basin.

1.5. Research Objectives

1.5.1. Main Objective

The main objective of this study is to perform bias correction and bias error propagation assessment of CMORPH satellite rainfall estimates for hydrological analysis by the Representative Elementary Watershed (REW) model in the Zambezi Basin.

1.5.2. Specific Objectives and Research Questions

The following specific objectives (SO) and research questions (RQ) are identified:

SO 1: To assess **performance of CMORPH satellite precipitation product** in the Zambezi Basin.

> RQ 1. What is the probability of rainfall detection by CMORPH for both daily and weekly time step in the Zambezi Basin, for the dry and wet season and for different rainfall intensities?
> RQ 2: Which sub-basins of the Zambezi show under- and overestimation of CMORPH in terms of mean, maximum and rainfall totals?
> RQ 3: Which of the three bias components (Hit, Missed and False biases) contribute to increased spatial and temporal variations of CMORPH bias?

SO 2: To evaluate the **performance of bias correction schemes** for CMORPH rainfall estimates in the Zambezi River Basin.

> RQ 4. How is the performance of CMORPH rainfall estimates affected by elevation and distance from large scale water bodies in the Zambezi Basin?
> RQ 5. What is the performance of bias correction schemes in removing bias for different rainfall rates and seasons?

SO 3. To perform a **hydrologic evaluation of bias corrected CMORPH** rainfall estimates at the Kabompo headwater catchment of the Zambezi River.

RQ 6. To what extent is bias correction and runoff mismatch affected by point-to- pixel and pixel-to-pixel rainfall comparisons?
R 7. How does REW hydrological model parameterization change when bias corrected SREs serve for model forcing instead of interpolated rain gauge data?
RQ 8. How is streamflow seasonality, and how are simulated high and low streamflows affected by CMORPH bias errors?

SO 4. To assess **propagation of CMORPH rainfall errors** to REW streamflow simulation mismatch in the Kabompo headwater catchment.

RQ 9. How suitable is time and space variable bias correction for assessing rainfall error propagation in the Zambezi basin?
RQ 10. What is the pattern of rainfall error propagation to streamflow mismatch in a multi-objective calibration framework that targets specific hydrograph characteristics?
RQ 11. To what extent is water balance closure affected by SRE error propagation?

1.6. Thesis outline

The eleven research questions are addressed in Chapters 4, 5, 6 and 7 of this thesis respectively. The thesis is structured as follows:

Chapter 2 provides a brief introduction of the study area, in situ and satellite-based data sets;

Chapter 3 introduces the REW model structure;

In **Chapter 4**, CMORPH satellite rainfall evaluations are carried out for rainfall occurrence and rate at sub-basin scale as well as at daily, weekly, and seasonal time scales by means of detection statistics: probability of detection *(POD)*, false alarm ratio *(FAR)*, critical success index *(CSI)* and frequency bias *(FBS)*, error decomposition and volumetric statistics;

Chapter 5 tests the influence of elevation and distance from large water bodies on bias for CMORPH rainfall estimates. Effectiveness of five linear/non-linear and time-space variant/invariant bias correction schemes is evaluated. Evaluation also covers for rainfall rates and climatic seasonality;

Chapter 6 assesses the performance of bias corrected CMORPH rainfall estimates as aspects of error propagation and streamflow mismatch are assessed.

REW based hydrologic modelling is performed from 2008-2013 in the Kabompo Basin. Comparison of rain gauge observations to CMORPH estimates was done at point to pixel scale, as well as pixel to pixel scale. Manual calibration of the REW model is by trial and error in which the model parameters were manually adjusted to optimize model performance for in situ-based rainfall. Manual recalibration of the model was also performed by changing one parameter at a time when uncorrected and bias corrected SRE was introduced.

Chapter 7 seeks an improved understanding of propagation effects of CMORPH rainfall errors to REW streamflow mismatch. Automated multi-objective calibration of the REW model is by means of the ε-NSGAII algorithm where a parameter set is optimized using in situ-based rainfall. To assesses effects of use of SREs, the model was recalibrated using ε-NSGAII algorithm. Findings are expected to provide new insights on the hydrologic implications of use of SREs and serves to improve applications in the Zambezi Basin such as for rainfall-runoff modelling;

Chapter 8 synthesizes the main findings of Chapters 4, 5, 6 with respect to the eleven research questions and directions for further research are presented as well.

Chapter 2: Study area and rainfall data sets

2.1. Study area

2.1.1. The Zambezi Basin

Chapters 4 and 5 are based on the Zambezi Basin. The Zambezi River is the fourth-longest river (~2,574 km) in Africa with basin area of ~1,390,000 km^2 (~4 % of the African continent). The river drains into the Indian Ocean and has mean annual discharge of 4,134 m^3/s (World Bank, 2010a). The river has its source in Zambia and forms boundaries of Angola, Namibia Botswana, Zambia, Zimbabwe and Mozambique (Fig. 2.1). The basin has considerable differences in elevation, topography and climatic seasonality and, as such, makes the basin well suited for this study. The basin is divided into three sub-basins i.e., the Lower Zambezi comprising the Tete, Lake Malawi/Shire, and Zambezi Delta basins, the Middle Zambezi made up of the Kariba, Mupata, Kafue, and Luangwa basins, and the Upper Zambezi constituted by the Kabompo, Lungwebungo, Luanginga, Barotse, and Cuando/Chobe basins (Beilfuss, 2012).

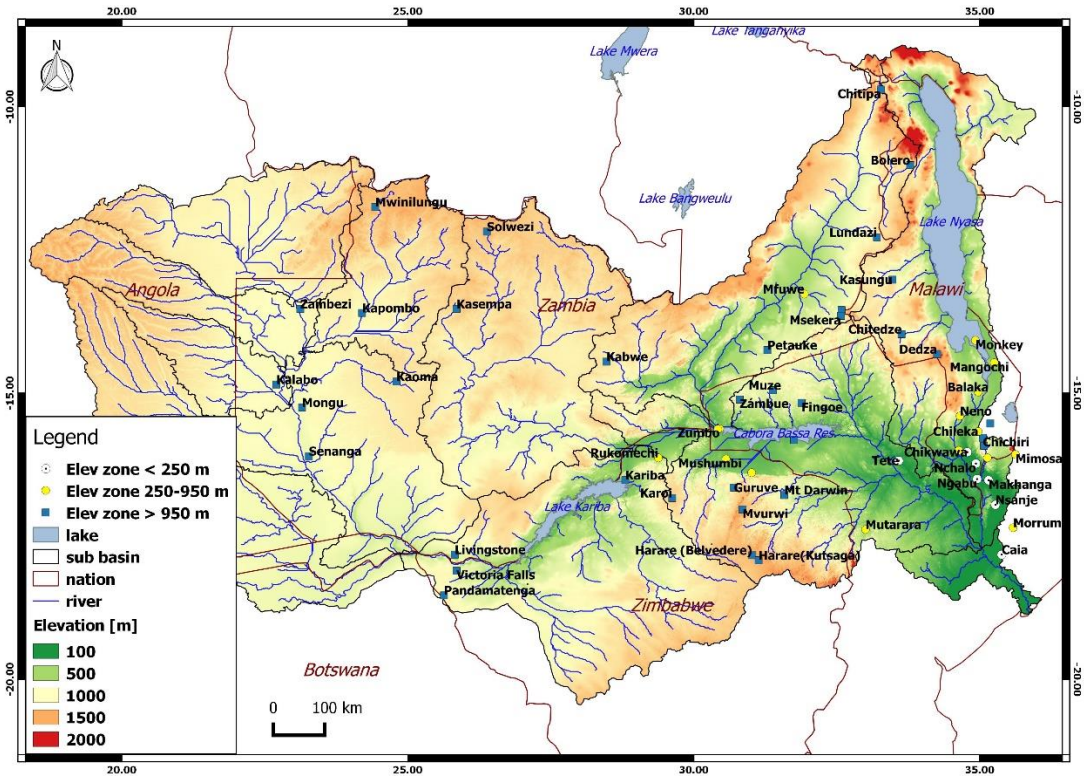

Figure 2.1: Zambezi River Basin from Africa with sub-basins, rivers, major lakes, elevation, and locations of the 60 rain gauging stations (in each respective elevation zone) used in this study.

The elevation of the Zambezi basin ranges from < 200 m (for some parts of Mozambique) to > 1500 m above sea level (for some parts of Zambia). Large scale water bodies in and around the basin are Kariba, Cabora Bassa, Bangweulu, Chilwa and Nyasa. Typical landcover types are woodland, grassland, water surfaces and cropland (Beilfuss *et al.*, 2000; Chisanga *et al.*, 2022).

The basin lies within the tropics between 10° and 20° S, encompassing humid, semi-arid and arid regions dominated by seasonal rainfall patterns associated with the Inter-Tropical Convergence Zone (ITCZ), a convective front oscillating along the equator. The movement of the ITCZ in Southern hemisphere results in the peak rainy season that occurs during the summer (October to April) and the dry winter months (May-Sept) is a result of the shifting back of ITCZ towards the equator (Cohen Liechti *et al.* 2012; Hughes, 2006). The weather system in South

Eastern parts such as Mozambique is dominated by Antarctic Polar Fronts (APF) and Tropical Temperate Troughs (TTTs) occurrence which are related to La Niña and Southern Hemisphere planetary waves, while El Niño-Southern Oscillation (ENSO) appears to play a significant role in causing dry conditions in the basin. The Zambezi River Basin is characterized by high annual rainfall (>1,400 mm/year) in the north and north-east areas and low annual rainfall (< 500 mm/year) in the south. Figure 2.1 shows that only 60 rain gauges are available in the vast area of 1.39 million km^2. The river and its tributaries are subject to seasonal floods and droughts that have devastating effects on the people and economies of the region, especially the poorest members of the population (Tumbare, 2005). It is not uncommon to experience both floods and droughts.

2.1.2. The Kabompo Basin

For hydrological modelling and error propagation analysis, the area of study is the Kabompo River Basin (Figure 2.2) of North-Western Zambia with size of approximately 72 000 km^2. The basin is a headwater catchment of the Zambezi River.

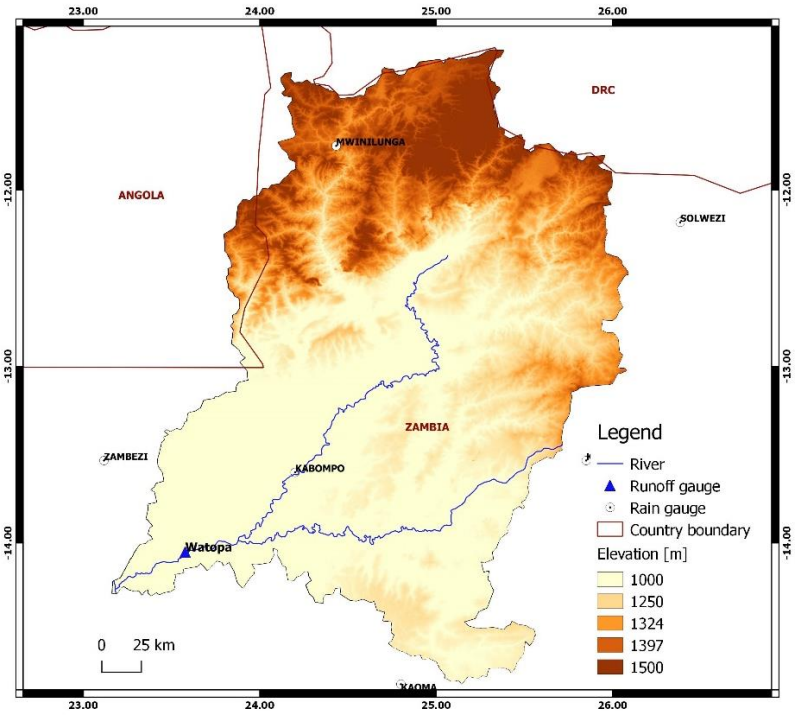

Figure 2.2: Kabompo Basin showing, elevation, rain and runoff gauging stations.

The Kabompo Basin experiences two distinctive seasons (a dry season from May to October and a wet season from November to April). The basin has mean annual rainfall ranging from 1500 mm/year in the North to 900 mm/year in the South. The minimum basin wide average monthly temperature for the period 2008-2013 is around 14 ºC whereas the maximum is around 22 ºC (Mwansa, 2018).

Silt-to-clay and sandy-textured soils make up the undulating plateau zones and slightly dissected plateau zones. Also found are soils influenced by waterlogged conditions near the Zambezi floodplain which have visual evidence of iron reduction (FAO/IIASA/ISRIC/ISS-CAS/JRC, 2009; Garrison, 2017). The geology is dominated by Kabompo granitic domes flanked by a sequence considered equivalent to the basal Lower Roan rocks which is a composition of the Katanga Supergroup (Muzumara, 2010). Vegetation in most part of the basin is classified as tropical grasslands or savanna. Specific vegetation types include grasslands, woodlands and forests. The area has protected forests (6 %) and parks (12 %). There is also increased population pressure causing increased deforestation (Mwansa, 2018). Economic activities include small-scale agriculture and mining. Muzumara (2010), describes that water related problems in the Kabompo Basin include water allocation to agriculture and ecosystems, unknown hydrological regime changes by land cover changes, and potential water resources impacts by mine tailing dams.

2.2. Gauge based data

For chapters 4 and 5, daily rain gauge data from 66 stations located in the Zambezi Basin were obtained from meteorological departments of Botswana, Mozambique, Malawi, Zimbabwe and Zambia. After initial screening, and quality control by intercomparing neighbouring stations, missing rainfall values were filled-in and duplicate entries and suspiciously high values were removed following Young *et al.* (2014). Additional quality control involved manual inspection of the runoff gauging stations, visual inspection of data gaps, comparison of mean annual precipitation (MAP) and mean annual runoff (MAR) in mm as well as checking for negative values or extreme high values. For other stations, instead of introducing additional uncertainty by filling in the missing values, the study left out the missing days from the analysis (i.e., comparison of gauge-CMORPH data, bias correction and hydrological modelling).

The poor data quality is attributed to a number of reasons: short station records as observed in Northern Zimbabwe raingauge stations, not concurrent records as observed in Southern Malawi as well as trees growing close to a raingauge, thus wrong place, as observed in a reconnaissance survey in Zambia's Kabompo catchment. Certain stations in the Zambezi Delta have an artificial influence such as the raingauge being removed from original location. Kanyemba station on the border between Zimbabwe and Zambia is occasionally disturbed by wildlife.

Time series of most stations cover the period 1998-2013 (see Table 2.1.) with a number of stations that are affected by data gaps. Stations are located at different elevations between 3 m to 1575 m (Table 2.2.) and are irregularly distributed across the basin. The minimum, maximum and average distance between the rain gauges is 3.5 km (Zumbo in Mozambique-Kanyemba in Zimbabwe), 1570 km (Mwinilunga in Zambia-Marromeu in Mozambique) and 565 km respectively. As such, the network is most dense in the Shire River sub-basin in Malawi and very sparse in Tete sub-basin in Mozambique. The Quando/Chobo sub-basin has no rain gauges at all. Distances to large scale open water bodies range between 5 km and 615 km (Table 2.2.). This allowed evaluation if elevation and distance to large scale open water bodies affect CMORPH performance.

After discarding some of the data which was judged as very uncertain during data quality check, the study remained and prioritized the rest of the 60 stations. All the stations are standard type rain gauges with a measuring cylinder whose unit of measurement is millimetres per day (mm/day). Double Mass Curves (DMCs) of nearby stations accompanied by statistical tests were plotted to further ascertain the quality of the 60 remaining stations.

Figure 2.1, shows a comparison of DMC hydrographs for selected pairs of nearby stations. The high R^2 for Harare (Belvedere) vs Harare (Kutsaga) (inter distance of 18 km) and Mvurwi vs Guruve stations (51 km apart) reveals that the stations can be trusted in the subsequent analysis. Stations have several data points spread uniformly along the x and y-axis but however instances when the data points deviate from the x = y line.

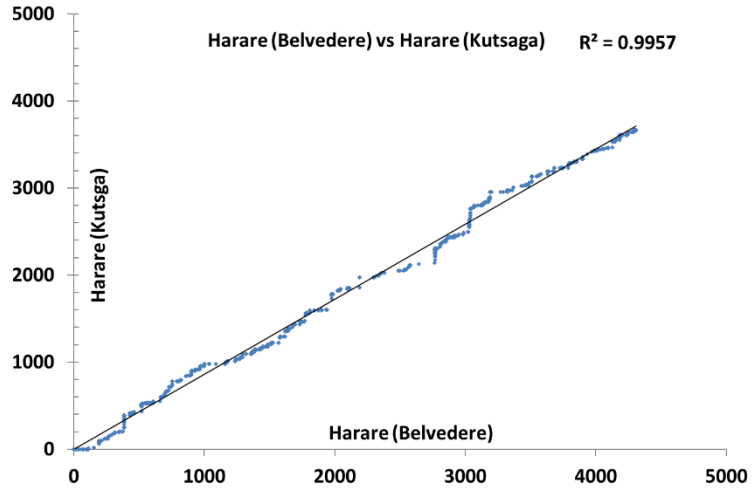

(a)

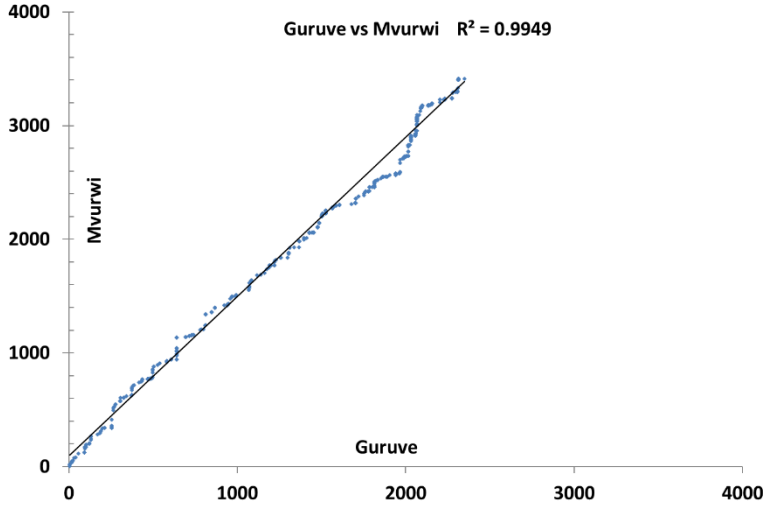

(b)

Figure 2.1. Double Mass Curve Analysis for (a) Harare (Belvedere) vs Harare (Kutsaga) and (b) Mvurwi vs Guruve stations in Kariba Catchment of the Zambezi Basin.

For the REW model simulation objectives, daily rain gauge data from 6 stations in the Kabompo Basin were used. These are Zambezi, Kabompo, Kaoma, Kasempa, Mwinilunga and Solwezi. The data series that overlap from 1973-2013 was obtained from the Meteorological Office of Zambia. Potential evapotranspiration at daily time step was estimated from the meteorological data using the FAO-Penman Monteith method as outlined in Allen *et al.* (1998). The locations of these stations cover a wide range of elevation values (~1000-1400 m).

For the same period, daily streamflow data were obtained for Watopa gauging station from the Department of Water Affairs and Water Resources Management Authority of Zambia. The relation between rainfall and streamflow was assessed as part of data screening. Watopa station has a long-term mean flow of 216 m^3/s (i.e., 1.9 × 107 m^3/year) with highest flows (up to 1570 m^3/s) that are received in March whereas the lowest flows (down to 36 m^3/s) are received in September. A field visit to the station shows that Kabompo's Watopa station has a fairly good rating curve, and compared to other stations in the Zambezi Basin, has less evidence of change of river section due to vegetation and siltation problems. Further analysis of runoff station quality involved water balance checking by calculating runoff coefficients (Q/P) between different subbasins.

Table 2.1. Rain gauge stations in the Zambezi Basin showing station code, sub-basin they belong to, years of data availability and elevation.

Station	**Code**	**Sub-basin**	**Zambezi classification**	**X Coord**	**Y Coord**	**Start date**	**End Date**	**% Gaps**	**Elevation (m)**
Marromeu	Mru	Zambezi Delta	Lower Zambezi	36.95	-18.28	29/05/2007	31/12/2013	0.37	3
Caia	Ca	Zambezi Delta	Lower Zambezi	35.38	-17.82	29/05/2007	31/12/2013	0.13	28
Nsanje	Ns	Shire	Lower Zambezi	35.27	-16.95	01/01/1998	31/12/2013	3.49	39
Makhanga	Mk	Shire	Lower Zambezi	35.15	-16.52	01/01/1998	31/12/2013	9.43	48
Nchalo	Nc	Shire	Lower Zambezi	34.93	-16.23	01/01/1998	31/12/2013	0.60	64
Ngabu	Ng	Shire	Lower Zambezi	34.95	-16.50	01/01/1998	3112/2010	0.74	89
Chikwawa	Chk	Shire	Lower Zambezi	34.78	-16.03	01/01/1998	31/12/2010	0.93	107

Tete	Te	Tete	Lower Zambezi	33.58	-16.18	29/05/2007	31/12/2013	0.17	151
Chingodzi	Chg	Shire	Lower Zambezi	34.63	-16.00	29/05/2007	10/01/2013	11.8	280
Zumbo	Zu	Shire	Lower Zambezi	30.45	-15.62	29/05/2007	12/09/2012	0.16	345
Mushumbi	Msh	Kariba	Middle Zambezi	30.56	-16.15	11/06/2008	11/12/2013	7.47	369
Kanyemba	Kny	Tete	Middle Zambezi	30.42	-15.63	01/01/1998	30/03/2013	5.86	372
Morrumbala	Mor	Zambezi Delta	Lower Zambezi	35.58	-17.35	29/05/2007	10/01/2013	13.3	378
Mágoè	Mag	Tete	Middle Zambezi	31.75	-15.82	01/01/2009	31/12/2013	9.6	427
Muzarabani	Mz	Tete	Middle Zambezi	31.01	-16.39	01/01/1998	31/12/2013	1.14	430
Monkey	Mon	Shire	Lower Zambezi	34.92	-14.08	01/01/1998	30/11/2010	0.00	478
Mangochi	Man	Shire	Lower Zambezi	35.25	-14.47	01/01/1998	31/12/2010	0.02	481
Rukomechi	Rk	Kariba	Middle Zambezi	29.38	-16.13	01/01/1998	31/12/2013	6.40	530
Mutarara	Mut	Shire	Lower Zambezi	33.00	-17.38	29/05/2007	10/01/2013	11.7	548
Mfuwe	Mf	Luangwa	Middle Zambezi	31.93	-13.27	01/01/1998	31/12/2010	2.70	567
Mimosa	Mim	Shire	Lower Zambezi	35.62	-16.07	01/01/1998	31/12/2010	3.96	616
Kariba	Kar	Kariba	Middle Zambezi	28.80	-16.52	01/01/1998	31/12/2013	0.01	618
Balaka	Bal	Shire	Lower Zambezi	34.97	-14.98	01/01/1998	30/04/2010	0.78	618
Thyolo	Thy	Shire	Lower Zambezi	35.13	-16.13	01/01/1998	31/12/2010	0.11	624
Chileka	Chil	Shire	Lower Zambezi	34.97	-15.67	01/01/1998	31/12/2013	0.60	744
Fingoe	Fin	Tete	Middle Zambezi	31.88	-15.17	01/01/2009	31/12/2013	5.9	881
Muze	Mze	Tete	Zambezi	31.38	-14.95	01/01/2009	31/12/2013	8.8	888
Neno	Nen	Shire	Lower Zambezi	34.65	-15.40	01/01/1998	01/01/2010	9.14	903
Zámbue	Zau	Tete	Middle Zambezi	30.80	-15.11	01/01/2009	31/12/2013	9.8	950
Mt Darwin	MtD	Tete	Middle Zambezi	31.58	-16.78	01/01/1998	02/03/2008	5.00	962
Chipata	Chip	Shire	Lower Zambezi	32.58	-13.55	01/01/1998	13/08/2003	1.11	995

Makoka	Mak	Shire	Lower Zambezi	35.18	-15.53	01/01/1998	31/12/2010	0.00	996
Livingstone	Liv	Kariba	Middle Zambezi	25.82	-17.82	01/01/1998	31/12/2013	0.00	996
Senanga	Sen	Barotse	Upper Zambezi	23.27	-16.10	01/01/1998	31/12/2013	8.90	1001
Petauke	Pet	Luangwa	Middle Zambezi	31.28	-14.25	01/02/1998	31/12/2013	0.40	1006
Msekera	Msk	Luangwa	Middle Zambezi	32.57	-13.65	01/03/1998	31/12/2015	19.7	1028
Kalabo	Kal	Lungue Bungo	Upper Zambezi	22.70	-14.85	01/01/1998	31/12/2011	5.20	1033
Mongu	Mong	Barotse	Upper Zambezi	23.15	-15.25	01/01/1998	31/12/2013	0.51	1052
Kasungu	Kas	Shire	Lower Zambezi	33.47	-13.02	01/01/2003	31/07/2013	0.00	1063
Victoria Falls	VF	Kariba	Middle Zambezi	25.85	-18.10	01/01/1998	31/12/2013	2.26	1065
Bolero	Bol	Luangwa	Middle Zambezi	33.78	-11.02	01/01/2003	31/05/2013	0.00	1070
Pandamatenga	Pan	Kariba	Middle Zambezi	25.63	-18.53	01/01/1998	31/12/2013	0.01	1071
Zambezi	Za	Lungue Bungo	Upper Zambezi	23.12	-13.53	01/01/1998	31/12/2013	1.60	1075
Kabompo	Kap	Kabombo	Upper Zambezi	24.20	-13.60	01/01/1998	30/04/2005	0.08	1086
Chichiri	Chic	Shire	Lower Zambezi	35.05	-15.78	01/01/1998	31/12/2010	0.00	1136
Chitedze	Chtd	Shire	Lower Zambezi	33.63	-13.97	01/01/2003	30/04/2013	0.00	1150
Lundazi	Lu	Luangwa	Middle Zambezi	33.20	-12.28	01/01/2003	30/04/2013	1.40	1151
Guruve	Gur	Tete	Middle Zambezi	30.70	-16.65	01/01/1998	30/03/2013	0.02	1159
Kaoma	Kao	Barotse	Upper Zambezi	24.80	-14.80	01/01/1998	31/11/2013	9.89	1162
Bvumbwe	Bv	Shire	Lower Zambezi	35.07	-15.92	01/01/1998	01/01/2011	0.00	1172
Kasempa	Kas	Kafue	Middle Zambezi	25.85	-13.53	01/01/1998	31/12/2013	9.10	1185
Kabwe	Kab	Luangwa	Middle Zambezi	28.47	-14.45	01/01/1998	13/10/2012	1.54	1209
Chitipa	Chit	Shire	Lower Zambezi	33.27	-9.70	01/01/2003	06/01/2013	0.05	1288
Mwinilunga	Mwi	Kabompo	Upper Zambezi	24.43	-11.75	01/01/1998	31/12/2013	4.81	1319
Karoi	Kar	Tete	Middle Zambezi	29.62	-16.83	01/01/1998	31/12/2004	15.08	1345

Solwezi	Sol	Kafue	Middle Zambezi	26.38	-12.18	01/01/1998	31/12/2013	0.02	1372
Harare (Belvedere)	HB	Tete	Middle Zambezi	31.02	-17.83	01/01/1998	31/03/2013	7.80	1472
Harare (Kutsaga)	HK	Tete	Middle Zambezi	31.13	-17.92	01/01/2004	30/09/2010	0.55	1488
Mvurwi	Mv	Tete	Middle Zambezi	30.85	-17.03	01/01/1998	11/12/2000	0.00	1494
Dedza	Ded	Shire	Lower Zambezi	34.25	-14.32	01/01/2003	31/10/2012	0.00	1575

Table 2.2: Topographic zones influenced by correlation between the satellite and gauge-based estimates as well as average distance from moisture sources.

Topographic zone (m)	**Average distance from moisture source (km)**	**Station membership**
< 250 (Zone 1)	68	Marromeu, Caia, Nsanje, Makhanga, Nchalo, Ngabu, Chikwawa, Tete, Tete (Chingodzi)
250- 950 (Zone 2)	45	Zumbo, Mushumbi, Kanyemba, Morrumbula, Mágoè, Muzarabani, Monkey, Mangochi, Rukomechi, Mutarara, Mfuwe, Mimosa, Balaka, Thyolo, Chileka
> 950 (Zone 3)	88	Fingoe, Muze, Neno, Zâmbue, Mt Darwin, Chipata, Makoka, Livingstone, Senanga, Petauke, Msekekera, Kalabo, Mongu, Kasungu, Victoria Falls, Bolero, Pandamatenga, Zambezi, Kabompo, Chichiri, Chitedze, Lundazi, Guruve, Kaoma, Bvumbwe, Kasempa, Kabwe, Chitipa, Mwinilungu, Karoi, Solwezi, Harare (Belvedere), Harare (Kutsaga), Mvurwi, Dedza, Morrumbala

2.3. Satellite derived data

2.3.1. CMORPH satellite rainfall

Time series (1998-2013) of CMORPH rainfall product (CMORPH version 0.x) at 8 km × 8 km, 30-minute resolution were selected. Selection of CMORPH satellite rainfall for this study is based on successful applications of bias corrected CMORPH estimates in African basins for hydrological modelling (Habib et al., 2014) and flood predictions in West Africa (Thiemig *et al.*, 2013). CMORPH has been operational since 1998 and data are available at the CPC of the National Centers for Environmental Prediction (NCEP) (http://www.ncep.noaa.gov/). Data for the period 1998-2013 was downloaded via the GeoNETCAST's ISOD toolbox which is available through the ILWIS GIS software (http://52north.org/downloads/). The rainfall is aggregated to 1-day totals to be consistent with rainfall station estimates at daily time interval. For descriptions on algorithms that are used to retrieve rainfall estimates from satellite observations, reference is made to Cohen Liechti *et al.* (2012). A detailed description on the CMORPH estimation algorithm is presented by Joyce *et al.* (2004) and to Jiang *et al.* (2016). For recent applications of CMORPH, the study refers to (Li, Yang and Hong, 2013; Habib *et al.*, 2014; Yang and Luo, 2014; Koutsouris, Chen and Lyon, 2016; Wehbe *et al.*, 2017).

2.3.2. Digital Elevation Model (DEM)

The Shuttle Radar Terrain Mission (SRTM) DEM based 30 m × 30 m DEM obtained from https://earthexplorer.usgs.gov/, was used to retrieve elevation values across the Zambezi domain, to delineate the sub-basin boundaries and to extract the major river drainage network of the study area. The DEM was further used to extract catchment attributes such as flow direction, drainage network, longest flow paths and catchment geometry.

2.3.3. Landuse and soils

Landuse and landcover information was obtained from Landsat satellites. Landsat 8 images (30 m resolution; path 174-175 and row 68-70) were downloaded from the United States Geological Survey (USGS) Global Visualization Viewer (GLOVIS) for the year 2016. Soil data were obtained from FAO soil database via http://www.waterbase.org/download_data.html. All the datasets were processed in ILWIS open-source GIS software (*https://52north.org/software/software-projects/ilwis).*

Chapter 3: The REW model

3.1. Modelling approach

The Representative Elementary Watershed (REW) rainfall-runoff model was used to perform the rainfall-runoff analysis for the Kabompo Basin using rainfall estimates with gauge-based estimates, uncorrected CMORPH estimates and bias corrected rainfall estimates. The model proposed by Reggiani *et al.* (1998) is a complex hydrological simulation tool, which is designed and developed for the simulation of the hydrological cycle of a watershed system, underlain by a regional aquifer, which extends beyond the topographic boundaries of the watershed. The modelling tool can be used for a series of hydrological studies, which look at different components of the hydrological cycle and processes that play a role at different time scales (Reggiani and Rientjes, 2005; Reggiani and Schellekens, 2003). For example, it can be used for event-based studies, such as the response of a watershed to an extreme hydrological event, or the behavior of the hydrological system under forcing conditions that are changing over longer time periods. Examples of possible applications are i) water balance assessments, ii) rainfall-runoff simulation (Reggiani and Rientjes, 2005), iii) groundwater recharge estimates (Zhang and Savenije, 2005; Reggiani and Rientjes, 2010), iv) hydrological impact assessments by climate and/or land use changes (Reggiani and Hassanizadeh, 2016).

In the REW model a watershed is partitioned into a series of discrete spatial units called Representative Elementary Watersheds (REWs) (Reggiani et al., 1998). REWs are identified by performing an analysis of the watershed topography and constitute a set of the interconnected elements that are organized around a tree-like structure of the stream channel network (Figure 3.1).

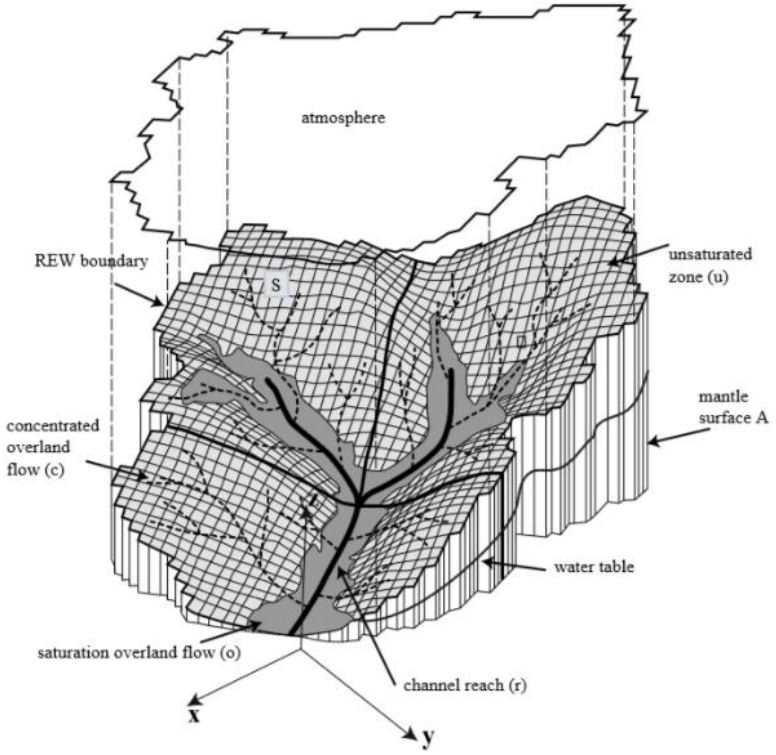

Figure 3.1: A REW as a 3-D spatial entity (Reggiani and Rientjes, 2005)

The volume occupied by a REW contains typical flow zones encountered in a watershed (Figure 3.2). Reggiani and Rientjes (2005) note that the following zones (sub regions) can be modeled explicitly and for every REW: the unsaturated zone flow (u-zone), saturated zone flow (s-zone), saturation overland flow (o-zone), concentrated overland flow, also known as Hortonian overland flow (c-zone) and channel zone (r-zone). The flow within the various domains extends over very different temporal scales, encompasses flow phenomena, such as unsaturated and saturated porous media flow (subsurface zones) as well as overland, and channel flow (land surface zones).

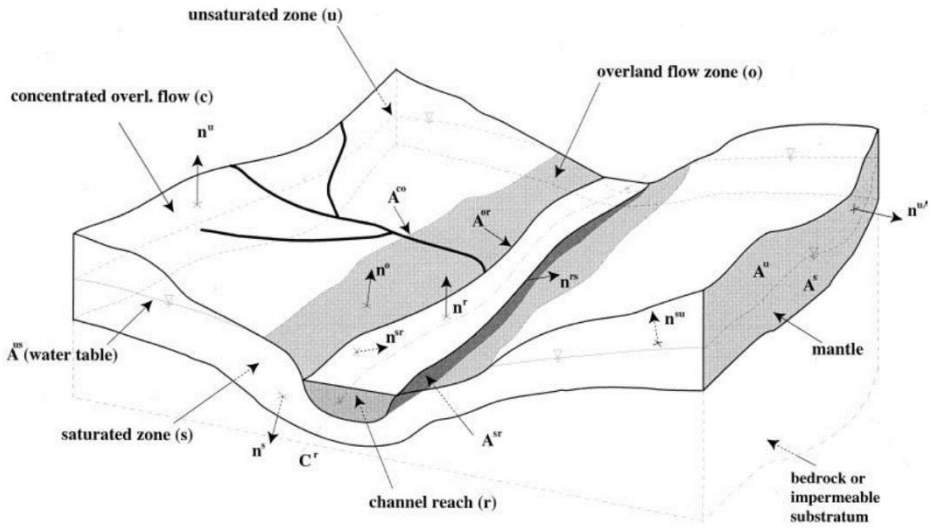

Figure 3.2.: Detailed view of the five sub-regions forming a REW (Reggiani et al., 1998). The actual flow within each element and zone (Qout) is assumed to be governed by the kinematic wave equation, which is obtained by combining the mass and momentum balance equation under the assumption of local steady-state. Detailed governing equations are shown in Reggiani et al. (2014).

The sub regions are chosen on the strength of previous field evidence about different processes that operate within catchments and subject to their flow geometries and time scales. For each of these sub regions, all associated variables and properties are spatially lumped quantities, and can vary only in time (Reggiani *et al.,* 2014).

The unsaturated and saturated zones form the subsurface regions of the REW, where the soil matrix coexists with water (and the gas phase in case of the unsaturated zone). The concentrated overland flow sub region includes: surface flow within rills, gullies and small channels, and the regions affected by Hortonian overland flow (Reggiani and Rientjes, 2005). The saturated overland flow sub region comprises the seepage faces, where the water table intersects the land surface and makes up the saturated portion of the REW land surface. REWs constitute 3D regions, with a vertical prismatic mantle surface defined by the REW boundaries (Figure 3.1). The REW boundaries coincide with the topographic divides (Zhang *et al.,* 2006). They delineate a well-defined area of the land surface that captures the precipitation. The contour of a REW mantle

surface coincides with the shape of the ridges defining a sub-basin. A schematic representation of a REW element is depicted in Figure 3.3.

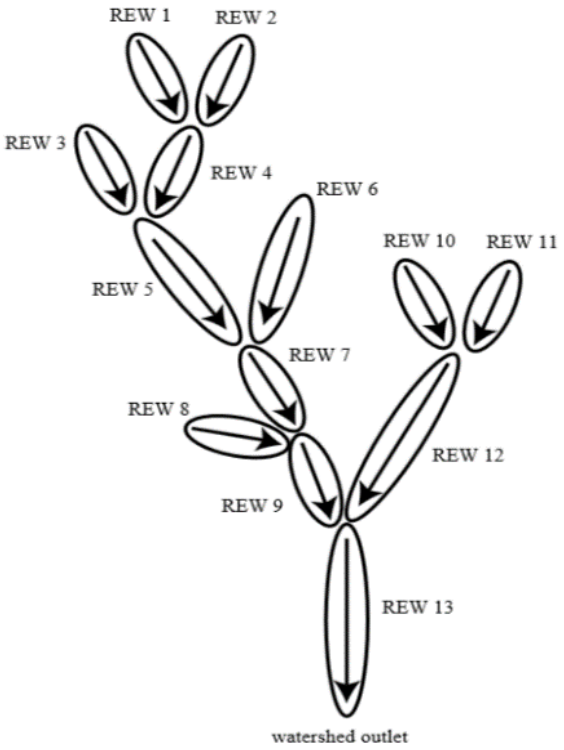

Figure 3.3: Organization of REWs around the structure of the network (Reggiani et al., 1999; Reggiani and Rientjes, 2005)

Reggiani *et al.* (1999) noted that a REW is delimited by the atmosphere at the top and by an impermeable layer at the bottom. The impermeable layer can be either defined by a horizontal surface or can be given by interpolation of bedrock depth for a series of irregular points. In order to account for hydrological variability within a REW with characteristics smaller than the REW, e.g., attributable to factors as landuse or soil properties, the unsaturated zone is subdivided into smaller units, or columns, labelled Representative Elementary Columns (RECs). These RECs are defined by overlapping a series of GIS maps such as landuse and soil type (Reggiani and Hassanizadeh, 2016). The procedure of subdividing the unsaturated zone allows attributing different soil properties and evapotranspiration rate depending on plant species to each smaller unit.

In the context of the REW approach, balance laws for mass, momentum, and energy are mapped from the microscale or point scale to the mega scale (or REW scale) by integration in space (Reggiani and Rientjes, 2005). Balance equations of mass and momentum are derived for each zone of each REW and they are directly applied to the sub-catchment scale. For the closure of the balance equations, watershed-scale hydrologic relations such as Darcy's law, Chezy's formula, and the Saint Venant equation, etc. are needed although some particular methods such as Hardy-Cross procedure for looping the REWs as a network (Reggiani and Rientjes, 2010), groundwater table interpolation is applied. The resulting conservation equations constitute a system of coupled Ordinary Differential Equations (ODE) leading to a simplification of the mathematical model (Zhang *et al.*, 2006). Those relations are also developed directly at the REW scale and are applied to the specific zones. Detailed descriptions of mass balance equations (Table 3.1) and the momentum equations (Table 3.2) are summarized (Reggiani and Rientjes, 2005).

Table 3.1. Mass Balance Equations

Zone	Mass Balance Equations
Unsaturated zone	$\Sigma\ \epsilon \frac{d}{dt}(s^u y^u \omega^u) = e^{us} + e^{u\ top} + e^{u}_{wg}$
Saturated zone	$\Sigma\ \epsilon \frac{d}{dt}(y^s \omega^s) = \sum_{i=1,N} e^{sm\ i} + e^{su} + e^{so} + e^{sr}$
Channel reach	$l^r \frac{d}{dt}(m^r) = e^{ro} + e^{rs} + e^{r\ in} + e^{r\ out}$
Overland flow	$\Sigma \frac{d}{dt}(y^o \omega^o) = e^{os} + e^{or} + e^{o\ top}$

Table 3.2. Momentum Balance Equations

Zone	Momentum Balance Equations
Unsaturated zone	$\Sigma\ \epsilon\ s^u y^u \omega^u \frac{d}{dt}\mathbf{v}^u - \Sigma\ \mathbf{g}\ \epsilon\ s^u y^u \omega^u = \sum_{i=1,N} \mathbf{T}^{um\ i} + \mathbf{T}^{us} + \mathbf{T}^{u\ top} + \mathbf{T}^{u}_{wg} + \mathbf{T}^{u}_{wm}$
Saturated zone	$\Sigma\ \epsilon\ y^s \omega^s \frac{d}{dt}\mathbf{v}^s - \Sigma\ \mathbf{g}\ \epsilon\ y^s \omega^s = \sum_{i=1,N} \mathbf{T}^{sm\ i} + \mathbf{T}^{s\ bot} + \mathbf{T}^{so} + \mathbf{T}^{sr} + \mathbf{T}^{su} + \mathbf{T}^{s}_{wm}$
Channel reach	$l^r\ m^r \frac{d}{dt}\mathbf{v}^r = \mathbf{g}\ m^r l^r + \mathbf{T}^{rs} + \mathbf{T}^{r\ out} + \mathbf{T}^{r\ in}$
Overland flow	$\Sigma\ \omega^o y^o \frac{d}{dt}\mathbf{v}^o = \Sigma\ \mathbf{g}\ \omega^o y^o + \mathbf{T}^{os} + \mathbf{T}^{or}$

3.2. Model Setup

The Kabompo Basin was discretized into a number of sub-watersheds (catchments) through a specific DEM technique using TAUDEM software (Saber and Yilmaz, 2016; Tarboton, 1997). The choice to use TAUDEM for digital terrain preprocessing was made because of the availability of open-source code.

NASA's Shuttle Radar Topography Mission (SRTM) Digital Elevation Model (DEM) at 30 m resolution (https://earthexplorer.usgs.gov/) was processed to extract the channel network by performing flow accumulation analysis. TAUDEM flags the DEM pixels belonging to the different drainage areas contributing to the individual network links. Once the network and the sub-basins are identified, 3-D REW volumes are extracted. This operation entails the calculation of the REW mantle surface areas, effective slopes and aspects. For this scope, the module REWANALYSIS has been developed. REWANALYSIS identifies neighboring REWs and respective lateral connectivity based on nearest neighbor analysis for individual pixels (Elgamal *et al.*, 2017). The contour curves separating two neighboring sub-basins are calculated, including their projections onto the x and y axes of the coordinate system. These curves are defined by the edgy line marking the separation curve between two pixels belonging to two separate but adjacent drainage areas or sub-basins (flagged by the TAUDEM algorithm). This makes it possible to establish lateral connectivity between REWs and the definition of the groundwater network topology in an automated fashion (see Reggiani and Rientjes, 2010). In this study, the Strahler order 1 was selected as threshold value, yielding 29 REWs of different size. Channel flow is routed using the mass-conservative Muskingum-Cunge-Todini approach (Reggiani *et al*., 2014). The Landsat 8 images (30 m resolution) over Kabompo Basin were classified into 5 classes (crops, forest, grass, open-water and urban areas) based on supervised classification using the Maximum Likelihood Classifier. Validation and accuracy assessment is by means of a confusion matrix (Foody, 2002). Different land-use types were the basis of partitioning of each REW in smaller REW Elements, this following (Elgamal *et al.*, 2017).

After assigning model parameter values, the required flux/no-flux boundary conditions and initial conditions were imposed following Reggiani et al. (1998). Initialization was for the end of the dry season that required a minimum base flow in the channel network, a minimum water content for the unsaturated zone, and hydraulic state values of the water table. The latter one is obtained by interpolating piezometric levels from a piezometer monitoring network via 2-D cubic spline functions to average water levels at the REW centroids (Reggiani and Rientjes, 2005). The bedrock elevations forming the lower aquifer boundary are assigned following a slightly inclined plane by exploiting geological survey data and using spatial interpolation. For the meteorological forcing of the model, daily measurements of rainfall are mapped from the coordinate points of the gauging stations through Kriging to the geometrical centroids of the REWs. A

reference evapotranspiration ET_0 (estimated from temperature, wind speed, solar radiation, net radiation, ground heat flux, and surface and aerodynamic resistance as input), also known as the FAO Penman-Monteith equation (Allen *et al.*, 1998), was derived through the same interpolation procedure. ET_0 only depends on climatic parameters. The computed streamflows are compared with daily values recorded at Watopa gauging station at the outlet.

Chapter 4: Performance evaluation of CMORPH satellite precipitation product in the Zambezi Basin*

4.1. Introduction

Understanding patterns and distributions of rainfall is central in assessing water resources of a catchment (Guo *et al.,* 2015; Meyer *et al.,* 2017; Zulkafli *et al.*, 2014). However, such understanding is often hindered by lack of rainfall stations and well-designed rain gauge networks (Chacon-Hurtado *et al.,* 2017; Nazaripour and Mansouri Daneshvar, 2016). Satellite rainfall estimates (SREs) offer an alternative to rainfall data from meteorological stations. By their coverage over large spatial domains, SREs are suitable for basin-wide applications such as shown by Dembélé and Zwart (2016), Jiang *et al.* (2016) and Meyer *et al.* (2017). In many basins where rainfall stations are absent or only sparsely available, SREs provide alternative and supplementary rainfall data (Haile *et al.*, 2014; Maidment *et al.* 2017). Studies by Maidment *et al.* (2017), Toté *et al.* (2015) and Valdés-Pineda *et al.* (2016) indicate the need for performance assessment of SREs before use. For such assessment, readings from rain gauges serve as ground truth and reference.

Satellite rainfall products such as GOES Precipitation Index (GPI) and the Merged Analysis of Precipitation (CMAP) are provided at relatively low temporal resolution of more than a day and at spatial resolution larger than 0.25^{o} × 0.25^{o}. Nowadays products such as The National Oceanic and Atmospheric Administration (NOAA) Climate Prediction Center-MORPHing (CMORPH) and Tropical Rainfall Measuring Mission (TRMM) are available at 0.1° × 0.1° and half hourly time interval. Such products provide information on rainfall to represent real world spatio–temporal distributions, to observe rainfall rates, and to assess occurrence, also for regions where installation of rain gauge techniques

*__This chapter is based on:__ W. Gumindoga, T.H.M. Rientjes, A.T. Haile, H. Makurira, and P. Reggiani (2019): Performance evaluation of CMORPH satellite precipitation product in the Zambezi Basin, *International Journal of Remote Sensing*, https://doi.org/10.1080/01431161.2019.1602791.

is limited (Awange *et al.* 2016; Koutsouris, Chen, and Lyon 2016; Valdés-Pineda *et al.* 2016).

The performance of SRE products in representing rainfall depths, rates and occurrences at daily and weekly time scales is largely unknown in the vast Zambezi Basin. Therefore, in this chapter, with daily rainfall station data from 66 stations located in the basin, the study seeks to understand the performance of CMORPH satellite-based rainfall estimates for the period 1998-2013. Specific objectives are i) to assess CMORPH rainfall detection capabilities (Probability of Detection, False Alarm Ratio, Critical Success Index and Frequency Bias) at daily and weekly time interval in the Zambezi sub-basins ii) to compare CMORPH estimates against gauge-based estimates for rainfall depth using standard error statistics iii) to evaluate the accuracy of CMORPH rainfall [mm] by assessing Hit bias, False bias and Missed bias.

4.2. Methodology

4.2.1. Comparison of satellite derived rainfall data with rainfall station observations

This study compares rainfall estimates from rainfall stations to CMORPH rainfall estimates at pixel scale following (Heidinger *et al.*, 2012; Li and Heap, 2011; Tobin and Bennett, 2010; Yin *et al.*, 2008). To represent spatial rainfall distributions, gauge estimates at daily interval were spatially interpolated at grid resolution and projection that matches the CMORPH rainfall estimates. For interpolation, the Inverse Distance Weighted interpolation (IDW) method (Parida *et al.* 2017; Shepard 1968) was used, to result in pixel based estimates. Whereas comparisons on a point-to-pixel basis commonly are affected by mismatch of spatial scales of observation as presented by Villarini *et al.* (2008), Haile *et al.* (2013a) and Haile *et al.* (2013b), this aspect is not further assessed.

4.2.2. Evaluation statistics at sub-basin level

By the size of the Zambezi River basin and the poor layout and uneven distribution of the network of rainfall stations, comparison results are best presented at sub-basin level. Therefore, CMORPH estimates are compared to counterparts from spatially interpolated rainfall estimates that are from pixels that overlay a rainfall station. CMORPH performance indicators for respective pixels are then averaged across each of the sub-basins. Assessment of performance of CMORPH for the nine sub-basins is performed using rainfall detection statistics,

standard statistics, and also by decomposing the accumulated error into Hit bias, Missed bias, and False bias for wet and dry seasons. Out of thirteen major sub-basins that make up the Zambezi basin, analysis is for nine sub-basins with at least 2 rainfall stations in a sub-basin.

Rainfall detection

Using 60 rainfall stations in the Zambezi Basin, categorical statistics were used to assess rainfall detection capability (i.e., rain or no-rain) of CMORPH (e.g. Dinku et al., 2010). Rainfall detection is assessed by Probability of Detection *(POD)*, False Alarm Ratio *(FAR)*, Critical Success Index *(CSI)* also known as Threat Score *(TS)* and Frequency Bias *(FBS)*. The rainfall threshold value for SREs used to distinguish rainfall/no-rainfall events was set to 0.5 mm/day (i.e., half of the tipping bucket measurement unit).

These are calculated from equations (4.1-4.4).

$$POD = \frac{hits}{hits+miss} \quad [4.1]$$

$$FAR = \frac{false\ alarm}{hits+false\ alarm} \quad [4.2]$$

$$CSI = \frac{hits}{hits+false\ alarm+miss} \quad [4.3]$$

$$FBS = \frac{hits+false\ alarm}{hits+miss} \quad [4.4]$$

Where *hits* implies that both CMORPH and rainfall stations detect rainfall. *False alarm* implies that rainfall is detected by CMORPH but not by the rain gauge. Miss implies that a rainfall event was not detected although it actually occurred as indicated by the gauge. When *miss* is zero, *POD* shows best value (1). Both *POD* and *FAR* ranges between 0 and 1 (Moazami *et al.* 2014). When both *miss* and *false alarm* are zero then *CSI* and *FBS* have best value (1). Higher values of *CSI* indicate better performance of CMORPH, a score of 0 indicates no skill (Prakash *et al.* 2014). *CSI* is sensitive to *hits* and penalizes for *miss* and *false alarms*. The *FBS* ranges from 0 to infinity with best score 1. All the 4 indices are rescaled in such a way that values (1) and (0) means better and poor performance respectively to maintain consistency in interpretation. SREs are averaged for each sub-basin with the number of rainfall stations indicated where CMORPH has > 50 % detection of rainfall occurrences and rain rates.

Standard statistics and bias

For this study, a comparison of CMORPH estimates with spatially interpolated, gauge based estimates is performed using mean, minimum, maximum, rainfall totals, standard deviation and *Rel. bias (%)* (Haile *et al.*, 2013b). Equations 4.5 and 4.6 apply.

$$Rel.\,bias\ (\%) = \frac{\sum_{i=1}^{n}(S_i - G_i)}{\sum_{i=1}^{n} G_i} \times 100\ \% \qquad [4.5]$$

where:

S_i = *rainfall estimate by satellite (mm/day) at a certain day (i)*

G_i = *rainfall estimate by rain gauge (mm/day) at a certain day (i)*

$$standard\ deviation = \sqrt{\frac{\sum_{i=1}^{n}(P_i - \overline{P})^2}{n-1}} \qquad [4.6]$$

where:

P = *rainfall estimate for CMORPH or gauge (mm/day)*

$\overline{P}$ = *CMORPH or gauge mean rainfall estimate (mm/day)*

n = *number of time steps (days)*

Bias decomposition

Total Bias (defined as *Rel. bias (%)* in equation 4.5) embodies accumulated SRE estimation errors by Hit bias *(HB)*, Missed bias *(MB)* and False bias *(FB)*. Hit bias occurs when rainfall is estimated by both satellite and rain gauge but estimates differ in amount (under or overestimation). Missed bias occurs when there is rainfall recorded by rain gauge but missed by the satellite. False rainfall bias occurs when there is no rainfall indicated by rain gauge although indicated by the satellite (Habib, Larson, and Graschel 2009; Likasa 2013). Using rainfall estimates by the satellite (S_i) and rainfall estimates by the rain gauge (G_i), bias components are mathematically expressed following equations [4.7-4.9]. Hit bias could be positive or negative, Missed and False bias always are negative and positive, respectively. Bias is expressed as a percentage of the gauge rainfall amount (mm/day) to allow direct comparison against biases reported from other stations, basins or regions.

$$HB = \sum_{i=1}^{n}(S_i - G_i)\ (when\ S_i > 0\ and\ G_i > 0) / \sum_{i=1}^{n} G_i \quad X\ 100\ \% \qquad [4.7]$$

$$MB = -\sum_{i=1}^{n} G_i\ (when\ S_i = 0\ and\ G_i > 0) / \sum_{i=1}^{n} G_i \qquad X\ 100\ \% \qquad [4.8]$$

$$FB = \sum_{i=1}^{n} S_i\ (when\ G_i = 0\ and\ S_i > 0) / \sum_{i=1}^{n} G_i \qquad X\ 100\ \% \qquad [4.9]$$

4.2.3. CMORPH performance evaluation according to rainfall rates and seasons

To explore CMORPH performance for different rainfall rates, five arbitrary classes are defined that indicate very light (< 2.5 mm/day), light (2.5-5.0 mm/day), moderate (5.0-10.0 mm/day), heavy (10.0-20.0 mm/day) and very heavy rainfall (> 20 mm/day) respectively. Furthermore, CMORPH rainfall was divided into wet and dry seasons to assess the influence of seasonal variation on rainfall detection and estimation by CMORPH and error decomposition. The wet season in Southern Africa occurs in October-March while the dry season is from April-September.

4.3. Results and Discussion

4.3.1. Rain detection

Rain detection at daily and weekly time interval

Table 4.1 shows CMORPH detection results for daily rainfall by means of Frequency Bias *(FBS)*, Probability of Detection *(POD)*, False Alarm Ratio *(FAR)* and Critical Success Index *(CSI)*. The number of stations in each sub-basin where CMORPH detects > 50 % of the rainfall occurrences is also shown. By *POD* and for the daily time interval, all the stations in Kabompo sub-basin detect > 50 % of the rainfall occurrences as compared to 18 stations for Shire River sub-basin and 5 stations for Luangwa sub-basin. The majority of stations show better detection at weekly interval than at daily interval. For example, all 22 stations in Shire River sub-basin detect > 50 % of rainfall occurrences.

When spatially averaged at sub-basin scale, *POD* for daily and weekly time interval indicates that > 60 % of the rainfall occurrences in 6 sub-basins is detected. Exceptions are for Kariba, Tete and Zambezi Delta sub-basins. The highest *POD* at daily interval is shown for the Kabompo sub-basin (0.9) in the

northern part of the basin, followed by Kafue (0.83) in the central part of the basin. As expected, CMORPH rainfall detection capability at weekly time interval is always higher than at daily time interval. The most significant improvement is for the Shire River sub-basin (daily *POD* = 0.6 and aggregated to a *POD* =1 for weekly timestep).

CSI shows that CMORPH detects > 50 % rainfall occurrences for 11 stations (out of 22) in the Shire River sub-basin at a daily time interval as compared to 18 stations at weekly time interval. At daily time interval, 4 sub-basins have CMORPH detecting 50 % of rainfall occurrences as compared to 8 sub-basins at weekly time interval. For some sub-basins, the actual detection *(CSI)* does not improve at weekly time interval showing that the missed rainfall counter balance the false rainfall. *FAR* close to 1 indicates best performance. For both stations in Kabompo sub-basin for daily and weekly time interval, CMORPH detects > 50 % of rainfall occurrences whereas this is only shown for 6 stations at daily and 8 stations at weekly time interval for Tete sub-basin. *FAR* shows only 3 sub-basins (Barotse, Kafue and Lungue Bungo) with *FAR* < 0.4 compared to 9 sub-basins for weekly estimates. *FAR* suggest lower false hits for weekly time interval as compared to daily time interval. *FBS* of 1 indicates good performance of CMORPH. For Luangwa sub-basin, 4 stations for daily time interval and all 6 stations for the weekly time interval contribute to CMORPH detection of > 50 % of the rainfall occurrence as compared to 1 station and 2 stations in Barotse sub-basin respectively. Best detection using *FBS* is for Kariba, Luangwa and Kabompo sub-basins.

Generally, rainfall detection capability of CMORPH varies from sub-basin to sub-basin and thus shows variation across the Zambezi Basin. This could be affected by the uneven distribution of rainfall stations across the sub-basins. Though in majority of sub-basins CMORPH performance in terms of *FBS, POD, FAR* and *CSI* generally improved from daily to weekly time step, further analysis shows that the change from daily to weekly time-step for each of the 9 sub-basins results in no significant correlation ($p < 0.05$) between integration length and CMORPH-gauge agreement. Studies (Cohen Liechti *et al.* 2012; Habib *et al.* 2012a; Mashingia *et. al*, 2014; Verdin and Klaver 2002) reveal improved CMORPH detection when time interval of analysis increases from daily to weekly, or longer.

Table 4.1. Rain detection (ratio value) of CMORPH by Frequency Bias (FBS), Probability of Detection (POD), False Alarm Ratio (FAR), and Critical Success Index (CSI) at daily and weekly time interval. With the exception of the FAR, the perfect score for each skill score would be 1 while the perfect FAR would be 0. The number of stations out of the total stations in each sub-basin contributing to performance > 50 % is indicated in brackets.

Time interval	Rainfall Detection [ ]	Barotse	Kabompo	Kafue	Kariba	Luangwa	Lungue Bungo	Shire River	Tete	Zambezi Delta
Daily	*FBS*	2.51 *(1/3)*	**0.93** *(2/2)*	2.13 *(1/2)*	4.06 *(4/7)*	3.21 *(4/6)*	2.73 *(2/2)*	1.17 *(15/22)*	-1.32 *(9/13)*	-4.21 *(1/3)*
	POD	0.79 *(3/3)*	**0.90** *(2/2)*	0.83 *(2/2)*	0.40 *(5/7)*	0.59 *(5/6)*	0.74 *(2/2)*	0.60 *(18/22)*	0.36 *(7/13)*	0.34 *(1/3)*
	FAR	0.57 *(2/3)*	**0.75** *(2/2)*	0.63 *(1/2)*	0.22 *(2/7)*	0.47 *4/6)*	0.58 *(2/2)*	0.44 *(10/22)*	0.24 *(6/13)*	0.31 *(1/3)*
	CSI	0.57 *(2/3)*	**0.75** *(2/2)*	0.63 *(2/2)*	0.18 *(3/7)*	0.47 *(4/6)*	0.58 *(2/2)*	0.44 *(11/22)*	0.24 *(5/13)*	0.31 *(1/3)*
Weekly	*FBS*	1.50 *(2/3)*	0.65 *(2/2)*	1.13 *(2/2)*	-1.03 *(6/7)*	**0.97** *(6/6)*	1.21 *(2/2)*	1.09 *(17/22)*	0.61 *(10/13)*	2.54 *(2/3)*
	POD	0.99 *(3/3)*	0.66 *(2/2)*	0.98 *(2/2)*	0.77 *(6/7)*	0.98 *(6/6)*	0.99 *(2/2)*	**1.00** *(22/22)*	0.65 *(11/13)*	0.50 *(2/3)*
	FAR	0.71 *(2/3)*	**0.96** *(2/2)*	0.90 *(2/2)*	0.32 *(4/7)*	0.62 *(4/6)*	0.83 *(2/2)*	0.65 *(16/22)*	0.54 *(9/13)*	0.51 *(2/3)*
	CSI	0.71 *(3/3)*	**0.96** *(2/2)*	0.90 *(2/2)*	0.22 *(4/7)*	0.62 *(5/6)*	0.83 *(2/2)*	0.65 *(18/22)*	0.65 *(9/13)*	0.51 *(2/3)*

Seasonal influences for rain detection

CMORPH rainfall detection in the dry and wet season was assessed. Figure 4.1 shows the daily rain detection of CMORPH by *POD, CSI, FBS* and *FAR* for wet and dry seasons in the Zambezi sub-basins. The miss rate (Missed Bias) is also plotted to help interpret the *FAR*. For the wet season, distinct better detection is indicated than for the dry season. *POD* decreases notably from the wet season to the dry season. CMORPH detects > 60 % of the rainfall occurrences in 8 sub-basins in the wet season whereas it detects < 12 % in all sub-basins in the dry season. For the dry season, 7 sub-basins have FAR > 0.75 whereas this is not

shown for any of the sub-basins in the wet season. The Missed Bias for the wet season consistently corresponds to high *FAR* experienced in the same season.

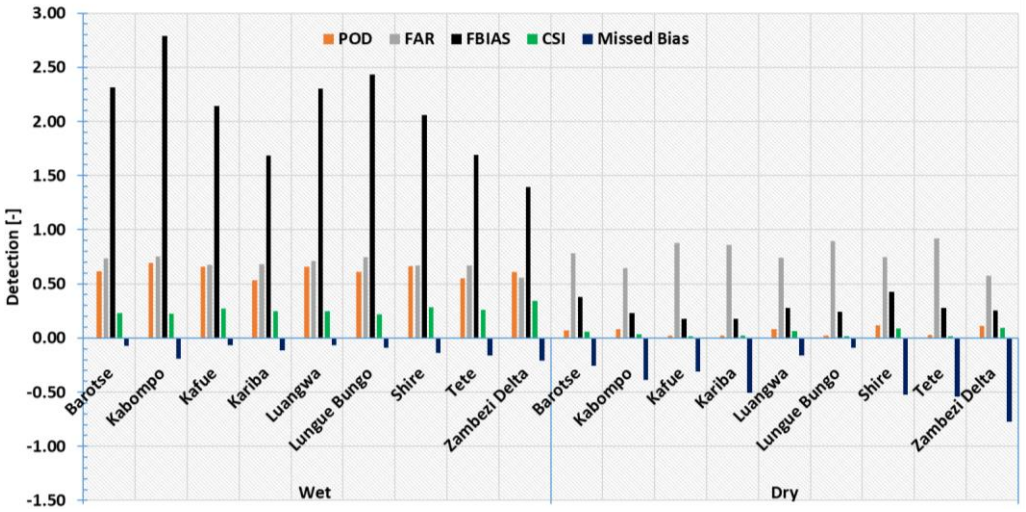

Figure 4.1. Daily rain detection of CMORPH by Probability of Detection (POD), False Alarm Ratio (FAR), Critical Success Index (CSI) and for two distinct seasons in the Zambezi basin. Left side shows CMORPH detection for wet season and the right side for the dry season. The Missed Bias is also plotted for easy interpretation of FAR.

FBS and *CSI* also show better rainfall detection for the wet season than the dry season. All the sub-basins in the wet season have *CSI* > 0.1 with highest values shown for Shire and Kafue sub-basins (*CSI* > 0.26).

Rainfall rates

In this study, estimates of rainfall rates are assessed by *POD, CSI, FAR* and *CSI*. Figure 4.2 shows that *POD* increases at higher rainfall rates, and that *FAR* decreases at higher rainfall rates. Improved *CSI* is shown at higher rainfall rates. Findings indicate that the performance of CMORPH improves at higher rainfall rates. About 70 % of the rainfall rates higher than 20 mm/day are detected by CMORPH in all the sub-basins except for the Zambezi Delta. This indicates much better detection than the 0-2.5 mm/day rate where < 37 % rainfall rate estimates are detected. There is improved *FBS* for very light rainfall (< 2.5 mm/day). *FBS* improves from medium (5-10 mm/day) to heavy rainfall (> 20 mm/day).

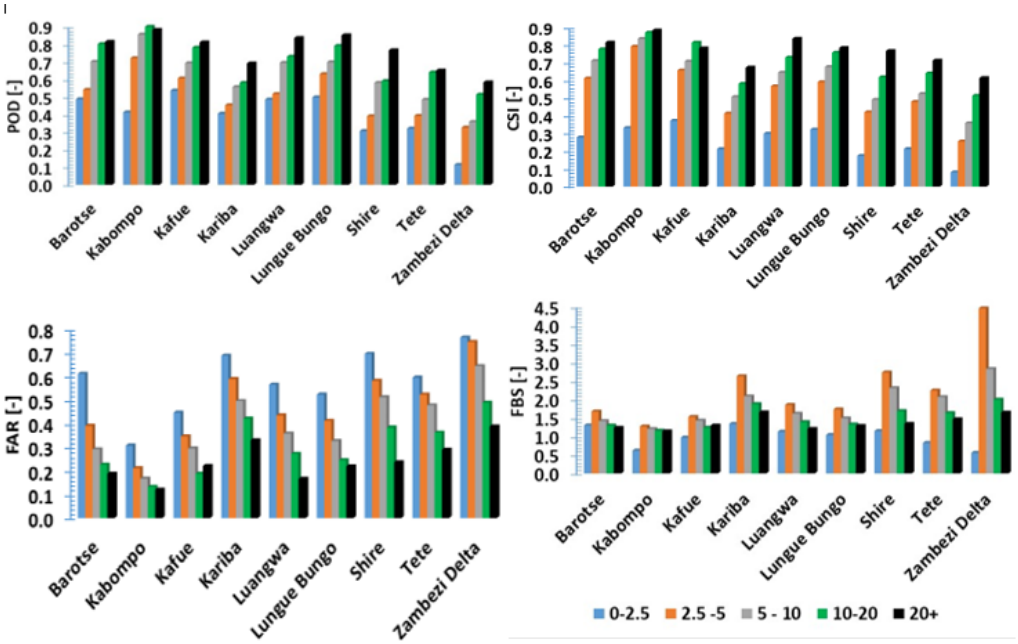

Figure 4.2: Detection capability for different rainfall rates: upper left panel= POD, upper right= CSI, lower left=FAR, Lower right=FBS

4.3.2. Standard error statistics and bias

Table 4.2 shows standard statistics for CMORPH and rain gauge estimates for the nine sub-basins. In general, both sources at daily time interval show large differences in terms of mean, maximum, standard deviation and rainfall totals for the 1998-2013 period. CMORPH underestimates and sometimes overestimates the gauge estimates (Table 4.2). For example, the 15-year period CMORPH total for Tete sub-basin in the South-eastern part of the basin is 8497 mm which is close to the actual rain gauge total of 8438 mm. CMORPH shows lower standard deviation (St. dev) compared to gauge-based estimates in all the nine sub-basins. An almost perfect match of St. dev for CMORPH and gauge is shown for Luangwa sub-basin (St. dev. of 8.3 mm/day and 8.6 mm/day for CMORPH and rain gauge respectively). CMORPH underestimates maximum rainfall in majority of the sub-basins whereas slight overestimation is shown for Kabompo, Kariba and Luangwa sub-basins.

Table 4.2: Standard statistics and Rel. bias (%) for the CMORPH and gauge daily estimates (1998-2013): Bold figures = overestimation by CMORPH.

Sub-basin	**Rainfall Estimate**	**Mean (mm/day)**	**St dev (mm/day)**	**Maximum (mm/day)**	**Rainfall total (mm)**	***Rel. bias (%)***
Barotse	CMORPH	2.0	6.1	93.7	9716.2	
	Gauge	2.3	7.7	127.0	11526.4	-2.1
Kabompo	CMORPH	2.5	6.9	**111.3**	10121.3	
	Gauge	3.2	8.1	101.4	13388.2	-22.8
Kafue	CMORPH	2.3	6.3	82.5	11993.8	
	Gauge	2.9	8.4	112.1	15012.6	-15.8
Kariba	CMORPH	1.5	6.2	**100.4**	6604.0	
	Gauge	1.7	6.7	98.4	8064.8	**23.8**
Luangwa	CMORPH	**2.9**	8.3	**107.7**	**13325.6**	
	Gauge	2.7	8.6	105.5	12230.8	-4.2
Lungue Bungo	CMORPH	2.3	6.9	125.2	12104.5	
	Gauge	2.7	8.8	146.2	14340.5	-9.0
Shire	CMORPH	2.4	7.5	112.0	**10303.7**	
	Gauge	2.6	9.0	143.9	11685.5	3.0
Tete	CMORPH	2.4	7.8	116.5	**8496.8**	
	Gauge	2.5	8.2	114.4	8437.8	4.7
Zambezi Delta	CMORPH	2.4	8.7	119.5	5418.5	
	Gauge	2.9	11.1	143.7	6549.8	-1.6
Entire basin	CMORPH	2.3	7.4	108.8	9350.3	
	Gauge	2.6	8.8	123.6	10778.6	-2.6

Table 4.2 also show that the northern sub-basins such as Kabompo and Barotse have underestimation of rainfall. The same can be said of the Zambezi Delta where the Zambezi River enters the Indian Ocean in Mozambique as well

as the western sub-basins such as Lungue Bungo. The study by Thiemig *et al.* (2012) however shows significant overestimation of CMORPH rainfall in the western part of the basin. Large *Rel. bias (%)* values are identified for southern sub-basins such as Kariba (23.8 %) which shows significant overestimation of rainfall. CMORPH also shows relatively high overestimations of rainfall in Luangwa and Shire River sub-basins.

The basin average statistics are also shown in Table 4.2, with a gauge mean value of 2.6 mm/day compared to a CMORPH underestimation value of -2.3 mm/day. The maximum and the rainfall totals also show underestimation by CMORPH. A *Rel. bias (%)* value of -2.6 % for the full basin indicates a slight underestimation, but it is still encouraging when compared to an underestimation value of 22.8 % in the Kabompo sub-basin.

4.3.3. CMORPH bias decomposition

Bias decomposition at daily and weekly time interval

Table 4.3 shows the CMORPH biases (Hit, Missed and False bias) for the daily and weekly time interval. All the sub-basins have negative Missed bias and positive False bias values. Hit bias values for the daily time interval vary from 9 % (Luangwa) to 32 % (Kafue) which is a wider range compared to the bias values for weekly time interval which ranges from -11 % (Kariba) to 19 % (Shire River). Fair agreement between CMORPH and rain gauge data is mainly at weekly time interval.

Table 4.3. Decomposition of CMORPH bias at daily time interval into its three components: Hit bias, Missed bias and False bias at daily and weekly time interval. Bold=best performance.

Time interval	Rainfall bias (%)	Barotse	Kabompo	Kafue	Kariba	Luangwa	Lungue Bungo	Shire River	Tete	Zambezi Delta
Daily	Hit	26.8	8.8	31.6	11.0	**8.6**	25.2	24.7	11.5	17.9
	Missed	-7.6	-23.1	-7.2	-16.1	**-6.9**	-9.2	-16.8	-19.0	-33.0
	False	21.0	**8.8**	19.2	54.1	24.3	18.6	31.9	36.6	38.1
	Hit	16.7	12.2	21.6	-11.3	**-6.0**	18.9	19.2	-3.3	9.3

Weekly	Missed	**-0.2**	-10.0	-0.4	-4.9	-0.6	**-0.2**	-2.6	-4.6	-15.5
	False	5.7	1.4	2.4	18.9	3.8	3.8	9.4	7.7	12.4

The poorest performance by means of Missed bias is -33 % and -16 % for the daily and weekly time interval respectively, all for the Zambezi Delta sub-basin. Excellent performance is shown for Barotse, Kafue and Lungue Bongo sub-basins where the Missed bias for the weekly time interval is -0.2 %. The highest False bias is 54 % (Kariba) as compared to the lowest (1 %) for Kabompo sub-basin. It can be noted that the main component contributing to bias is the one with high magnitude but that Missed and False biases have opposite signs and thus counteract (Haile *et al.*, 2013b). The sign of the Hit bias is determined by the magnitudes of satellite rain and gauged rain amounts. It is also noted that the number of rainfall stations in each sub-basin vary from minimum of 2 and maximum of 22 and thus affecting the results of performance that is at sub-basin scale. Even with reduced temporal resolution (from daily to weekly) bias decomposition components in some cases are still high. Future studies should also aim at analysis on shorter time interval such as the hourly or sub-daily time intervals.

Seasonal influences on bias decomposition

The study assessed seasonal influences on bias decomposition. Figure 4.3. presents bias decomposition factors (computed daily over Zambezi sub-basins) between CMORPH and rain gauge estimates for the wet and dry seasons. Results show that bias decomposition terms for the dry season are higher than the wet season. For example, from wet season to dry season, Hit bias decreases and the magnitude of False and Missed bias increases. There is significant underestimation for the dry season for Kariba, Tete and Zambezi Delta. Bias decomposition terms vary for the two distinct seasons but also from sub-basin to sub-basin.

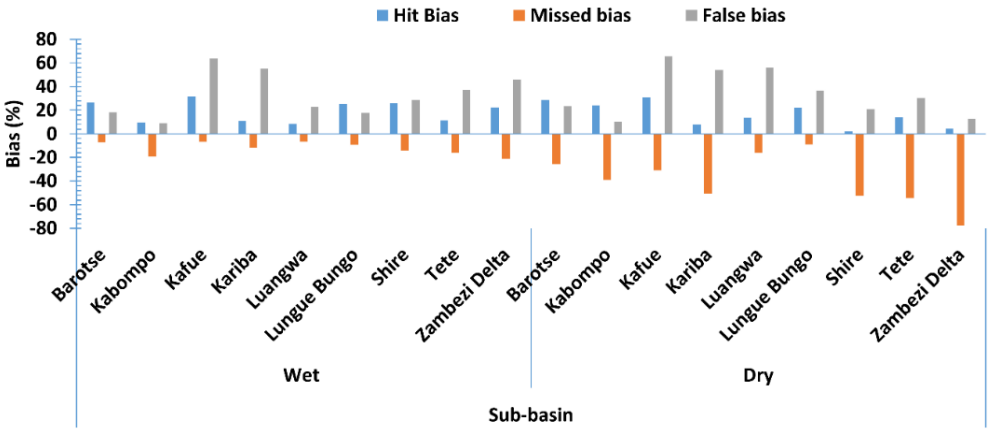

Figure 4.3. Bias decomposition at daily time interval for wet and dry seasons.

Bias decomposition for different rainfall rates

Figure 4.4. shows bias decomposition for selected rainfall rate classes. Results show that there is no consistent pattern of CMORPH performance for the different rainfall rates. Ringard *et al.* (2015) in the Guiana Shield found that CMORPH performance decreases for highest rainfall rates. However, Jamandre and Narisma (2013) found that SREs (TRMM) in the Philippines have better estimates for rainfall with rate > 50 mm/day. Results also show that for all sub-basins (except for Zambezi Delta and Shire River sub-basins), the Hit bias is highest for very heavy rainfall (> 20 mm/day) and is lowest for very light rainfall (0-2.5 mm/day). Missed bias (always negative) increases in terms of magnitude from very light rainfall to heavy rainfall. An example is shown for Tete sub-basin where Missed bias changes from -49 % to -85 %. Findings on False bias in this study also reveal poor performance for very heavy rainfall for the majority of the sub-basins.

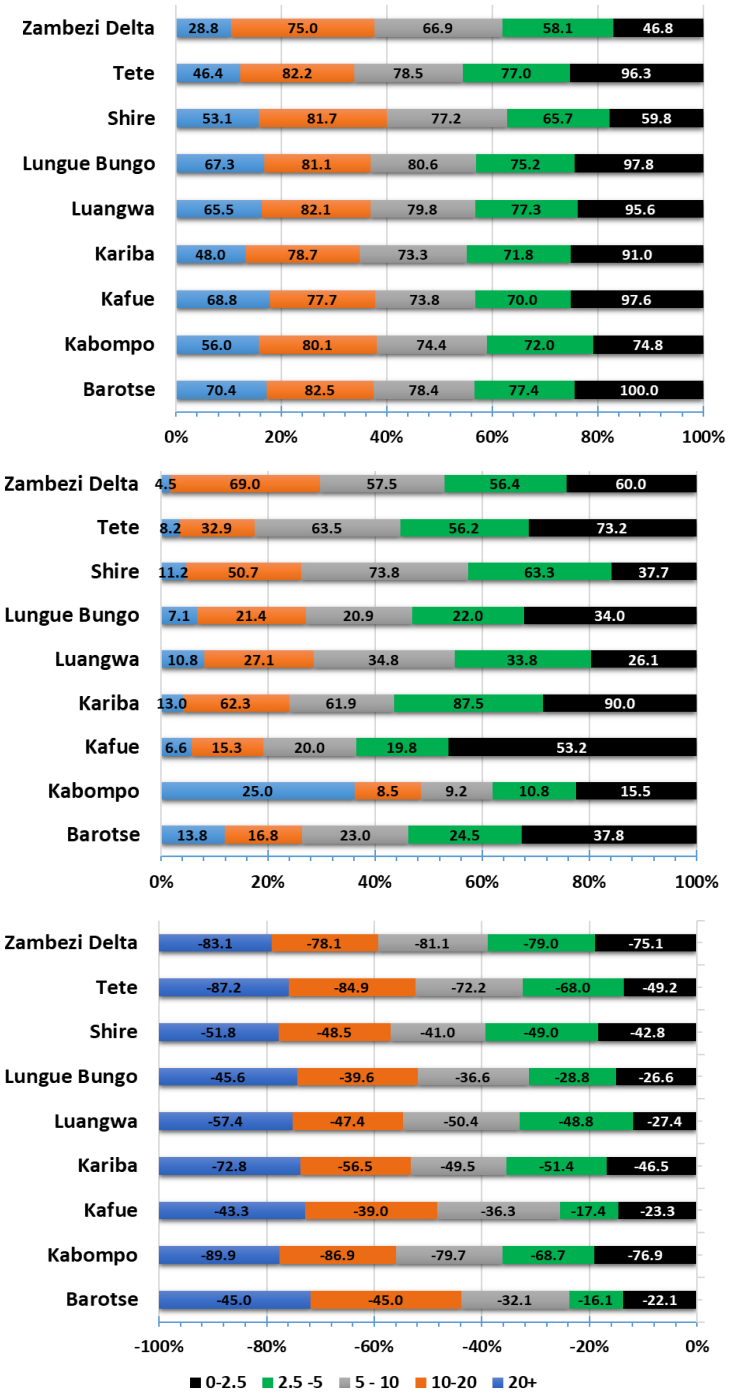

Figure 4.4: Bias decomposition (%) for different rainfall rates (mm/day) at daily time interval: upper panel= Hit bias, middle= Missed bias, lower =False Bias

4.4. Conclusions

Time series data of only 60 meteorological stations were available for the vast Zambezi River basin that must be considered as a poorly gauged basin. Despite the very low network density, results presented in this study are perceptive since findings underline the importance to assess satellite rainfall data before data can be used in water resources applications. Five conclusions are:

i. Using *POD, FAR, CSI* and *FBS* rainfall detection statistics shows that the probability of rainfall detection by CMORPH for both daily and weekly time interval in the Zambezi Basin in general is satisfactory. CMORPH correctly detects 50 % of the rainfall events in most sub-basins which is considered satisfactory following (Gao and Liu, 2013; Katiraie-Boroujerdy *et al.*, 2013; Tobin and Bennett, 2010). Rainfall detection is highest in the Kabompo sub-basin where rain gauged network has highest density, and poorest in the Zambezi Delta sub-basin where network is very low. This study shows that satellite rainfall detection for the Zambezi Basin is better for the wet season than for the dry season.

ii. CMORPH performance assessment for rainfall depth show large differences in terms of mean, maximum, standard deviation, rainfall totals and *Rel. bias (%)* for the 1998-2013 period. CMORPH underestimates or overestimates respective gauge measurements for single sub-basins by up to 24 %. Overall findings show that *Rel. bias (%)* of CMORPH estimates by considering all stations is larger than 25 %. As such the study concludes that direct application of the CMORPH product in Zambezi basin is not possible and bias correction is advocated.

iii. Total bias decomposition into Hit, Missed and False biases reveals that all three components contribute to large spatial and temporal variations of bias in the Zambezi sub-basins. The sensor type and retrieval algorithm may play a key role on the magnitude of False bias in CMORPH rainfall which has been noted by Gebregiorgis and Hossain (2013). Bias decomposition of CMORPH suggest better performance of CMORPH in the wet season and no optimal observed pattern for the different rainfall rates.

iv. The time interval has an important influence on CMORPH performance, such accords to other studies in the basin (Cohen Liechti *et al.*, 2012; Mashingia

et al., 2014). At a daily time interval, there is poor detection of rainfall events whereas accumulation to weekly interval show improved performance of the CMORPH products. This probably results from positive and negative errors that may counter effect, and that are more pronounced at weekly interval. However, it should be noted that the rainfall threshold was not changed when daily data was aggregated to weekly data. For instance, the 0.5 mm/day used can be hydrological significant but 0.5 mm/week is not considered hydrological significant.

v. CMORPH performed well in capturing rainfall rates. At higher rainfall rates detection increases. CMORPH rainfall detection capability is better in the wet season than the dry season (20 % improvement). Findings provide meaningful information on the ability of CMORPH to successfully reproduce observed measurements at particular periods throughout the year, and performance in different seasons.

vi. Overall, the study shows that CMORPH bias is too high to ignore bias correction before SREs can be applied for water resources management.

Chapter 5: Performance of bias correction schemes for CMORPH rainfall estimates in the Zambezi River Basin*

5.1 Introduction

Correction schemes for rainfall estimates are developed for climate models (Maraun, 2016; Grillakis *et al.,* 2017; Switanek *et al.,* 2017), for radar approaches (Cecinati *et al.,* 2017;Yoo *et al.,* 2014) and for satellite-based, multi-sensor approaches (Najmaddin *et al.,* 2017;Valdés-Pineda *et al.,* 2016). In this chapter, focus is on satellite rainfall estimates (SREs) to improve reliability in spatio-temporal rainfall representation. Correction schemes rely on assumptions that adjust errors in space and/or time (Habib *et al.,* 2014). Some correction schemes consider correction only for spatial distributed patterns in bias, commonly known as space variant/invariant. Approaches that correct for spatially averaged bias have roots in radar rainfall estimation (Seo *et al.,* 1999) but are unsuitable for large scale basins (> 5,000 km^2) where rainfall may substantially vary in space (Habib *et al.,* 2014). Studies by Tefsagiorgis *et al.* (2011) in Oklahoma (USA) and Müller and Thompson (2013) in Nepal concluded that space variant correction schemes are more effective in reducing CMORPH and TRMM bias than space invariant correction schemes. In a study conducted in the Upper Blue Nile basin in Ethiopia, Bhatti *et al.* (2016) show that CMORPH bias correction is most effective when bias factors are calculated for 7-day sequential windows.

Bias correction schemes based on regression techniques have reported distortion of frequency of rainfall rates (Ines and Hansen, 2006; Marcos *et al.,* 2018). Multiplicative shift procedures tend to adjust SRE rainfall rates, but Ines and Hansen (2006) reported that they do not correct systematic errors in rainfall frequency of climate models. Non-multiplicative bias correction schemes preserve the timing of rainfall within a season (Fang *et al.,* 2015; Hempel *et al.,* 2013). Studies that have applied non-linear bias correction schemes such as

*__This chapter is based on:__ W. Gumindoga, T.H.M. Rientjes, A.T. Haile, H. Makurira and P. Reggiani (2019): Performance of bias-correction schemes for CMORPH rainfall estimates in the Zambezi River Basin, *Hydrology and Earth System Sciences (HESS)*. https://doi.org/10.5194/hess-23-2915-2019.

Power Function report correction of extreme values (depth, rate and frequency) thus mitigating the underestimation and overestimation of CMORPH rainfall (Vernimmen *et al.,* 2012). The study by Tian (2010) in the United States noted that the Bayesian (likelihood) analysis techniques are found to over-adjust both light and heavy CMORPH rainfall.

This study uses daily CMORPH and rain gauge data for Upper, Middle, and Lower Zambezi basins to (i) evaluate if performance of CMORPH rainfall is affected by elevation and distance from large scale open water bodies (ii) evaluate the effectiveness of linear/non-linear and time-space variant/invariant bias correction schemes and (iii) assess the performance of bias correction schemes to represent different rainfall rates and climate seasonality. Analysis serves to improve reliability of SREs applications in water resource applications in the Zambezi basin such as for rainfall-runoff modelling.

5.2 Methodology

5.2.1. Comparison of CMORPH and gauge rainfall

The study compares gauge rainfall at point scale to CMORPH satellite derived rainfall estimates at pixel scale (point-to-pixel). Comparison is at a daily time interval covering the period 1998-2013, following Cohen Liechti *et al.* (2012), Dinku *et al.* (2008), Haile *et al.* (2014), Hughes (2006), Tsidu (2012) and Worqlul *et al.* (2014) who report on point-to-pixel comparisons in African basins. Unlike point-to-pixel comparison, Worqlul *et al.* (2014) describe that for pixel-to-pixel comparison, there is demand for a well distributed rain gauge network that would not hamper accurate interpolation.

5.2.2. Elevation and distance from large scale open water bodies

Rientjes *et al.* (2013b), Habib *et al.* (2012b) and Haile *et al.* (2009) for the Nile Basin reveal that performance of SREs is effected by elevation. Findings in the latter three studies signal that performance possibly also may be affected by presence of Lake Tana. To assess both influences, the Zambezi Basin was classified into 3 elevation zones for which the hierarchical cluster 'within-groups linkage' method in the Statistical Product and Service Solutions (SPSS) software was used (Table 5.1). Based on Euclidian distance to large scale open water bodies, 4 arbitrary distance zones are defined to group stations (Table 5.1). A detailed description on the individual stations, their elevation and distance to large scale open water bodies is provided in Table 2.1. The Advanced Spaceborne

Thermal Emission and Reflection Radiometer (ASTER) based DEM of 30 m resolution was used to represent elevation across the Zambezi Basin. The Euclidian distance of each rain gauge location to large scale open water bodies is defined in a GIS environment through the distance calculation algorithm. Large scale open water bodies are defined as perennial open water bodies with surface area > 700 km^2. The threshold is defined based on knowledge of the water bodies in the Zambezi basin study area and the detailed fieldwork the authors have conducted over the years in various other study areas in Africa (such as Lake Tana in Ethiopia and Lake Naivasha in Kenya). The relationship between lake surface area and CMORPH bias on 300 water bodies in the study area shows that at a threshold > 700 km^2, a signal is induced to warrant the removal from the analysis of all water bodies with surface area < 700 km^2.

Table 5.1: Elevation and distance from large scale open water bodies.

Zone ID	Elevation (m)	No. of stations	Mean elevation of stations (m)
Zone 1	< 250	8	90
Zone 2	250-950	21	510
Zone 3	> 950	31	1140
Zone ID	Distance (km)	No. of stations	Mean distance to large scale open water bodies (km)
Zone 1	< 10	4	5
Zone 2	10 - 50	10	35
Zone 3	50 - 100	18	80
Zone 4	> 100	28	275

5.2.3. Bias correction schemes

Bias correction schemes evaluated in this study are the Spatio-temporal bias *(STB)*, Elevation zone bias *(EZ)*, Power transform *(PT)*, Distribution transformation *(DT)*, and the Quantile mapping based on an empirical distribution *(QME)*, this by the aim to correct for bias while daily rainfall variability is preserved. The five schemes are chosen based on merits documented in literature (Bhatti *et al*., 2016; Habib *et al.,* 2014; Teutschbein and Seibert, 2013; Themeßl *et al.,* 2012; Vernimmen *et al.,* 2012). It is noted that findings on the performance

of selected bias correction schemes in literature do not allow for generalization but findings only apply to the respective study domains (Wehbe *et al.,* 2017; Jiang *et al.,* 2016; Liu *et al.,* 2015; Haile *et al.,* 2015).

In the procedure to define a time window for bias correction, the study follows Habib *et al.* (2014) and Bhatti *et al.* (2016) who in the Lake Tana Basin (Ethiopia) carried out a sensitivity analysis on moving time windows and on sequential time windows. Window lengths between 3 and 31 days are tested. Findings indicated that a 7-day sequential time window for bias factors is most appropriate but only when a minimum of five rainy days were recorded within the 7-day window with a minimum rainfall accumulation depth of 5 mm, otherwise no bias is estimated (i.e., a value of 1 applies as bias correction factor). Preliminary tests in this study on 5 and 7-day moving and sequential windows on 20 individual stations distributed over the three elevation zones indicates that the 7-day sequential approach is well applicable in the Zambezi Basin. As such, the approach was selected.

The bias correction factors are calculated using only rain days (rainfall $\geq$ 1 mm/day). Otherwise in cases where both the gauge and satellite have zero values (Rain gauge *(G)* = 0 and CMORPH *(S)* = 0), correction is not applied and the SRE value remains 0 mm/day.

Following Bhatti *et al.* (2016), the bias correction factors of the rain gauges were spatially interpolated so that SREs at all pixels can be corrected. For interpolation, the Universal Kriging was applied. Thus, to systematically correct all CMORPH estimates, station based bias factors for each time window are spatially interpolated to arrive at spatial coverage across the study area and to allow for comparison with other approaches.

Spatio-temporal bias correction (STB)

This linear bias correction scheme has its origin in the correction of radar-based precipitation estimates (Tesfagiorgis *et al.,* 2011) and downscaled precipitation products from climate models. The CMORPH daily rainfall estimates (*S*) are multiplied by the bias correction factor for the respective sequential time window for individual stations resulting in corrected CMORPH estimates (STB) in a temporally and spatially coherent manner (Equation [5.1]).

$$STB = S\frac{\sum_{t=d}^{t=d-l} G(i,t)}{\sum_{t=d}^{t=d-l} S(i,t)} \qquad [5.1]$$

where:

G = gauged rainfall (mm/day)

i = gauge number

d = day number

t = julian day number

l = length of a time window for bias correction

The advantages of this bias correction scheme are that it is straightforward and easy to implement due to its simplicity and modest data requirements. However, just like any multiplicative shift procedures of bias correction, *STB* has challenges in correcting systematic errors in rainfall frequency particularly the wet-day frequencies (Lenderink *et al.,* 2007; Teutschbein and Seibert, 2013).

Elevation zone bias correction (EZ)

This bias scheme is proposed in this study and aims at correcting satellite rainfall for elevation influences. This method groups rain gauge stations into 3 elevation zones based on station elevation. The grouping in this study is based on the hierarchical clustering technique, expert knowledge about the study area but also guided by relevant past studies in the basin (e.g., World Bank, 2010b; Beilfuss, 2012). Each zone has the same bias correction factor but differs across the three zones. In the time domain bias factors vary following the 7-day sequential window approach. The corrected CMORPH estimates (*EZ*) at daily time interval are obtained by multiplying the uncorrected CMORPH daily rainfall estimates (*S*) by the daily bias correction factor of each elevation zone.

$$EZ = S\frac{\sum_{t=d}^{t=d-l}\sum_{i=1}^{i=n} G(i,t)}{\sum_{t=d}^{t=d-l}\sum_{i=1}^{i=n} S(i,t)} \qquad [5.2]$$

The merit of this bias correction scheme is that the effects of elevation on rainfall depth are accounted for.

Power transform (PT)

The non-linear *PT* bias correction scheme has its origin in studies of climate change impact (Lafon *et al.,* 2013). Vernimmen *et al.* (2012) show that the scheme could be applied to correct satellite rainfall estimates for use in hydrological modelling and drought monitoring. The *PT* method uses an exponential form to adjust the standard deviation of rainfall series. The daily bias corrected CMORPH rainfall *(PT)* for a pixel that overlays a station is obtained using equation:

$$PT = aG(i,t)^{b} \qquad [5.3]$$

Where:

G = gauged rainfall (mm/day)

a = prefactor such that the mean of the transformed CMORPH values is equal to the mean of rain gauge rainfall

b = factor calculated such that for each rain gauge the coefficient of variation (CV) of CMORPH matches the gauge-based counter parts
i = gauge number

t = day number

Optimized values for *a* and *b* are obtained through the generalized reduced gradient algorithm (Fylstra *et al.,* 1998). Values for *a* and *b* vary for the 7-day sequential window since correction is at daily time base. In the case of utilising the *PT* method in a certain area (or for a certain period), the bias correction factor is spatially interpolated to result in comparable estimates with other bias correction schemes. The advantage of the bias scheme is that it adjusts extreme precipitation values in CMORPH estimates (Vernimmen *et al.,* 2012). *PT* has reported limitations in correcting wet-day frequencies and intensities (Leander *et al.,* 2008; Teutschbein and Seibert, 2013).

Distribution transformation (DT)

DT is an additive bias correction approach which has its origin in statistical downscaling of climate model data (Bouwer *et al.,* 2004). The method transforms a statistical distribution function of daily CMORPH rainfall estimates to match the distribution by gauged rainfall. The procedure to match the CMORPH distribution function to gauge rainfall-based counter parts is described in equations [5.4-5.6]. The principle to matching is that the difference in the mean value and differences in the variance are corrected for, in the 7-day sequential

window. First, the bias correction factor for the mean is determined by equation [5.4]:

$$DT_u = \frac{G_u}{S_u} \qquad [5.4]$$

G_u *and* S_u are mean values of 7-day gauge and CMORPH rainfall estimates.

Secondly, the correction factor for the variance $(DT\tau)$ is determined by the quotient of the 7-day standard deviations, $G\tau$ and $S\tau$, for gauge and CMORPH respectively.

$$DT\tau = \frac{G\tau}{S\tau} \qquad [5.5]$$

Once the correction factors, that vary within a 7-day time sequential window, are established, they are then applied to correct all daily CMORPH estimates *(S)* through equation [5.6] to obtain corrected CMORPH rainfall estimate *(DT).* The parameters DT_u and are developed for respective 7-day sequential windows, but correction is at daily time intervals.

$$DT = (S(i,t) - Su)DT\tau \; + DTu * S\tau \qquad [5.6]$$

Uncorrected CMORPH daily values are returned if [5.6] results in negative values. The merit of this bias correction scheme is that it corrects wet-day frequencies and intensities. The disadvantage of this bias correction scheme is that adding the gauge based mean deviation to the satellite data destroys the physical consistency of the data. In addition, the method might result in the generation of too few rain days in the wet season, and sometimes the mean of daily intensities might be unrealistically corrected (Johnson and Sharma, 2011; Teutschbein and Seibert, 2013).

Quantile mapping based on an empirical distribution (QME)

This is a quantile based empirical-statistical error correction method with its origin in empirical transformation and bias correction of regional climate model-simulated precipitation (Themeßl *et al.,* 2012). The method corrects CMORPH precipitation based on empirical cumulative distribution functions (*ecdfs*) which are established for each 7-day time window and for each station. The bias corrected rainfall *(QME)* using quantile mapping are expressed in terms of the empirical cumulative distribution function (*ecdf*) and its inverse (*ecdf-1*). Parameters apply to a 7-day sequential window but correction is then at daily time

interval with bias spatially averaged for the entire domain to allow for comparison with other approaches.

$$QME = ecdf_{obs}^{-1}(ecdf_{raw}(S(i,t))) \quad [5.7]$$

Where:

$ecdf_{obs}$ = *empirical cumulative distribution function for the gauge-based observation*

$ecdf_{raw}$ = *empirical cumulative distribution function for the uncorrected CMORPH*

The advantage of this bias scheme is that it corrects quantiles and preserves the extreme precipitation values (Themeßl *et al.,* 2012). However, it also has its limitation due to the assumption that both the observed and satellite rainfall follow the same proposed distribution, which may introduce potential new biases.

5.2.4. Rainfall rates and seasons

To assess the performance of SREs for different classes of daily rainfall rates, five classes are defined which indicate: very light (< 2.5 mm/day), light (2.5-5.0 mm/day), moderate (5.0-10.0 mm/day), heavy (10.0-20.0 mm/day) and very heavy rainfall (> 20.0 mm/day).

Furthermore, gauged rainfall was divided into wet and dry seasonal periods to assess the influence of seasonality on performance of bias correction schemes. The wet season in the Zambezi Basin spans from October-March whereas the dry season spans from April-September.

5.2.5. Evaluation of CMORPH estimates

Corrected and uncorrected CMORPH satellite rainfall estimates were evaluated with reference to rain gauge rainfall using statistics that measure systematic differences (i.e., *Rel. bias (%)* and Mean Absolute Error (*MAE*)), measures of association (e.g., correlation coefficient and Nash Sutcliffe Efficiency (*NSE)*) and random differences (e.g., standard deviation of differences and coefficient of variation) (Haile *et al.,* 2013). *Rel. bias (%)* (defined in equation 4.5) is a measure of how the satellite rainfall estimate deviates from the rain gauge rainfall, and the result is normalised by the summation of the gauge values. A positive value indicates overestimation whereas a negative value

indicates underestimation. The correlation coefficient *R* (ranging between +1 and −1) represents the linear dependence of gauge and CMORPH data. *MAE* is the arithmetic average of the absolute values of the differences between the daily gauge and CMORPH satellite rainfall estimates. The *MAE* is zero if the rainfall estimates are perfect and increases as discrepancies between the gauge and satellite become larger. *NSE* indicates how well the satellite rainfall matches the rain gauge observation and it ranges between - ∞ and 1, with *NSE* = 1 meaning a perfect fit (Nash and Sutcliffe, 1970).

Equations [5.8-5.10] apply.

$$R = \frac{\sum_{i=1}^{n}(G_i-\bar{G})(S_i-\bar{S})}{\sqrt{\sum_{i=1}^{n}(G_i-\bar{G})^2}\sqrt{\sum_{i=1}^{n}(S_i-\bar{S})^2}} \quad [5.8]$$

$$MAE = \frac{1}{N}\sum_{i=1}^{n}|S_i - G_n| \quad [5.9]$$

$$NSE = 1 - \frac{\sum_{i=1}^{n}(G_i-S_i)^2}{\sum_{i=1}^{n}(G_i-\bar{G})^2)} \quad [5.10]$$

where:

S = satellite rainfall estimate (mm/day), at a certain day (i)

$\bar{S}$ *= mean of the satellite rainfall estimate (mm/day)*

G = rainfall by a rain gauge (mm/day), at a certain day (i)

$\bar{G}$ *= mean value of rainfall recorded by a rain gauge (mm/day)*

n = length of bias correction window in days.

5.2.6. Test for differences of mean

To detect significant differences between gauge and satellite rainfall (corrected and uncorrected) and differences amongst the five bias correction methods, the study applied paired t-test and analysis of variance (ANOVA) tests.

Paired t-tests

A paired t-test was used to test whether there is a significant difference between rain gauge, uncorrected and bias corrected CMORPH satellite rainfall for the 52 rain gauges. Results are summarized for the Upper, Lower and Middle Zambezi. The paired t-test compares the mean difference of the values to zero.

The test depends on the mean difference, the variability of the differences and the amount of data. The null hypothesis (H0) is that there is no difference in mean of daily rain gauge and satellite rainfall (uncorrected or bias corrected). If the p-value is less than or equal to 0.05 (5 %), the result is deemed statistically significant, i.e., there is a significant relationship between the rain gauge and satellite rainfall (Wilks, 2006; Field, 2009).

Analysis of Variance (ANOVA) test

The ANOVA-test aims to test whether there is a significant difference amongst the five bias correction techniques. The Null hypothesis (H0) is that there are no differences amongst the five bias correction schemes. The study further determined which schemes differ significantly using three post-hoc tests, namely: Tukey HSD, Scheffe and the Bonferroni (Brown, 2005; Kucuk *et al.,* 2018). Results are summarized for the Upper, Lower and Middle Zambezi.

5.2.7. Taylor diagram

The study applied a Taylor diagram to evaluate differences in data sets generated by respective bias correction schemes by providing a summary of how well bias correction results match gauge rainfall in terms of pattern, variability and magnitude of the variability. Visual comparison of SRE performance is done by analysing how well patterns match each other in terms of the Pearson's product-moment correlation coefficient (*R*), root mean square difference (*E*), and the ratio of variances on a 2-D plot (Lo Conti *et al.,* 2014; Taylor, 2001). The reason that each point in the two-dimensional space of the Taylor diagram can represent the above three different statistics simultaneously is that the centred pattern of root mean square difference (E^i), and the ratio of variances are related by the following:

$$E^i = \sqrt{\sigma_f^2 + \sigma_r^2 - 2\sigma_f \sigma_r R} \qquad [5.12]$$

where:

σ_f *and* σ_r = *standard deviation of CMORPH and rain gauge rainfall, respectively.*

Development and applications of Taylor diagrams have roots in climate change studies (Smiatek *et al.,* 2016; Taylor, 2001) but also has frequent applications in environmental model evaluation studies (Cuvelier *et al.,* 2007; Dennis *et al.,* 2010; Srivastava *et al.,* 2015). Bhatti *et al.* (2016) proposed the use of Taylor Diagrams for assessing effectiveness of SREs bias correction schemes. The most effective bias correction schemes will have data that lie near a point marked 'reference' on the x-axis, relatively high correlation coefficient and low root mean square difference. Bias correction schemes matching gauged based standard deviation have patterns that have the right amplitude.

5.2.8. Quantile-quantile (q-q) plots

A q-q plot is used to check if two datasets (in this case gauge vs CMORPH rainfall) can fit the same distribution (Wilks, 2006). A q-q plot is a plot of the quantiles of the first data set against the quantiles of the second data set. A 45-degree reference line is also plotted. If the satellite rainfall (corrected and uncorrected) has the same distribution as the rain gauge, the points should fall approximately along this reference line. The greater the departure from this reference line, the greater the evidence for the conclusion that the bias correction scheme is less effective (NIST/SEMATECH, 2001).

The main advantage of the q-q plot is that many distributional aspects can be simultaneously tested. For example, changes in symmetry, and the presence of outliers can all be detected from this plot.

5.2.9. Cross validation of bias correction

Spatial cross-validation

The spatial cross-validation procedure (hold-out sample) applied in this study, involves the withdrawal of 8 in-situ stations from the sample of 60 when generating bias corrected SREs for all pixels across the study area. Corrected SREs are then compared to the rain gauge rainfall of the withdrawn stations to evaluate closeness of match. From the sample of 8, only 2 stations were selected in the < 250 m elevation zone, 3 stations in the 250 - 950 m zone and 3 stations in > 950 m elevation zone. Stations selected have elevation close to the average elevation zone value and are centred in an elevation zone. Thus 52 stations were left for applying the bias correction methods and spatial interpolation. As performance indicators to evaluate results of cross-validation, the study used the

Rel. bias (%), *MAE*, *R* and the estimated ratio which is obtained by dividing CMORPH rainfall totals and gauge-based rainfall totals for the 1999-2013 period.

Temporal cross-validation

For evaluation of SREs in the time domain this study followed Gutjahr and Heinemann (2013) to omit rainfall (both from gauge and satellite) for the 1998-1999 hydrological year to remain with 14 years for bias correction of SREs. Bias corrected estimates for the 14 years are then evaluated against estimates for the 1998-1999 period that served as reference. For evaluation, the study used the *Rel. bias (%)*, *MAE*, correlation coefficient and the estimated ratio, which values were averaged for the Upper, Middle and Lower Zambezi but also for the wet and dry seasons.

5.3 Results and Discussion

5.3.1. Performance of uncorrected CMORPH rainfall

The spatially interpolated values of *Rel. bias (%)* across the Zambezi Basin are shown in Figure 5.1. Areas in the central and western part of the basin have *Rel. bias* relatively close to zero suggesting good performance of the uncorrected CMORPH product. However, relatively large negative *Rel. bias* values (-18 %) are shown in the Upper Zambezi's high elevated areas such as Kabompo and northern Barotse Basin, in the south-eastern part of the basin such as Shire River Basin and in the Lower Zambezi's downstream areas where the Zambezi River enters the Indian Ocean. CMORPH overestimates rainfall in Kariba, Luanginga, and Luangwa basins by positive *Rel. bias* values. As such CMORPH estimates do not consistently provide results that match rain gauge observations. Since CMORPH estimates have pronounced error (-10 > *Rel. bias (%)* > 10), SRE bias needs to be removed before the product can be applied for hydrological analysis and in water resources applications. It can be seen that the Inverse Distance interpolation approach results in stations relatively close to each other to have over- and underestimates of the rainfall. An example is station Kalabo which belongs to Luanginga sub basin (*Rel. bias (%)* > 10 %) and Mongu which belongs to Barotse basin (*Rel. bias (%)* < -15 %). The same can be observed for many other locations in the Zambezi Basin. The two stations are 68 km apart. Figure 5.2 also shows contours for rain gauge mean annual precipitation (MAP) in the Zambezi Basin with higher values in the northern parts of the basin (Kabompo and Luangwa) compared to regionalized estimates of MAP such as in Shire River and Kariba sub-basins.

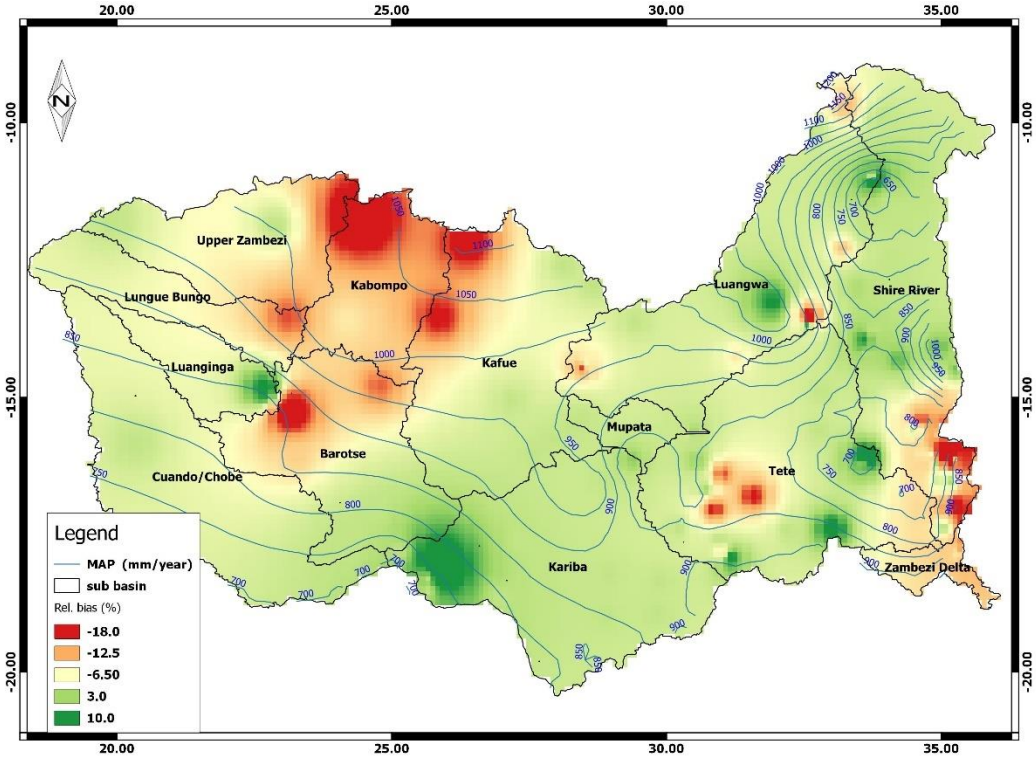

Figure 5.1: The spatial variation of Rel. bias (%) for gauge vs uncorrected CMORPH daily rainfall (1998-2013) for the Zambezi Basin. The gauge-based isohyets for Mean Annual Precipitation (MAP) are shown in blue.

5.3.2. Effects of elevation and distance from large scale open water bodies on CMORPH bias

Figure 5.2. shows Taylor diagrams with a comparison of basin lumped estimates of daily uncorrected time series (1999–2013) of CMORPH and gauge-based rainfall for the 3 elevation zones (Figure 5.2a) and 4 distance zones from large scale open water bodies (Figure 5.2b). Figures 5.2a and 5.2b show that standard deviations in the elevation zones and the distance zones (except for the < 10 km distance zone) are lower than the reference/rain gauge standard deviation which is indicated by the black arc (value of 8.45 mm/day). The stations in the high elevation zone (> 950 m) and long-distance zone (> 100 km) reveal lower variability than stations at lower elevation and shorter distance zones. With respect to the reference line, CMORPH estimates that are lumped for respective elevation zones and distance to a large water body do not match standard deviation of rain gauge-based counterparts. Figure 5.2a and 5.2b also show that

CMORPH standard deviations that are close to gauge-based rainfall apply to lower elevation and shorter distance zones. Based on the Taylor diagrams, the statistics (root mean square difference, correlation coefficient and standard deviation) for uncorrected CMORPH show increasing performance for increasing elevation and increasing distance from large scale water bodies. Specifically, stations in the lower elevation zones (< 250 m) have lower *R* and higher *E* than the higher elevation zones (> 950 m). For shorter distance zones lower *R* and higher *E* is shown than for longer distance zones (> 100 km). These findings suggest that in general effects of distance to large scale water body are minimal except for distances < 10 km.

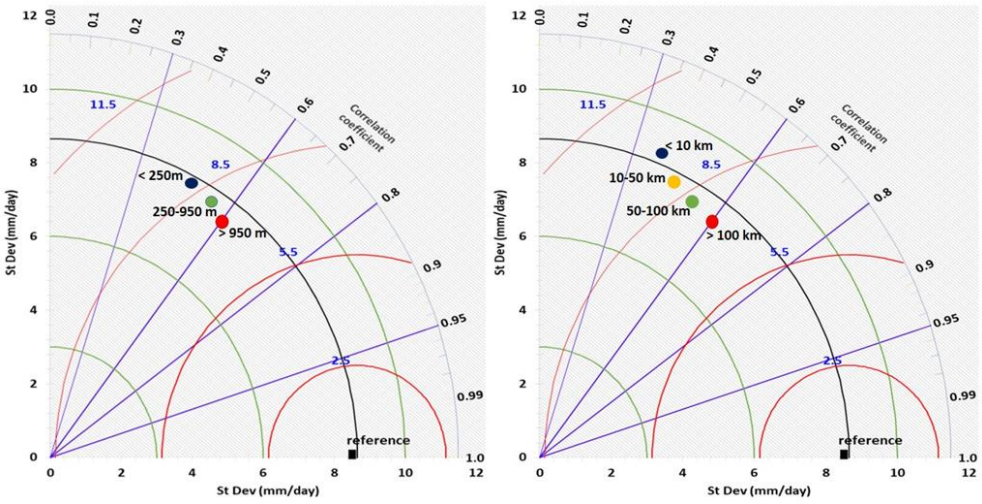

a) Elevation zones *b) Distance zones*

Figure 5.2. Time series of rain gauge (reference) vs CMORPH estimations, period 1999-2013, for elevation zones (Figure 5.2a) and distance zones (Figure 5.2b) in the Zambezi Basin. The correlation coefficients for the radial line denote the relationship between CMORPH and gauge-based observations. Standard deviations on both the x and y axes show the amount of variance between the two-time series. The standard deviation of the CMORPH pattern is proportional to the radial distance from the origin. The angle between symbol and abscissa measures the correlation between CMORPH and rain gauge observations. The root mean square difference (red contours) between the CMORPH and rain gauge patterns is proportional to the distance to the point on the x-axis identified as "reference". For details, see Taylor (2001).

5.3.3. Evaluation of bias correction

Standard statistics

Figure 5.3 shows frequency-based statistics (mean and maximum) on accuracy of uncorrected CMORPH (R-MORPH) and corrected rainfall estimates for each bias correction method. Comparison is based on the gauge rainfall values shown for the bars to the left of the R-MORPH for each of the three Zambezi basins. The ratio of cumulated estimates (1999-2013) from rain gauge and CMORPH estimates for the Lower, Middle and Upper Zambezi sub-basins are shown. Results show that the bias of CMORPH moderately reduced for each of the five bias correction schemes. However, the effectiveness of the schemes varies spatially with best performance in Lower and Upper Zambezi sub-basin and relatively poor performance in the Middle Zambezi sub-basin.

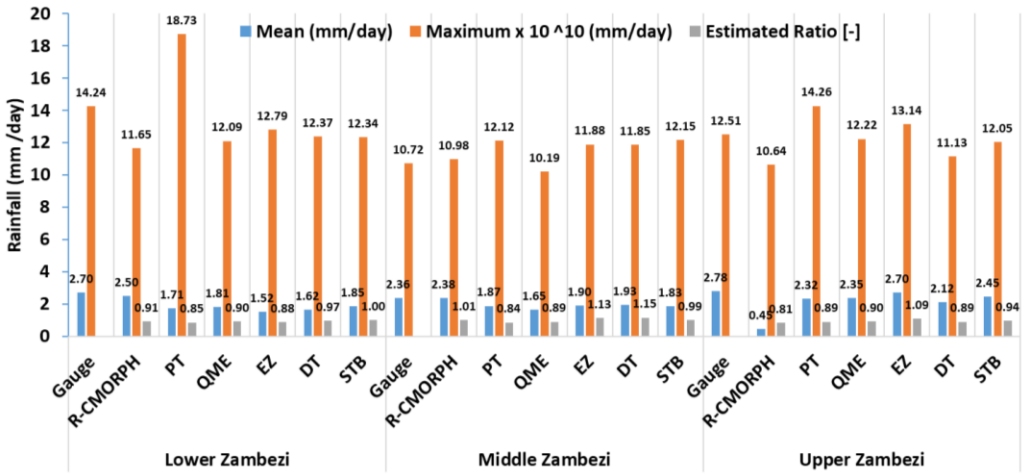

Figure 5.3: Frequency based statistics (mean, max and estimated ratio of gauged sum vs CMORPH sum for 1999-2013) of uncorrected (R-MORPH) and corrected CMORPH for Lower, Middle and Upper Zambezi Basin.

Judging by the three performance indicators (mean, max and estimated ratio), results indicate that *STB* bias correction scheme is consistently effective in removing CMORPH rainfall bias in the Zambezi Basin. *STB* and *PT* effectively adjust for the mean of CMORPH rainfall estimates. Statistics in Figure 5.3 confirm these findings especially for the Upper Zambezi sub-basin where the mean of corrected estimates improved by > 60 % from the mean of uncorrected estimates. In addition, *PT* in the Lower Zambezi, *QME* in both Middle and Upper

Zambezi and *STB* in the Upper Zambezi were also effective (improvement by 16 %) in correcting for the highest values in the rainfall estimates. *STB* performs better than other bias schemes in reproducing rainfall for the Lower and Upper Zambezi sub-basin, where the ratio of gauge total to corrected CMORPH total is close to 1.0.

Figure 5.4. shows the mean absolute error *(MAE)* and Relative bias (*Rel. bias*) on the left axis and Nash Sutcliffe Efficiency *(NSE)* on the right axis as measures to evaluate performance of bias correction schemes in the Zambezi Basin.

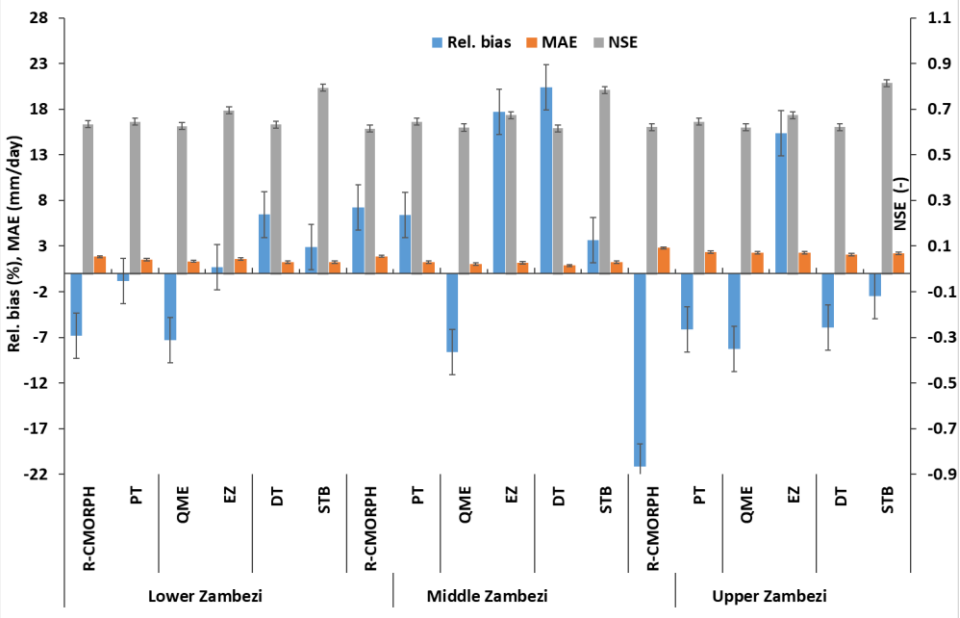

Figure 5.4: Rel. bias (%), Mean Absolute Error (left axis) and Nash Sutcliffe (NSE) (right axis) of corrected and uncorrected CMORPH (R-CMORPH) daily rainfall averaged for the Lower Zambezi, Middle Zambezi and Upper Zambezi for 1999-2013 period.

The effectiveness of the bias correction by all schemes varies over the different parts of the basin but is higher in the Lower and Upper Zambezi than in the Middle Zambezi. The *STB*, *PT* and *EZ* show improved performance by exhibiting smaller *MAEs* compared to the uncorrected CMORPH (R-CMORPH). A greater improvement is shown for the Middle Zambezi where the uncorrected *MAE* of 1.89 mm/day is reduced to 0.86 mm/day after bias correction by the elevation zone bias correction scheme *(EZ)*. The signal on improved performance for the Lower and Middle Zambezi as compared to the Upper Zambezi is also

evident for the majority of the bias correction techniques. However, relatively large error remains in the *MAE*.

NSE for *STB* is larger than 0.8 for all three Zambezi sub-basins. This is followed by *EZ* with *NSE* larger than 0.7 for the three sub-basins. The lowest *NSE* is for *QME* which is close to 0.65 for all three sub-basins. Best results for reducing *Rel. bias (%)* are obtained by *EZ* in the Lower Zambezi (*Rel. bias* of 0.7 % ~ absolute bias of 0.10 mm/day) and Upper Zambezi (0.22 % ~0.23 mm/day), *PT* in the Lower and Middle Zambezi (-0.84 % ~0.18 mm/day) and *STB* in all the basins (< 3.70 % ~0.24 mm/day). Gao and Liu (2013) over the Tibetan Plateau asserts that *EZ* is valuable in correcting systematic biases to provide a more accurate precipitation input for rainfall-runoff modelling. Significant underestimation for the uncorrected (-21.16 % ~0.44 mm/day) and for bias corrected CMORPH are shown for the Upper Zambezi sub-basin.

Significance testing

Table 5.2 shows results of statistical tests to assess whether there is a significant difference ($p < 0.05$) between rain gauge vs uncorrected and bias corrected CMORPH satellite rainfall for each of the 52 rain gauge stations. Results are summarised for the Upper, Middle and Lower Zambezi and in the Zambezi basin. The null hypothesis is rejected for *PT* (Lower Zambezi), *DT* (Upper Zambezi) and *QME* (all the 3 sub-basins) since $p < 0.05$. This means that statistically the above-mentioned bias correction schemes results deviate from the gauge. The null hypothesis is accepted for *STB* and *EZ* (all three sub-basins), *DT* (Lower and Upper Zambezi) and *PT* (Middle and Upper Zambezi), since $p > 0.05$ showing the effectiveness of these bias correction schemes. Compared to uncorrected satellite rainfall (R-MORPH), results also reveal that the bias corrected satellite rainfall is closer to the gauge-based rainfall.

Table 5.2: Paired t-tests for the Upper, Middle and Lower Zambezi. The mean difference is significant at the 0.05 level. Bold shows significant values.

Basin	Rainfall Estimate	t-value	Mean Std. Error	p-value (0.05)
Lower Zambezi	R-CMORPH	8.95	0.04	**0.04**
	DT	39.86	0.09	0.35
	PT	21.08	0.04	**0.03**

	QME	23.99	0.04	**0.04**
	EZ	36.43	0.03	0.27
	STB	14.7	0.04	0.46
Middle Zambezi	R-CMORPH	3.27	0.03	**0.001**
	DT	41.9	0.07	0.24
	PT	26.02	0.03	0.14
	QME	18.38	0.03	**0.00**
	EZ	26.60	0.02	0.07
	STB	23.6	0.03	0.09
Upper Zambezi	R-CMORPH	4.28	0.08	**0.00**
	DT	22.63	0.14	**0.01**
	PT	12.98	0.07	**0.05**
	QME	13.27	0.07	**0.00**
	EZ	13.73	0.07	0.14
	STB	13.62	**0.07**	**0.08**

Analysis of variance (ANOVA test)

The ANOVA test resambles a t-test except that the test was used to compare mean values from three or more data samples. Results of ANOVA shows that there is a significant ($p < 0.05$) difference in the mean values of the 5 bias correction results across the three sub-basins. This warranted the running of a post-hoc test to determine which schemes differ significantly. The contingency matrix in Table 5.3 shows results of the post-hoc test results summarized for the Tukey HSD, Scheffe and the Bonferroni methods but also for the Upper, Lower and Middle Zambezi. Table 5.3 also show that *STB*, *PT* and *EZ* are significantly different from the distribution transformation technique *(DT)* for the three sub-basins. *STB*, the best performing bias correction scheme identified using majority of the indicators, is also significantly different from *QME* and *EZ*. *QME* which has poorly performed is significantly different from *EZ*. Results are important for

further application of the bias correction schemes for studies such as flood, drought and water resources modelling.

Table 5.3: ANOVA post-hoc tests for the results of the five bias correction schemes ($p<0.05$). The checklist table gives an indication (symbol) where two bias correction scheme's results are significantly different from each other. Where there is no symbol, it means that the schemes' results are not significantly different. Different symbols represent Upper, Middle and Lower Zambezi basins.

	STB	PT	QME	DT	EZ
STB			√	x √ ♀	√
PT			♀	x √ ♀	
QME	√				♀
DT	x √ ♀	x √ ♀	x √		x ♀
EZ	√			x √ ♀	
	Key	x	Upper Zambezi		
		√	Lower Zambezi		
		♀	Middle Zambezi		

Taylor Diagrams

Figure 5.5. shows the Taylor diagram for time series of rain gauge (reference) observations vs CMORPH bias correction schemes averaged for the Lower Zambezi (UZ), Middle Zambezi (MZ) and Upper Zambezi (UZ). Absolute values used to develop the Taylor diagram are shown in Appendix 2. The position of each bias correction scheme and uncorrected satellite rainfall (R-MORPH) on Figure 5.6 shows how closely the rainfall by uncorrected CMORPH (R-MORPH) matches rain gauge observations as well as effectiveness of each of the bias schemes. Overall, all bias correction schemes show intermediate performance in terms of bias removal. Only the *PT* and *STB* for the Lower Zambezi sub-basin lie on the line of standard deviation (brown dashed arc) and means the standard deviation of the data for the two bias correction schemes match the gauge observations. This also indicates that rainfall variations after *PT* and *STB* bias correction for the Lower Zambezi resembles gauge based standard deviation. Note however that *STB* performs better than *EZ* as shown by the superior correlation coefficient. Compared against the reference line of mean standard deviation (8.5 mm/day), the rainfall standard deviation for most bias correction

schemes is below this line and as such exhibit low variability across the Zambezi Basin.

Figure 5.5. also shows that most of the bias correction schemes have standard deviation range of 6.0 to 8.0 mm/day. There is a consistent pattern between the bias correction schemes that have low *R* and high *RMSE* difference indicating that these schemes are not effective in bias removal. Overall, the best performing bias correction schemes (*STB* and *EZ*) have $R > 0.6$, standard deviation relatively close to the reference point and $RMSE < 7$ mm/day. The uncorrected CMORPH (R-MORPH) lies far away from the marked reference (gauge) point on the x-axis suggesting an intermediate overall effectiveness of the bias correction schemes such as *STB, EZ, DT* and *PT* in removing error as they are relatively closer to the marked reference point.

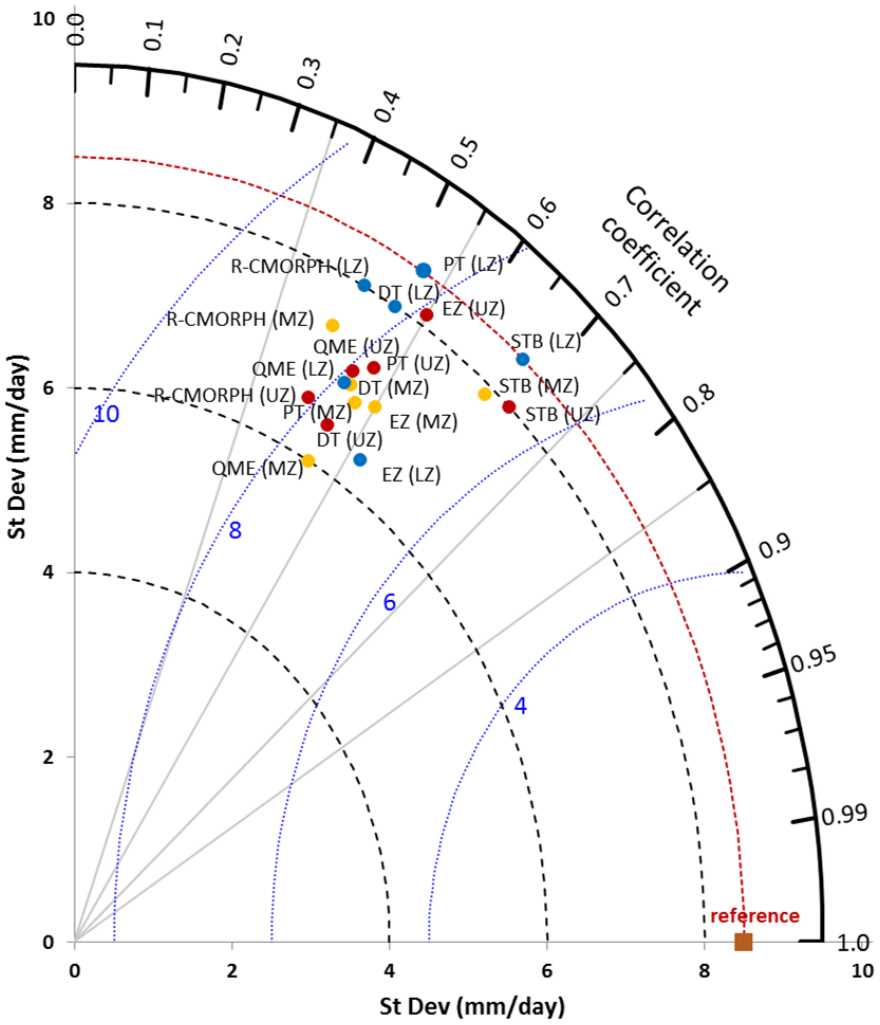

Figure 5.5: Taylor's diagram on Rain gauge (reference) observations and CMORPH bias corrected estimates (all 5 schemes) as averaged for the Lower Zambezi (LZ), Middle Zambezi (MZ), and Upper Zambezi (UZ) for the period 1999-2013. The distance of the symbol from point (1, 0) is also a relative measure of the bias correction scheme performance. The position of each symbol appearing on the plot quantifies how closely precipitation estimates by respective bias correction scheme's matches counterparts by rain gauge. The dashed blue lines indicate the root mean square difference (mm/day).

The least performing bias correction scheme is *QME* with relatively large *RSMD* (> 8 mm/day) and with low *R* (< 0.49) and standard deviation (< 6.5 mm/day). Inherent to the methodology of most of bias correction schemes (e.g. *QME*) is that the spatial pattern of the SRE does not change and therefore *R* for a

specific station for daily precipitation does not necessarily improve. The bias correction results by the Taylor Diagram in Figure 5.6 corroborates with findings shown in Figure 5.4 and Figure 5.5 for mean, max, ratio of rainfall totals and bias as performance indicators.

q-q plots

Figure 5.6. shows q-q plots for the Upper, Middle and Lower Zambezi for gauge rainfall against uncorrected and bias corrected CMORPH rainfall. Results show that *STB's* q-q plots for bias corrected CMORPH across the 3 basins has majority of points that fall approximately along the 45-degree reference line. This means that the *STB* bias corrected satellite rainfall has closer distribution to the rain gauge as compared to the uncorrected CMORPH counterparts suggesting effectiveness of the bias correction scheme. Other bias correction schemes such as *QME, EZ* and *PT* have data points showing a greater departure from the 45-degree reference line so performance is less effective.

In some instances, in both the Upper, Middle and Lower Zambezi, bias corrected values are significantly higher than the corresponding gauge values whereas in some instances there is serious underestimation. All q-q plots also show that for all bias correction schemes, the differences between gauge and satellite rainfall are smallest for low rainfall rates (< 2.5 mm/day) and increasing for very heavy rainfall (> 20.0 mm/day). In more detail, all the bias correction schemes show a larger difference for the transition area from low to heavy rainfall. *QME* and *PT* are not in good agreement with the rest of the bias correction schemes for higher rainfall estimates (40 and 60 mm/day).

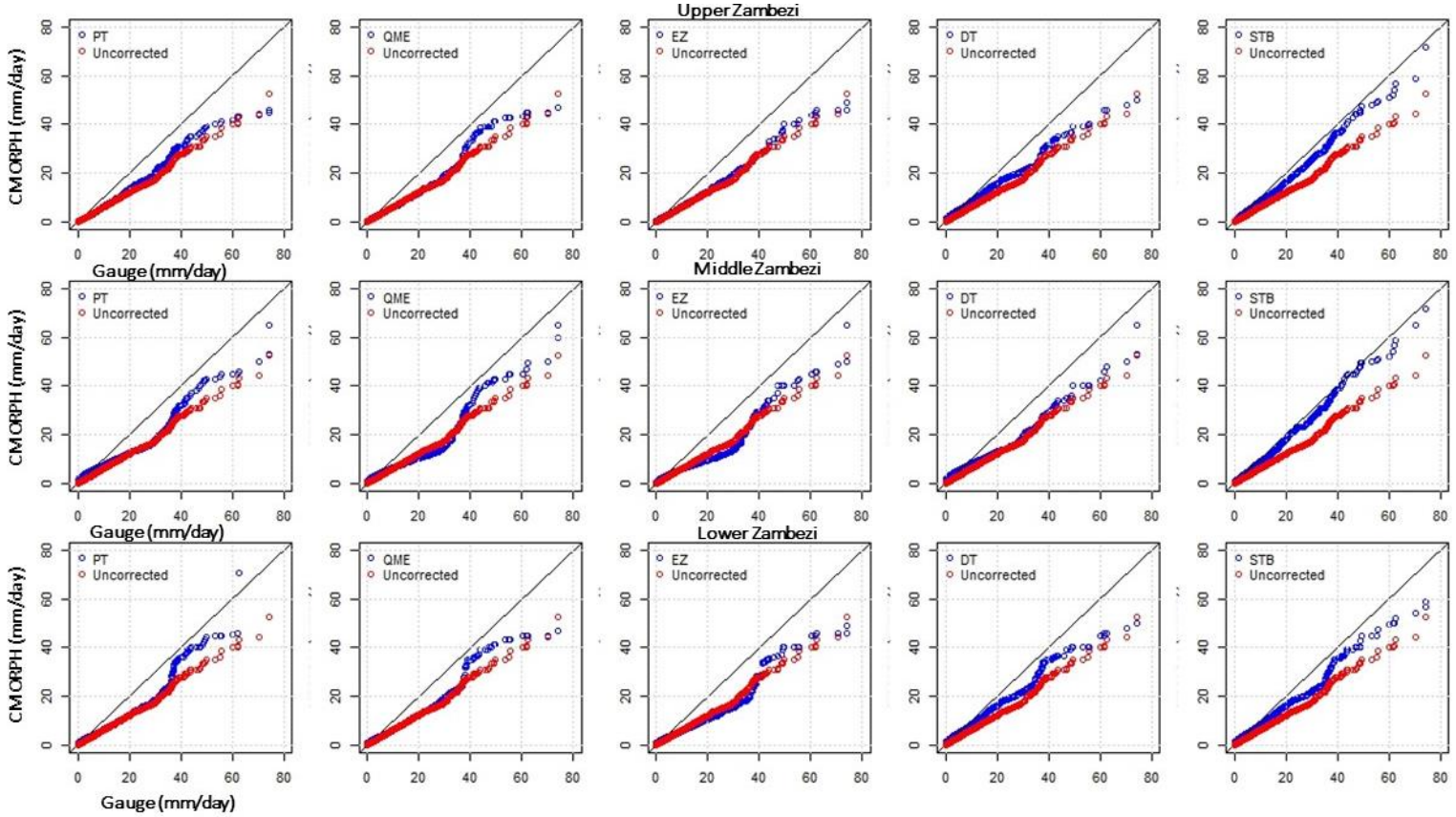

Figure 5.6: q-q plot for gauge vs satellite rainfall (uncorrected and PT, QME, EZ, DT and STB corrected) for the Upper (top panes), Middle (middle panes) and Lower (bottom panes) Zambezi.

CMORPH rainy days

Occurrence (%) of rainfall rates in the Zambezi Basin for each bias correction scheme is shown in Figure 5.7. The highest percentage (80-90 %) is shown for very light rainfall (0.0-2.5 mm/day). A smaller percentage is shown for 2.5-5.0 mm/day which is the light rainfall class. Smallest percentage (< 5 %) is shown for very heavy rainfall (> 20 mm/day). The CMORPH rainfall corrected with *STB*, *PT* and *DT* matches the gauge-based rainfall (%) in the Lower, Middle and Upper Zambezi suggesting good performance. All five bias correction schemes in the Zambezi Basin generally tend to overestimate very light rainfall (< 2.5 mm/day). There is a small difference for moderate rainy days classification of 10.0-20.0 mm/day. For *QME* in the Middle and Upper Zambezi, there is overestimation by > 80 %. There is underestimation of rainfall greater than 20 mm/day.

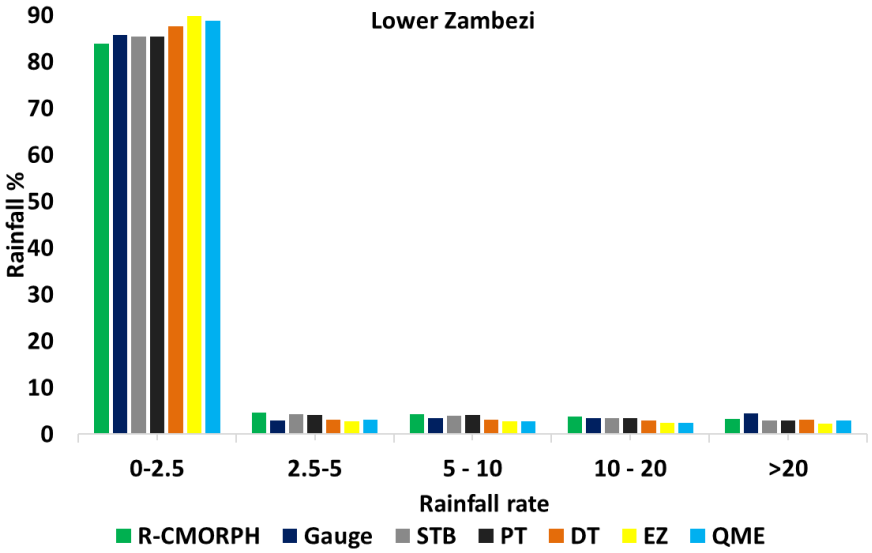

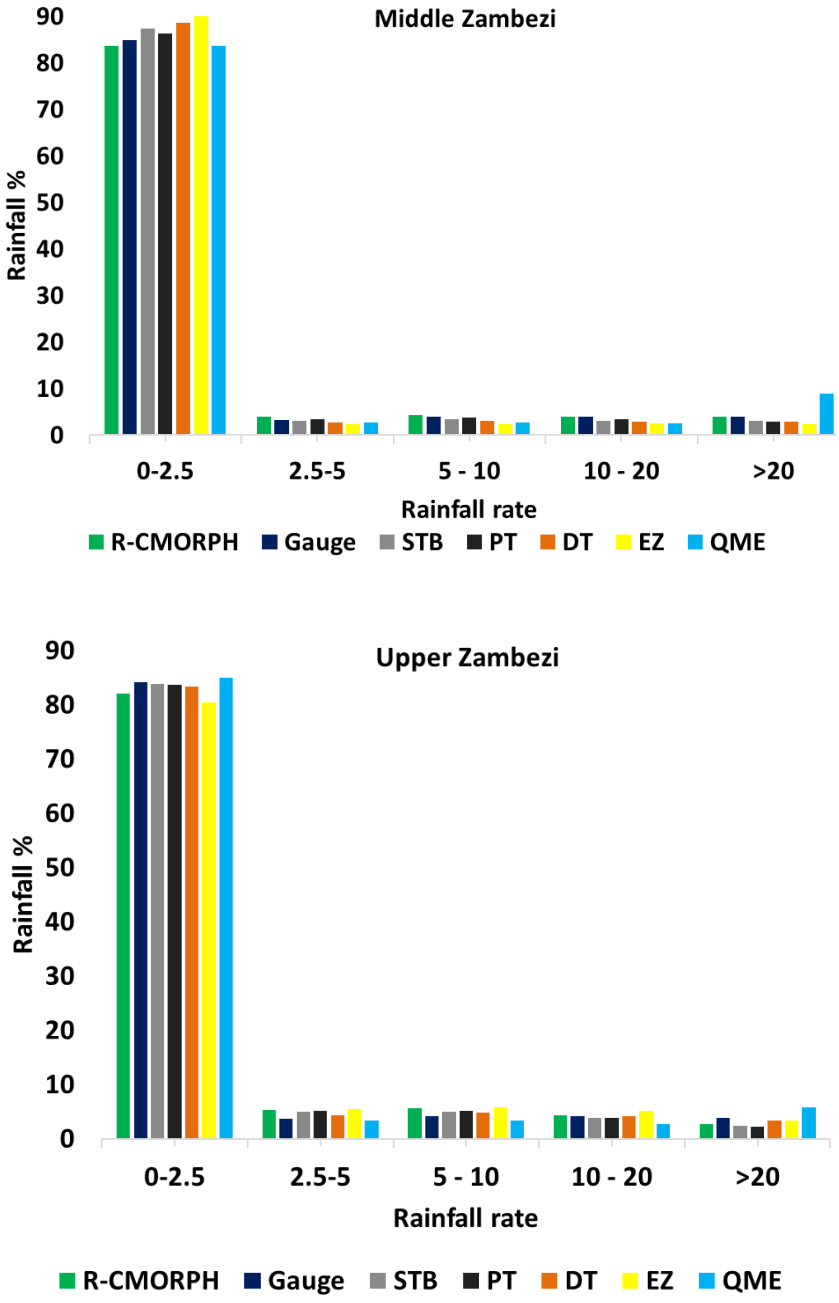

Figure 5.7: Percentage occurrence for rainfall rate classes for Lower, Middle and Upper Zambezi

Figure 5.8. gives the bias correction performance for the different rainy-day classes. Results of bias removal varies for the Lower, Middle and Upper Zambezi. Comparatively, the *STB* and *EZ* show effectiveness in bias removal with an average bias correction of 0.97 % and 3.6 % in the whole basin respectively. Results show more effectiveness in reducing the *Rel. bias (%)* for light (2.5-5.0 mm/day) and moderate (5.0-10.0 mm/day) rainfall compared to the heavy (10.0-20.0 mm/day) and very heavy (> 20.0 mm/day) rainfall across the whole basin.

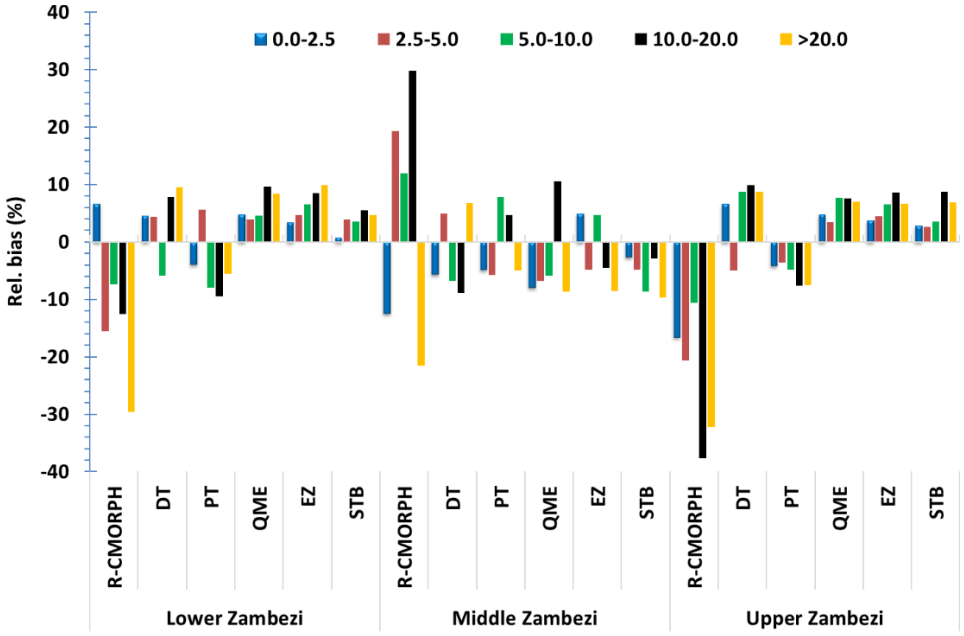

Figure 5.8: Bias correction (%) for respective rainfall rate (mm/day) classes

5.3.4. Spatial cross-validation

Table 5.4 shows the cross-validation results on bias correction for 8 rain gauge stations in the wet and dry seasons. It is evident that CMORPH has a considerable bias, although this bias is not always consistent for all 8 validation stations. Overall, Mutarara station has the highest positive bias (overestimation) whereas Makhanga has the highest negative bias (underestimation) for uncorrected CMORPH. Bias is effectively being removed by the *STB* followed by the *EZ* bias correction schemes. Bias is more effectively removed for the wet season than for the dry season. For the dry season, the *STB* shows good performance for Mkhanga and Nchalo stations, whereas good performance is shown for Kabompo and Chichiri stations. However, the *MAE* is higher for the wet season than for the dry

season. Correlation coefficient for bias corrected satellite rainfall is higher for the wet season than for the dry season.

*Table 5.4: Cross validation results for the bias correction procedure with 8 gauging stations for the dry and wet season. Stations lie at average elevation zone and sort of centred in an elevation zone. R-CMORPH is the uncorrected R-CMOPRPH estimate. DT, PT, QME, EZ and STB are the bias corrected rainfall estimate. Bold values indicate best performance. * = zone 1: elevation of < 250 m, ** = zone 2: elevation range of 250 - 950 m and *** = zone 3: elevation > 950 m*

		Dry Season (April-Sept)			Wet Season (Oct-March)			
Station	Rainfall Estimate	*Rel. bias (%)*	*MAE* mm/day	Correlation	Estimated Ratio	*Rel. bias (%)*	*MAE* (mm/day)	Correlation
Makhanga*	R-CMORPH	-28.69	1.23	0.42	0.87	-21.17	8.63	0.43
	DT	-1.37	0.53	0.56	0.99	-1.66	3.96	0.65
	PT	-5.62	0.52	0.54	0.95	-3.5	4.67	0.64
	QME	1.98	0.54	0.54	0.95	-0.64	4.86	0.65
	EZ	2.10	0.47	0.55	1.03	-0.11	4.08	0.58
	STB	0.77	0.61	0.56	1.04	0.5	5.06	0.62
Nchalo*	R-CMORPH	-33.05	1.13	0.42	0.84	-25.18	8.05	0.38
	DT	-0.23	0.73	0.56	0.96	-2.61	3.65	0.50
	PT	-4.28	0.68	0.54	0.93	-6.48	5.05	0.59
	QME	1.90	0.72	0.53	0.81	-0.56	5.29	0.53
	EZ	0.35	0.63	0.54	0.99	**0.22**	4.4	0.60
	STB	-0.43	0.73	0.58	0.96	-1.23	5.54	0.61
Rukomichi**	R-CMORPH	-23.05	0.93	0.42	0.86	-21.18	6.69	0.31
	DT	-0.23	0.90	0.56	0.94	-6.2	3.51	0.60
	PT	-4.28	0.73	0.54	0.93	-2.48	3.62	0.59
	QME	1.90	0.75	0.53	1.03	-0.56	3.88	0.54

	EZ	0.35	0.71	0.54	0.99	**0.22**	3.5	0.60
	STB	-0.43	0.76	0.58	0.94	-1.26	3.33	0.61
Mutarara**	R-CMORPH	20.15	0.24	0.49	1.10	20.1	2.34	0.50
	DT	11.4	0.18	0.60	1.03	8.7	1.23	0.63
	PT	8.4	0.12	0.55	0.91	4.3	1.28	0.68
	QME	5.7	0.14	0.63	1.1	8.1	1.4	0.65
	EZ	-12.8	**0.09**	0.54	0.95	1.9	1.23	0.69
	STB	4.5	0.14	0.53	1.1	2.1	1.33	**0.73**
Mfuwe**	R-CMORPH	40.2	0.28	0.45	0.85	35.4	6.4	0.48
	DT	2.9	0.62	0.53	0.96	4.6	3.9	0.62
	PT	3.7	0.22	0.55	0.92	7.9	5.25	0.65
	QME	3.9	0.30	0.55	0.93	5.4	5.68	0.64
	EZ	6.1	0.24	0.54	0.92	3.8	5.18	0.56
	STB	5.4	0.26	0.65	0.93	1.2	4.66	0.65
Kabombo***	R-CMORPH	25.3	0.70	0.44	0.95	24.3	3.8	0.48
	DT	7.7	0.32	0.51	0.96	5.7	3.5	0.62
	PT	9.2	0.13	0.54	1.10	8.7	3.0	0.64
	QME	2.7	0.32	0.62	1.10	2.8	3.2	0.63
	EZ	5.6	0.22	0.53	0.91	3.3	2.7	0.54
	STB	19	0.13	0.62	1.01	9.3	2.7	0.64
Chichiri***	R-CMORPH	34.5	1.56	0.47	0.8	-37.3	4.7	0.45
	DT	12.2	0.60	0.51	0.85	5.5	3.2	0.51
	PT	9.4	0.42	0.52	1.04	-7.8	4.1	0.54
	QME	8.4	0.92	0.56	1.05	-13.0	4.1	0.64
	EZ	-13	0.61	0.60	0.94	-9.9	4.2	0.60
	STB	3.2	0.45	0.63	0.98	-14.3	2.1	0.65

Chitedze***	R-CMORPH	41.5	0.90	0.47	1.06	42.3	5.4	0.48
	DT	16.7	0.53	0.54	0.98	-13.2	3.3	0.62
	PT	-16.5	0.44	0.55	0.99	22.2	4.5	0.65
	QME	18.2	0.41	0.57	1.04	18.5	4.3	0.64
	EZ	11.7	0.32	0.57	1.02	8.4	4.6	0.55
	STB	3.9	0.23	0.60	0.03	-8.2	3.7	0.65

5.3.5. Temporal cross-validation

The same performance indicators in spatial cross-validation are calculated for the temporal cross-validation. Results are presented in Table 5.5. The *MAE* is higher for the wet season than for the dry season. The difference in effectiveness in the error removal between the dry and wet season is much larger. *STB* outperforms both bias correction methods but does also have problems correcting the estimated ratios. After the correction, the correlation coefficient much improved. The fact that *MAE* remains relatively large indicates that errors remain locally large. These values are almost in the same range to the performance indicators obtained from the main performance assessment period (1999-2013). The estimated ratio shows improvement for the Middle Zambezi compared to the Lower and Upper Zambezi.

Table 5.5: Temporal-cross validation results for the period 1998-1999 for the wet and dry season.

		Dry Season (April-Sept)				Wet Season (Oct-March)		
	Rainfall Estimate	*Rel. bias (%)*	*MAE* (mm/day)	Correlation	Estimated Ratio	*Rel. bias* (%)	*MAE* (mm/day)	Correlation
Lower Zambezi	*R-CMORPH*	-28.26	1.10	0.42	0.86	-22.51	7.79	0.37
	DT	-0.61	0.72	0.56	0.96	-3.49	3.71	0.58
	PT	-4.73	0.64	0.54	0.94	-4.15	4.45	0.61
	QME	1.93	0.67	0.53	0.93	-0.59	4.68	0.57

	EZ	0.93	0.60	0.54	1.00	0.11	3.99	0.59
	STB	-0.03	0.70	0.57	0.98	-0.66	4.64	0.61
Middle Zambezi	*R-CMORPH*	28.55	0.41	0.46	0.97	26.60	4.18	0.49
	DT	7.33	0.37	0.55	0.98	6.33	2.88	0.62
	PT	7.10	0.16	0.55	0.98	6.97	3.18	0.66
	QME	4.10	0.25	0.60	1.04	5.43	3.43	0.64
	EZ	-0.37	0.18	0.54	0.93	3.00	3.04	0.60
	STB	9.63	0.18	0.60	1.01	4.20	2.90	0.67
Upper Zambezi	*R-CMORPH*	38	1.23	0.47	0.93	2.5	5.05	0.465
	DT	14.45	0.565	0.525	0.915	-3.85	3.25	0.565
	PT	-3.55	0.43	0.535	1.015	7.2	4.3	0.595
	QME	13.3	0.665	0.565	1.045	2.75	4.2	0.64
	EZ	-0.65	0.465	0.585	0.98	-0.75	4.4	0.575
	STB	3.55	0.34	0.615	0.505	-11.25	2.9	0.65

5.4 Discussion

The study presents methods to assess the performance of bias correction schemes for CMORPH rainfall estimates in the Zambezi River Basin. For correction, sequential windows of 7 days that count 5 rainy days with rainfall threshold of 5 mm/day were applied. First, the study aimed at evaluating if performance of CMORPH rainfall is affected by elevation and distance from large scale open water bodies. Results in Taylor diagrams show that effects of distances > 10 km are minimal in this study. For distance < 10 km, results in the same Taylor diagrams shows some effect with increased CMORPH estimation errors although not clearly identifiable by the limited number of gauging stations at distance < 10 km. More pronounced effects of bias effects at short distances (< 10 km) is shown in Haile *et al.* (2009) for the Lake Tana, Ethiopia. The low number of gauge stations constrains clear identification of bias as effected by the short distance. The low number of stations also constrains detailed analysis on dependencies of observation time series. To assess bias effects at distances < 10 km the study advocates installation of a well-designed network of rain gauges

with stations located at preselected locations that would allow sound geostatistical analysis on small scale rainfall variability and spatial correlation analysis. Ciach and Krajewski (2006) present such analysis for a dense experimental network of 53 stations. The inter-station distance of the rain gauges in this study is too large to capture the effect of distance to large scale open water bodies on CMORPH rainfall error. For instance, such distance exceeds 350 km for most of Upper Zambezi Basin. Findings in this study show that effects of distance would be captured at distances 10-25 km or shorter.

The rainfall-elevation bias correction also shows minimal signal. Contrary to this finding, Romilly and Gebremichael (2011) showed that the accuracy of CMORPH at monthly time base is related to elevation for six river basins in Ethiopia. A similar finding was reported by Haile *et al.* (2009), Katiraie-Boroujerdy *et al.* (2013) and Wu and Zhai (2012) who found that performance of CMORPH is affected by elevation. However, Vernimmen *et al.* (2012) concluded that TRMM Multi-satellite Precipitation Analysis (TMPA) 3B42RT performance was not affected by elevation ($R^2 = 0.0001$) for Jakarta, Bogor, Bandung, Java, Kalimantan and Sumatra regions (Indonesia). The study by Gao and Liu (2013) showed that the bias in CMORPH rainfall over the Tibetan Plateau is affected by elevation. Whereas distance from large scale open water bodies and elevation have been assessed separately for this study, Habib *et al.* (2012a) revealed that both aspects interact in the Nile Basin to produce unique circulation patterns to affect the performance of SRE.

Second, this study evaluated the effectiveness of linear/non-linear and time-space variant/invariant bias correction schemes. The bias correction results by means of evaluation indicators such as Taylor Diagrams, q-q plots, ANOVA and standard statistics such as mean, max, ratio of rainfall totals and bias reveal that the *STB* is the best performing bias correction method in this study. This method by its nature, consider correction for temporal and spatial distributed patterns in bias, commonly known as space and time variant/invariant and thus effective in bias removal. This study did not investigate effects of the applied sequential windows of 7 days for each bias correction scheme separately but note that other window lengths possibly could yield more favourable results for bias schemes such as *PT, DT* and *QME*. As indicated by Habib *et al.* (2013), correction should improve hydrological applications by improved rainfall representation. This applies to Zambezi basin as well with demands for applications of the product such as for drought analysis, flood prediction, weather forecasting and rainfall-runoff modelling. The study is unique as it assesses the importance of space and

time aspects of CMORPH bias for rainfall-runoff modelling in a data scarce catchment. Findings in this study on cross and temporal validation contribute to efforts that aim towards enhancing applications of satellite rainfall products. The study site was the Zambezi Basin, an example of many world regions that can benefit from satellite-based rainfall products for resource assessments and monitoring.

Third, an assessment of the performance of bias correction schemes to represent different rainfall rates and climate seasonality is presented. Findings in this study show that bias is overestimated most for the very light rainfall (< 2.5 mm/day), which is also the range that shows the best bias reduction, that in turn is most effective during the wet season. Results also show that there is underestimation of rainfall larger than 20 mm/day. The poor performance of correction for the heavy rainfall class is caused by, sometimes, large mismatch of high rain gauge values versus low CMORPH values. This leads to unrealistically high CMORPH values which remain poorly corrected by bias schemes. Results are consistent with findings by Gao and Liu (2013) in the Tibetan Plateau who found consistent under and overestimation of occurrence by CMORPH for rainfall rates > 10 mm/day. A study by Zulkafli *et al.* (2014) in French Guiana and North Brazil noted that the low sampling frequency and the consequently missed short-duration precipitation events in between satellite measurements resulted in underestimation, particularly for rainfall > 20 mm/day.

Lastly, spatial and temporal cross validation reveal effectiveness of bias correction schemes. The hold-out sample of 8 stations in this work showed the applicability of different bias correction methods under different geographical domains. Based on correlation coefficient and *MAE,* this study showed that effectiveness in bias removal in the wet season is higher than in the dry season. This result is contrary to Vernimmen *et al.* (2012) who showed that for the dry season, bias for PT decreased in Jakarta, Bogor, Bandung, East Java and Lampung regions after bias correction of monthly TMPA 3B42RT precipitation estimates over the period 2003–2008. Ines and Hansen (2006), for semi-arid eastern Kenya, showed that multiplicative bias correction schemes such as *STB* were effective in correcting the total of the daily rainfall grouped into seasons. Habib *et al.* (2014) evaluated sensitivity of *STB* for the dry and wet season and concluded that the bias correction factor for CMOPRH shows lower sensitivity for the wet season as compared to the dry season. Findings in this study also reveal that bias factors for all the schemes are more variable in the dry season

than in the wet season and cause poor performance of the bias correction schemes in the dry season.

5.5 Conclusions

The following is concluded:

i. Analysis on gauge and CMORPH rainfall estimates show that performance increases for areas at higher elevation (> 950 m) in the Zambezi Basin and that CMORPH has largest mismatch at low elevation. Such analysis was performed for rain gauges within elevation classes of < 250 m, 250 - 950 m and > 950 m. The match between gauge and CMORPH estimates improved at increasing distance to large scale open water bodies. This was shown for rain gauges located in between distances of 10 - 50 km, 50 - 100 km and > 100 km to a large scale open water body. For distances < 10 km errors by CMORPH increased but the small sample size of stations and the weak signal require further study. To assess how bias is affected at short distance to a large scale water body, a specifically designed and dense gauging network is advocated (see Ciach and Krajewski, 2006) that allow evaluation of small scale rainfall variability. A detailed analysis on small spatial variability and spatial correlation analysis of rain gauged observations presumably is prerequisite before effects of satellite rainfall at short distance to a large scale water body can be assessed.

ii. For each of the five bias correction methods applied, accuracy of the CMORPH satellite rainfall estimates improved. Assessment through standard statistics, Taylor Diagrams, t-tests, ANOVA and q-q plots shows that STB is most effective in reducing rainfall bias as comparted to remining bias correction schemes. Findings on bias correction indicate that the temporal aspect of CMORPH bias is more important than the spatial aspect in the Zambezi Basin. Quantile-quantile (q-q) plots for all the bias correction schemes in general show that bias corrected rainfall is in good agreement with gauge-based rainfall for low rainfall rates but that high rainfall rates are largely overestimated.

iii. Differences in the mechanisms that drive precipitation throughout the year could result in different biases for each of the seasons, which motivated this study to calculate the bias correction factors for dry and wet seasons separately. As such CMORPH rainfall time series were divided to assess the influence of seasonality on performance of bias correction schemes. Overall,

the bias correction schemes reveal that bias removal is more effective in the wet season than in the dry season.

iv. The study assessed whether bias correction varies for different rainfall rates of daily rainfall in the Zambezi Basin. There is overestimation of very light rainfall (< 2.5 mm/day) and underestimation of very heavy rainfall (>20 mm/day) after application of the bias correction schemes. Bias was more effectively reduced for the very light (< 2.5 mm/day), to moderate (5.0-10.0 mm/day) rainfall compared to the heavy (10.0-20.0 mm/day) and very heavy (> 20 mm/day) rainfall. Overall, the *STB* and *EZ* more consistently removed bias in all the rainy days compared to the three other bias correction schemes. Effects of length of sequential window sizes for selected bias correction schemes is not investigated but different lengths possibly could yield more favourable results for *PT, QME* and *DT* bias correction schemes.

v. Analysis serves to improve reliability of SREs applications in hydrological analysis and water resource applications in the Zambezi basin such as in drought analysis, flood prediction, weather forecasting and rainfall-runoff modelling.

Chapter 6: Hydrologic evaluation of bias corrected CMORPH rainfall estimates at the headwater catchment of the Zambezi River *

6.1 Introduction

The global importance of SREs has led to a large number of studies aimed to assess the accuracy of various SRE products for streamflow simulation. The major limiting factor in the adoption of SREs for streamflow simulation is that they contain random and systematic errors also known as bias (Maggioni and Massari, 2018). Sampling errors are determined by the satellite orbit, swath width, and space-time characteristics of the rainfall (Kling *et al.*, 2014). Errors in rain detection and rain rate estimation can both play an important role in streamflow simulation (Vu *et al.*, 2018). In this study, focus is on the National Oceanic and Atmospheric Administration (NOAA) Climate Prediction Center-MORPHing rainfall product (CMORPH) (Joyce *et al.*, 2004; Wehbe *et al.*, 2017) which is one of the most widely-used precipitation products of satellite remote sensing that provides tremendous information for hydrological application. Studies on CMORPH in the Southern Africa's Zambezi River Basin (Lekula *et al.*, 2018; Meyer *et al.*, 2017; Toté *et al.*, 2015) show evidence that necessitates bias correction of the product.

Hydrological modelling by use of CMORPH rainfall estimates commonly is assessed at catchment scale with specific focus on the streamflow simulation (Bajracharya *et al.*, 2014; Liu *et al.*, 2017; Thiemig *et al.*, 2013). In catchments where uncorrected CMORPH has been used for streamflow simulation, such often caused unsatisfactory model performance. Few examples are the following. For Shehong basin in southeast China the CREST model had poor performance in streamflow simulation (Ma *et al.*, 2018). Tong *et al.* (2014) report on an application of uncorrected CMORPH to the upper Yellow and Yangtze River

---

***This chapter is based on the paper:** W. Gumindoga, T.H.M. Rientjes, P. Reggiani A.T. Makurira H and Haile A. (2020): Hydrologic evaluation of bias corrected CMORPH rainfall estimates at the headwater catchment of the Zambezi River, *Physics and Chemistry of the Earth 115 (2020) 102809*. https://doi.org/10.1016/j.pce.2019.11.004

Basins on the Tibetan Plateau to result in poor performance of the Variable Infiltration Capacity (VIC) hydrologic model on a daily and monthly time interval. Gosset *et al.* (2013) used two simplified hydrological models in West Africa (SCS in Niger and GR4J in Benin) to illustrate that a correction is needed for CMORPH rainfall. In both Niger and Benin, the bias in the annual simulated runoff volume more than doubled for uncorrected CMORPH. The above studies concluded that SREs cannot be used directly as meteorological forcing term in hydrological models without bias correction. Studies further shows that hydrologic simulations using uncorrected SREs are inferior in performance to simulations that employ even just a few ground-based rain gauges (Stisen and Sandholt, 2010), to illustrate that bias correction is a necessity.

In this study the spatial and temporal aspects of the bias are used to correct the bias of CMORPH at a daily timescale. Studies show that the time and space bias correction method (Bhatti *et al.,* 2016; Gumindoga *et al.,* 2017; Habib *et al.,* 2014a) yields reasonable streamflow performance over African Basins. Habib *et al.* (2014b) calibrated the Hydrologiska Byråns Vattenbalansavdelning (HBV-96) streamflow model in the Gilgel Abay basin (Ethiopia) using gauge and CMORPH rainfall inputs for the year 2003–2004 to evaluate the effect of bias correction in CMORPH on HBV-96 model simulations. Results show that the streamflow hydrograph that is simulated by considering spatial temporal variability in the CMORPH bias produced the best result compared to other schemes that do not consider spatial temporal variability in the rainfall bias. Observations were made for patterns, observed peak flows and volumes with observed streamflow hydrographs as reference. In the Awash River basin in Ethiopia, Likasa (2013) reports improved model performance of the HBV-96 rainfall-runoff model after spatial and temporal aspects in the bias corrected CMORPH rainfall are considered to force the model. In developing a bias correction approach for this work, preference was to keep bias correction simple to remove most important biases (the mean, variability and autocorrelation structure).

Hydrologic model recalibration has been proven to be a viable strategy for improving model performances when SREs served to force the model behavior, such for basins of different size, and climatology across regions of the world (Falck *et al.,* 2015). Habib *et al.* (2014) and Liu *et al.* (2017) show that for optimal model performance, model parameters of streamflow models should be recalibrated when rain gauge inputs are replaced by bias corrected SREs as model forcing terms. By difference in rainfall estimates, use of bias corrected rainfall as compared to rain gauge rainfall will affect water storage in respective model

stores (Habib *et al.,* 2014a; Valdés-Pineda *et al.,* 2016). It is likely that model recalibration is able to reduce for model simulation discrepancies and to obtain optimal model performances according to a pre-defined criterion (Behrangi *et al.*, 2011; Tobin and Bennett, 2010).

The objective of this study is to evaluate application of CMORPH SREs for streamflow modelling in the Kapombo River basin by the REW model. The specific objectives are i) to evaluate time and space variable bias correction for streamflow simulation ii) to assess how the REW hydrological model parameterization changes when uncorrected and bias corrected SREs serve for model forcing instead of rain gauge data and iii) to apply parameter sensitivity analysis for low and high flows. Analysis serves to improve applications of SREs in the Zambezi basin such as for rainfall-runoff modeling.

6.2 Methodology

6.2.1. Comparison of rainfall estimates by CMORPH and rain gauges

In this study, and for all pixels in the study area, the study compares time series of rain gauge rainfall with uncorrected and corrected CMORPH SRE using two approaches. The first approach that is commonly referred to as point-to-pixel comparison, compares rain gauge rainfall at point scale (i.e. gauge funnel scale) to CMORPH SRE at pixel scale (see Cohen Liechti *et al.*, 2012; Dinku *et al.*, 2008; Haile *et al.*, 2014; Hughes, 2006; Tsidu, 2012; Worqlul *et al.*, 2014). In the second approach that is commonly referred to as pixel-to-pixel comparison, the study compares spatially interpolated gauged rainfall estimates at pixel scale to CMORPH based counter parts at equal spatial grid resolution and projection (Heidinger *et al.*, 2012; Li and Heap, 2011; Tobin and Bennett, 2010; Yin *et al.*, 2008). Spatially interpolated rain gauge rainfall serves to represent rainfall distributions across the area of study.

In the procedure to select a suitable interpolation method, a sensitivity analysis based on two interpolation techniques: Universal Kriging (Fang *et al*., 2015) and Inverse Distance Weighted interpolation (IDW) (Parida *et al.,* 2017; Shepard, 1968) is carried out. A conclusion was drawn on which technique is most effective in representing mean annual rainfall in the Kabompo Basin for the dry and wet season (2000-2015 period). The study indicated that the IDW performed better than Universal Kriging for the dry and wet season in the representation of mean annual rainfall and peak streamflow. As such, IDW was selected as the

interpolation technique for the pixel-to-pixel rainfall estimation method. Studies by Parida *et al.* (2017) and Bhatti *et al.* (2016) employed IDW technique for interpolating daily rainfall from rain gauges at respective point locations to grid points for comparison with CMORPH estimates.

6.2.2. Bias correction of CMORPH SRE

Bias correction approach

In this part of this thesis study, bias in CMORPH rainfall estimates was assessed and subsequently corrected using a time and space linear multiplicative shift bias correction technique, also known as the Spatio-temporal bias correction. Detailed description of the procedure is found in section 5.3.3. as well as equation [5.1].

Evaluation of corrected and uncorrected CMORPH estimates

Corrected and uncorrected CMORPH SRE (S_i) are evaluated with reference to rain gauge rainfall (G_i) at a certain day *(i)* for the period covering 2003-2015. Comparison is for the following performance indicators: mean, minimum, maximum, rainfall totals, standard deviation, relative bias *(Rel. bias (%))*, correlation coefficient *(R)* and Nash Sutcliffe Efficiency *(NSE)*. *Rel. bias*, *R* and *NSE* are described in equations 5.8, 5.9 and 5.11 respectively in Chapter 5. *RMSE* represents aggregated squared residual errors between CMORPH and rain gauge rainfall. *RMSE* needs to be minimized so smaller values indicate that performance of SRE's has improved (Chai *et al.*, 2014). Equations [6.1] apply.

$$RMSE = \sqrt{\frac{1}{n}\sum_{i=1}^{n}(S_i - G_i)^2} \qquad [6.1]$$

where:

n = *length of bias correction window in days*

For graphical evaluation, a Taylor diagram was applied that provide a statistical summary of how well time series of the different rainfall estimates (corrected and uncorrected) match in terms of the Pearson's product-moment correlation coefficient *(R)*, root mean square difference *(E)*, and the ratio of variances on a 2-D plot (Baker and Taylor, 2016; Taylor, 2001). Equation [*5.12*] applies.

Besides patterns that have the right amplitude, the effectiveness of a bias correction scheme is seen in terms of data that lie near a point marked 'reference' on the x-axis, relatively high correlation coefficient and low root mean square difference.

6.2.3. Cross-validation of bias correction

In this study, CMORPH is evaluated in the time domain by omitting gauge and SRE for the 1998-1999 hydrological year to remain with 15 years (2000-2015) for bias correction (after Gutjahr and Heinemann, 2013). The 15 year-bias corrected estimates are cross validated against estimates for 1998-1999 period that served as reference. Performance indicators used for evaluation are *Rel. bias (%),* correlation coefficient and the estimated ratio which were all averaged for the Kabompo Basin but also summarised for the wet and dry seasons. The wet season for the Kabompo basin covers the months October-March whereas the dry season covers April-September.

6.2.4. Modelling approach

The selected hydrological modelling approach is based on the discretization of a watershed into three-dimensional units, so called Representative Elementary Watersheds (REWs). In first publications on the REW approach (Reggiani *et al.*, 1998), the model is described as an innovative hydrological model that simulates runoff and streamflow at the sub-watershed scale. In this study, SRE data as well as satellite-based land cover and terrain data are prepared as model inputs. In the modelling approach, REWs make up the semi-distributed model domain. REWs constitutes a set of interconnected prismatic volumes that are organized around the stream channel network. Detailed descriptions on REW flow algorithms and typical model implementation are found in Chapter 3 as well as in Reggiani *et al.* (1999) and Reggiani and Rientjes (2005). Recent applications of the model are found in Reggiani *et al.* (2014), Reggiani and Hassanizadeh (2016), Elgamal *et al.* (2017).

6.2.5. Calibration strategy

As a first step in the modelling to evaluate effects of use of SREs, the model was initialized, calibrated and validated based on in situ rain gauge observations. Initialization or warming of the model was for the hydrological year October 2003–September 2004. Based on the split-sample test, the period October 2004–September 2007 was selected for model calibration and the period 2008–2010 for model validation. Results of streamflow simulation were evaluated by comparing observed and simulated streamflow by Nash-Sutcliffe Efficiency *(NSE)* and

Relative Volume Error *(RVE)* (equations 6.3 and 6.4 respectively) objective functions. In hydrological modelling practice a *NSE* of 0.6 in general indicates fair model performance, a value 0.8 indicates good performance. *RVE* can vary between +∞ and −∞ with optimum value of 0. A *RVE* between +5 % to −5 % indicates a well performing model whereas a *RVE* between +5 % and +10 % and −5 % and −10 % indicates fair model performance (Janssen and Heuberger, 1995). Interpreting model performance indices is not trivial and refer to Rientjes *et al.* (2011) as well as Schaefli and Gupta (2007) for further discussion. Equation 6.2 – 6.3 applies.

$$NSE = 1 - \frac{\sum_{i=1}^{n}(Q_{sim,i} - Q_{obs,i})^2}{\sum_{i=1}^{n}(Q_{obs,i} - \overline{Q_{obs}})^2} \quad [6.2]$$

$$RVE = \frac{\sum_{i=1}^{n}(Q_{sim,i} - Q_{obs,i})}{\sum_{i=1}^{n} Q_{obs,i}} \times 100\ \% \quad [6.3]$$

where:

Q_{obs} = *observed streamflow (m^3/s) at a certain day i*

$\bar{Q}_n$ = *mean of observed streamflow (m^3/s)*

Q_{sim} = *simulated streamflow (m^3/s) at a certain day i*

n = *number of time steps,*

In this thesis chapter, calibration was performed by trial and error in which the model parameters were manually adjusted to optimize model performance. Initial values for the following parameters were set by considering values from previous studies (Reggiani and Rientjes, 2005, 2010; Varado *et al.*, 2006): Soil porosity, Saturated hydraulic conductivity, At a station depth scaling exponent, Discharge area scaling coefficient and Water content at saturation.

The first step in calibration aimed at simulation of baseflow in the dry season after which calibration aimed at higher streamflow in the wet season. Further optimization aimed at matching streamflow for recession periods, for rising limb of the simulated hydrograph and for timing of the peak flow discharges.

6.2.6. Model parameter optimization using different rainfall inputs

Following the calibration procedure described above, model simulations were evaluated for uncorrected and for bias corrected rainfall for the period 2008-2013.

Uncorrected and bias corrected CMORPH estimates were extracted for each of the 29 REWs to represent rainfall across the study area. Since this study aims to assess how optimized model parameter values are affected by bias in the rainfall input, the model was manually recalibrated for the parameters listed in section 6.3.4 when bias corrected and uncorrected rainfall SREs serves as rainfall forcing. Since rainfall inputs are dissimilar, it is hypothesised that parameter values and model performance as measured by *NSE* and *RVE* objective functions are affected when in situ rainfall was replaced by SREs. Parameters were manually adjusted one by one in the model to find best fit for in situ-based rainfall and SRE.

Rainfall bias is defined as the systematic differences (errors) between gauge and SREs. Mismatch between simulated and observed streamflow is subject to respective rainfall input data source and thus streamflow results are affected by rainfall bias. Mismatch in this study is expressed for mean daily values for the period 2008-2013. *Rel. bias (%)* is calculated for gauge vs SRE and further between simulated and observed flow. Any effect of rainfall bias to affect streamflow simulation results is referred to as SRE error propagation.

6.2.7. Sensitivity analysis for flow categories and seasons

The Chapter applies parameter sensitivity analysis for daily streamflow. Three classes are defined from 3 quantiles which indicate low (25th percentile), intermediate (25th -50th percentile) and high flows (75th percentile). For this, quantiles are developed for the period 2008-2013 from the flow duration curve via the FDC 2.1 software *https://hydrooffice.org/Downloads?Items=Software*. Flows were also divided into wet and dry seasonal periods to assess the influence of seasonality on parameter sensitivity. The *NSE* and *RVE* serve for performance assessment.

6.3 Results

6.3.1. Results on rainfall bias correction

Table 6.1. shows the *Rel. bias (%)* from 2004-2013 for the uncorrected and corrected CMORPH estimates with reference to the gauge-based rainfall. Uncorrected CMORPH shows substantial overestimation of rainfall for the point-to-pixel (> 15 %) and for pixel-to-pixel (> 13 %) rainfall comparison respectively. Significant underestimation of rainfall is also shown for point-to-pixel (< -21 %) and for pixel-to-pixel (< -10 %) rainfall comparison. After bias correction, substantial improvement for correlation coefficient *(R)* at daily base is observed

for Kasempa station in the point-to-pixel comparison (0.19 to 0.72) as well as for pixel-to-pixel rainfall comparison (0.37 to 0.79). In all 6 stations, bias correction for rainfall totals is effective. The study refers to Mwinilunga station in the Northern part of the basin where the ratio between rain gauge and CMORPH estimates improved after bias correction from 1.07 to 1 for point-to-pixel, and from 1.16 to 1.02 for pixel-to-pixel rainfall estimates. After bias correction, the highest *NSE* is shown for Solwezi station (7.0) for pixel-to-pixel rainfall comparison.

Table 6.1: Statistical scores for bias corrected and uncorrected CMORPH vs gauge-based rainfall (2004-2013) Top rows show point-to-pixel comparison, bottom rows show pixel-to-pixel comparison. UC shows uncorrected CMORPH, BC shows bias corrected CMORPH. Bold shows best performance.

		Kalabo		**Kaoma**		**Kasempa**		**Mwinilunga**		**Solwezi**		**Zambezi**	
		UC	BC	UC	BC	UC	BC	UC	BC	UC	BC	UC	BC
Point - to - pixel	*Rel. bias (%)*	9.94	4.33	12.16	3.84	15.91	-5.8	-21.86	-4.04	20.8	2.74	5.97	2.29
	RMSE	3.29	-2.4	3.25	1.86	8.39	-4.63	3.17	**0.14**	-2.69	7.67	-5.4	4.11
	R	0.23	0.41	0.27	0.63	0.19	0.74	0.26	0.65	0.16	0.55	0.15	0.58
	NSE	0.59	0.64	0.61	0.64	0.65	0.68	0.58	0.63	0.63	0.65	0.64	0.69
	Ratio	1.07	0.98	1.1	1.03	1.3	0.94	1.07	**1**	1.14	1.01	0.83	1.02
Pixel-to - Pixel	*Rel. bias (%)*	7.19	2.83	9.9	4.8	13.29	-3.75	-10.27	-3.43	10.29	2.48	-4.86	**-0.86**
	RMSE	4.19	2.63	8.92	3.33	8.44	6.2	-6.05	2.05	-6.23	-2.45	7.44	5.44
	R	0.35	0.67	0.42	0.71	0.37	**0.79**	0.53	0.68	0.41	0.71	0.42	0.68
	NSE	0.62	0.64	0.61	0.69	0.64	0.69	0.67	0.69	0.68	**0.70**	0.67	0.69
	Ratio	1.06	1.01	1.02	1 1	0.83	**1**	1.16	1.02	1.10	1.02	1.07	1.01

The Taylor Diagram (Figure 6.1) shows effectiveness of the bias correction scheme when results of individual stations are combined and presented for the whole basin. In terms of bias removal, the pixel-to-pixel rainfall comparison shows better performance than the point-to-pixel comparison. This is evidenced by the position of the red rectangle representing the pixel-to-pixel bias corrected rainfall estimate which is relatively closer to the reference point and almost lies at the reference line of rain gauge standard deviation. The performance for the Kabompo basin as a whole, resembles that reported for individual stations.

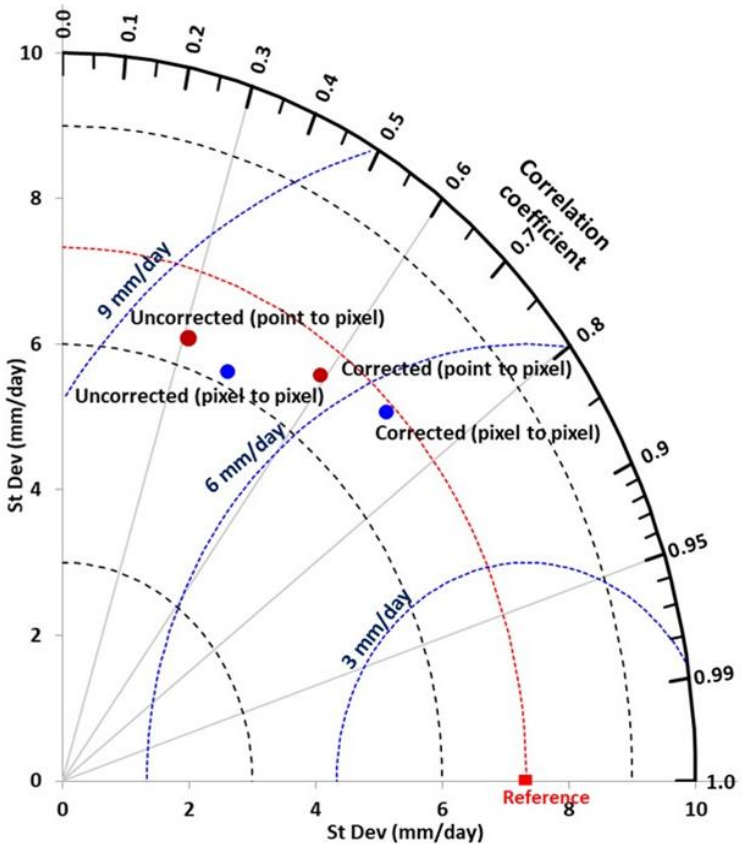

Figure 6.1: Taylor's diagram showing comparison between the daily time series of rain gauge (reference) observations vs CMORPH corrected rainfall averaged for the Kabompo Basin for the period 2000-2015. The distance of the symbol from point (1, 0) is a relative measure of the bias correction performance. The position of each symbol appearing on the plot quantifies how closely precipitation estimates by a respective bias-correction scheme match counterparts by rain gauges. The blue contours show RMSE (mm/day).

6.3.2. Results of split-sample cross-validation

Table 6.2. shows performance indices for the dry and wet season, calculated for *Rel. bias (%)*, correlation and estimated ratio within the split-sample cross-validation framework. Results are summarised for the Kabompo basin but comparison of rain gauge and CMORPH rainfall achieved by the point-to-pixel and pixel-to pixel techniques. There is much more improved correlation for the wet season as compared to the dry season. Negative *Rel. bias (%)* which imply underestimation by CMORPH are observed for the wet season (max of -11.59 %) as compared to the dry season. Positive *Rel. bias (%)* which signify overestimation are observed in the dry season (max of 33.28 %), this for uncorrected CMORPH. On the opposite, estimated ratio's shows much more improvement for the dry season than the wet season. Except for the estimated ratio, *Rel. bias (%)* and correlation coefficient *(R)* shows better performance for the pixel-to-pixel than for the point-to-pixel comparisons. Results for the split sample cross-validation approach resembles the ones obtained in the main performance assessment period (2000-2015). The linear bias correction scheme results are applicable in the two time periods.

Table 6.2: Cross-validation results for the period 1998-1999 for the wet and dry seasons

		Dry Season (April-Sept)			Wet Season (Oct-March)		
	Rainfall Estimate	*Rel. bias (%)*	*R*	Estimated Ratio	*Rel. bias (%)*	*R*	Estimated Ratio
Point-to-pixel	Uncorrected	20.15	0.44	0.92	-11.59	0.49	0.78
	Bias corrected	4.80	0.59	**1.00**	**1.17**	0.61	1.01
Pixel-to-pixel	Uncorrected	33.28	0.47	0.95	14.55	0.52	0.84
	Bias corrected	6.59	0.61	0.98	-3.53	**0.69**	0.97

6.3.3. REW model results

Calibration and validation results

In this study, calibration was based on the gauge-based rainfall estimates. In all cases (point-to-pixel and pixel-to-pixel), manually calibrated parameters sets were applied for uncorrected and bias corrected rainfall inputs. Figure 6.2. shows

the REW model calibration results. The REW model is able to reproduce the streamflow hydrograph for wet seasons with *NSE* of 0.70 and *RVE* of 3 %. The time to peak for the simulated streamflow for the 2005 season lags behind the observed streamflow. The *NSE* for the point-to-pixel comparison is 0.78 and the model shows overestimation of streamflow (*RVE* = 4%). The model overestimates peaks with threshold > 800 m^3/s. In Elgamal *et al.* (2017) using the REW approach in Magdalena River Basin, Colombia, underestimation of highest peaks is shown, and possibly may be attributed to an uncertain stage-discharge relationship for high flows, or model deficiencies in representing the mechanisms that contribute to rapid response of the subsurface system.

Figure 6.3. shows observed and simulated streamflow for the validation period (2007-2010). The model is able to reproduce the observed streamflow although highest peaks are overestimated. *NSE* and *RVE* for the validation period are 0.67 and 8 %, respectively, and indicate satisfactory model performance. As such rainfall is accumulated to cause gradual changes in storage and delayed streamflow.

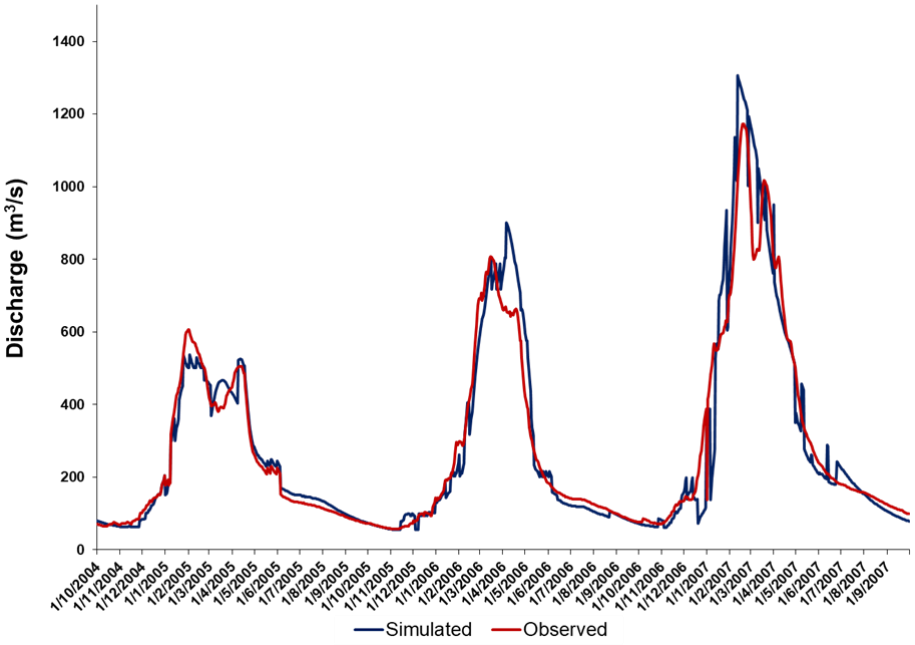

Figure 6.2: Results of streamflow for Sept 2004 - October 2007 by manual model calibration using in situ-based rainfall input.

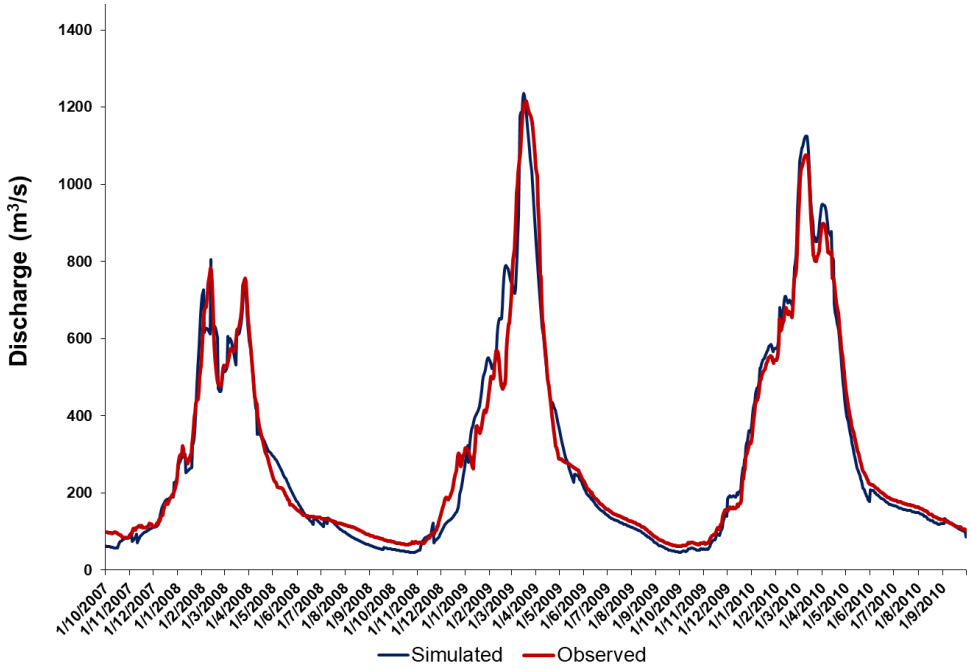

Figure 6.3: Results of model validation for the period Sept 2007-October 2010 by manual model calibration using in situ-based rainfall input.

Effects of uncorrected and bias corrected CMORPH rainfall on streamflow simulation

For the 2008-2013 period, the REW model is used to evaluate how corrected and uncorrected CMORPH rainfall estimates effect simulated streamflow. Note that the following REW model parameters were recalibrated for respective rainfall sets, and were applied for each case: Soil porosity, Saturated hydraulic conductivity, At a station depth scaling exponent, Discharge area scaling coefficient and Water content at saturation. Table 6.3. shows that the simulated streamflow hydrograph using rain gauge rainfall generally resembles the observed streamflow and indicates the best performance as compared to the use of uncorrected and bias corrected SREs. The uncorrected CMORPH estimates (point-to-pixel) show substantial overestimations for the mean streamflow (observed 296. m^3/s vs uncorrected CMORPH 332 m^3/s), as well as the 4-year streamflow totals (54.0×10^4 vs 59.2×10^4 m^3/s). Underestimations for the uncorrected CMORPH are found in the pixel-to-pixel comparison (mean discharge and streamflow total). When the model is forced with bias corrected CMORPH, the match between observed and simulated streamflow much improved for the pixel-to-pixel comparison (*NSE* = 0.69 and *RVE* = -3.8 %)

although overestimation and underestimation are still observed. For the point-to-pixel comparison, *NSE* and *RVE* also are satisfactory (0.62 and 5.4 %, respectively) but performance is little lower than for pixel-to-pixel comparison.

Table 6.3: Streamflow characteristics for observed and model simulations (Sept 2008-Oct 2013) for rain gauge, uncorrected and bias corrected rainfall inputs. RVE and NSE are shows as well. Bold = best performance. It should be clear what parameter set(s) have been used. only the set for in situ rainfall or the manually recalibrated sets.

		Observed runoff	Rain gauge simulated runoff	Uncorrected CMORPH simulated runoff	Bias corrected CMORPH simulated runoff
Point-to-pixel	Max (m^3/s)	1215	1285	1039	1291
	Mean (m^3/s)	296	3001	332	3156
	Streamflow total (m^3/s)	54.0×10^4	53.3×10^4	59.2×10^4	53.5×10^4
	RVE (%)		5.0	9.8	**5.4**
	NSE		0.70	0.59	0.62
Pixel-to-pixel	Max (m^3/s)	1215	1285	1125	**1227**
	Mean (m^3/s)	296	301	224	**292**
	Streamflow total (m^3/s)	54.0×10^4	53.3×10^4	49.9×10^4	53.3×10^4
	RVE (%)		5.0	-6.0	**-3.8**
	NSE		0.70	0.62	**0.69**

Figure 6.4. shows that for point-to-pixel rainfall comparison, 29 % *Rel. bias* in uncorrected CMORPH rainfall transform to 36 % streamflow increases whereas for pixel-to-pixel comparision, 18 % uncorrected CMORPH bias

transforms to 26 % streamflow increase. For bias corrected CMORPH, rainfall bias of 8 % transforms to 6 % streamflow reduction in the point-to-pixel rainfall comparison whereas 3 % of corrected CMORPH rainfall bias transforms to 2 % streamflow reduction. The amplification of streamflow by bias for uncorrected CMORPH rainfall input and the reduction of streamflow by bias for corrected CMORPH is referred to as error propagation. Overal, it can be observed that small changes in rainfall input propagate to a larger volumetric change in runoff simulation.

It should be noted that the model was manually recalibrated for the REW model parameter values when bias corrected and uncorrected rainfall SREs serves as rainfall forcing. Results show that even after re-calibration of the model, the bias cannot be totally eliminated. Since the manual re-calibration is not easily reproducible, the next chapter assesses the effect of automated parameter estimation with an optimization algorithm.

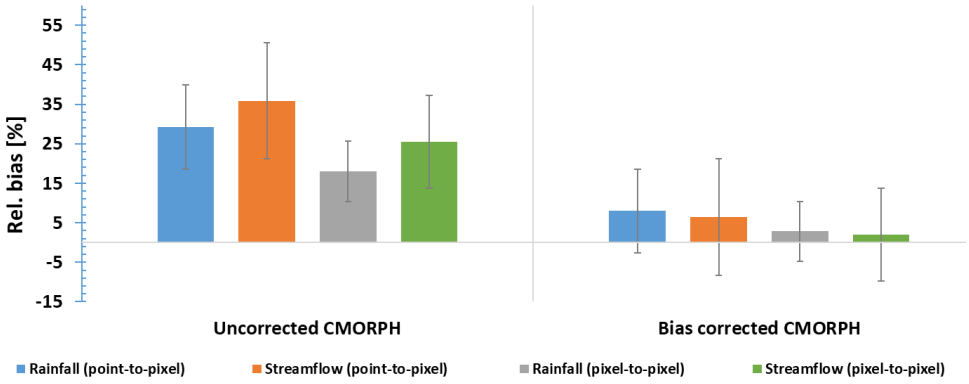

Figure 6.4: Rel. bias (%) change from rainfall input to REW streamflow simulation for point-to-pixel and pixel-to-pixel (2008-2013).

Parameter sensitivity analysis for low, intermediate and high flows

The study assessed how optimised model parameter values are affected by error in the rainfall inputs before and after bias correction is applied. As such, the model is manually recalibrated for each case following the introduction of uncorrected and bias corrected SRE. In theory, each rainfall input represents a specifc model forcing condition and may result in different parameter values and model performance as measured by *NSE* and *RVE*. The result of a simple sensitivity analysis achieved by manually changing one model parameter value while keeping others at their optimal value indicates that soil porosity and

saturated hydraulic conductivity are the most sensitive model parameters. Table 6.4. shows that when using rain gauge rainfall for the full period (2008-2013) most of the optimized parameter values are within the allowable value ranges for both the point-to-pixel and pixel-to-pixel comparisons. Through SRE recalibation, results also show that optimized parameter values are sensitive to the rainfall input as shown by some unexpected high or low parameter values. In particular even after bias correction, sensitive parameters that control the volume of the simulated hydrograph showed large changes of up to 21 % compared to the parameters using rain gauge input (both pixel-to-pixel and point-to-pixel input). Factors that control ground water table depth and thus groundwater contributions to simulate base flows are less affected. The largest discrepancy between optimized parameter values for gauge based and bias corrected SREs is found where there is largest rainfall underestimation. It can be noted that findings do not directly apply to other basins since model parameter optimization results are basin specific.

The study also notes that rainfall bias changes in the time domain over respective satellite pixels and thus it is uncertain how magnitude of bias affects streamflow characteristics. The aim is to evaluate parameter sensitivity for low, intermediate and high flows and to assess how *NSE* and *RVE* are affected subject to sensitivity. Model parameter values for intermediate flows are close to the initial values. Figure 7.8 shows that for high flows, large rainfall bias results in much more pronounced effects on the parameters than for low flows. This again affects parameters and refer to Valdés-Pineda *et al.* (2016) and Alazzy *et al.* (2017).

In the pixel-to-pixel and point-to-pixel comparison and for the low, intermediate and high flows, bias corrected CMORPH has improved *NSE* and *RVE*. The satisfactory model performance indicates the potential of CMORPH in water budget studies after applying a linear bias correction. The basin average CMORPH correction coefficients can be used to correct the bias of CMORPH where there is limited or no gauged rainfall data for the Kabompo basin. Findings indicate that the effect of different rainfall forcing becomes more tangible after recalibration.

Parameter sensitivity analysis for wet and dry season

Table 6.5. shows calibrated values of the REW model parameters for the dry and wet season. The values fall within their acceptable ranges and represent fairly the characteristics of the Kabompo basin's components, such as soil porosity,

saturated hydraulic conductivity, at a station depth scaling exponent and discharge area scaling coefficient. The soil porosity which is a function of the soil type, ranges from a lowest value of 0.5 to a highest of 0.65. Based on knowledge of the area, the higher porosity values were for the areas of sandy soil and wetland areas. Much more improved values are shown for the wet season as compared to the dry season. The saturated hydraulic conductivity slightly changed from its original value after calibration in the wet season. Major changes were observed for the dry season. After bias correction highest calibrated hydraulic conductivity of 0.008 m/s was shown for the point-to-pixel comparison as compared to 0.005 m/s for the pixel-to-pixel comparison.

6.4 Discussion

Rainfall-runoff modelling with bias corrected SREs is not yet explored in the Kabompo basin despite the strategic importance of the basin. This study aimed to evaluate effectiveness of a linear bias correction scheme for CMORPH SRE for the period 2004-2013. Application of the scheme resulted in a reduction of bias by > 20 %. The magnitude of the bias factors and the biases reported in Kabompo catchment resemble findings in Asadullah *et al.* (2008) for different regions in Uganda where daily CMORPH rainfall was used. Overall, pixel-to-pixel comparison shows better performance than point-to-pixel comparison as indicated by majority of the statistical indicators. Results of cross-validation for both corrected and uncorrected CMORPH confirm this finding. Availability of six irregularly distributed rain gauges over the Kabompo Basin, yielded meaningful results using the pixel-to-pixel comparison by improved match between the observations. The limitations of the pixel-to-pixel based interpolation techniques is that by this approach, centers of pixel distances may even become larger than actual station distances.

The study carried out REW model simulations to assess the effects of SREs on simulated streamflow. The model parameters were manually adjusted to optimize model performance for in situ-based rainfall. When SREs were introduced, manual recalibration of the model was done through changing one parameter at a time. The objective functions chosen here are the Nash Sutcliffe (*NSE*) of daily streamflow and Relative Volume Error (*RVE*). It is shown that REW model performance improved using bias corrected SRE as compared to uncorrected SRE input. The result indicated that use of bias corrected SRE improved REW model efficiency for *RVE* and *NSE*, by 58 % and 11 % respectively. Across the globe, substantial improvements are shown in model

simulations which are reported with other SREs other than CMORPH. In the Tibetan Plateau, application of bias corrected CMORPH resulted in improved *NSE* for the HEC-HMS model calibration but observed peak streamflows were consistently underestimated (Alazzy *et al.,* 2017). The study by Najmaddin *et al.* (2017) in the Lesser Zab catchment in Iraq showed a *Rel. bias (%)* of -37.6 % when forcing the Leicester Model for Semi-Arid Regions (LEMSAR) (Pullan *et al.,* 2016) with uncorrected TMPA-3B42 rainfall, but improved to -2.6 % after bias correction. After bias correction *NSE* improved from 45 - 66 %. Liu *et al.* (2017) noted that the use of bias corrected SREs in the Mekong River Basin has a promising prospect on the hydrological process simulation in data-sparse tributaries as revealed through the BTOPMC model Takeuchi *et al.* (1999).

The study also aimed to apply parameter sensitivity analysis for low and high flows and for the wet and dry season. Improvement in the satellite streamflow simulations was mainly due to recalibrating model parameters to account for errors in SREs. However, there is a limit to the improvement resulting from parameter adjustments, as can be seen from the relatively poor performance of CMORPH even when the model was calibrated with satellite data. Such was observed for dry season and also for low and high flows.

Table 6.4. Calibrated values of the REW model parameters using gauge, uncorrected and bias corrected CMORPH. Numbers in brackets represent pixel-to-pixel rainfall input and outside bracket the point-to-pixel rainfall input. The last two rows show the NSE and RVE values.

		Full period (2008-2013)				Low flows			Intermediate flow			High flow		
Parameter	**Unit**	**Initial parameter**	**Gauge**	**Uncorrected CMORPH**	**Bias corrected CMORPH**	**Gauge**	**Uncorrected CMORPH**	**Bias corrected CMORPH**	**Gauge**	**Uncorrected CMORPH**	**Bias corrected CMORPH**	**Gauge**	**Uncorrected CMORPH**	**Bias corrected CMORPH**
Soil porosity	-	0.5	0.55	0.65 (0.55)	0.6 (0.65)	0.45	0.55 (0.55)	0.5 (0.55)	0.52	0.55 (0.53)	0.6 (0.50)	0.6	0.68 (0.75)	0.55 (0.65)
Saturated Hydraulic conductivity	m/s	0.0005	0.007	0.020 (0.0010)	0.008 (0.007)	0.006	0.030 (0.0020)	0.007 (0.0065)	0.006	0.003 (0.001)	0.006 (0.007)	0.006	0.001 (0.001)	0.0004 (0.0006)
Water table depth	m	15	15.5	16 (16.5)	15 (15.4)	15.1	15.8 (14.5)	14.4 (15.8)	15.5	16 (16.5)	15 (15.4)	16.8	16 (16.5)	15 (15.4)
At a station depth scaling exponent	---	0.4	0.35	0.60 (0.65)	0.2 (0.35)	0.34	0.50 (0.60	0.2 (0.35)	0.35	0.60 (0.65)	0.2 (0.35)	0.45	0.64 (0.70)	0.45 (0.39)
Discharge area scaling coefficient	---	2.00E-06	2.00E-05	2^e-6 (2^e-3)	2^e-3 (2^e-4)	2.50E-06	2^e-4 (2^e-3)	2^e-4 (2^e-3)	2.40E-05	2^e-6 (2^e-3)	2^e-4 (2^e-4)	1.10E-04	2^e-4 (2^e-5)	2^e-5 (2^e-4)
Initial water content	---	0.3	0.35	0.45 (0.46)	0.3 (0.40)	0.25	0.48 (0.50)	0.35 (0.48)	0.45	0.49 (0.50)	0.35 (0.45)	0.45	0.55 (0.65)	0.54 (0.55)
Water content at saturation	---	0.5	0.7	0.45 (0.55)	0.2 (0.5)	0.6	0.49 (0.45)	0.6 (0.5)	0.65	0.35 (0.70)	0.6 (0.55)	0.65	0.59 (0.55)	0.3 (0.8)
NSE	---			0.59 (0.55)	0.72 (0.72)		0.48 (0.50)	0.65 (0.62)		0.59 (0.55)	0.72 (0.72)		0.60 (0.58)	0.75 (0.70)
RVE	%			6.2 (5.6)	4.6 (7.4)		9.0 (8.4)	6.6 (5.4)		6.8 (6.6)	5.6 (5.4)		10.4 (7.6)	4.8 (7.8)

Table 6.5. Calibrated values of the REW model parameters using gauge, uncorrected and bias corrected CMORPH for the wet and dry season. Numbers in brackets represent pixel-to-pixel rainfall input and outside bracket the point-to-pixel rainfall input. The last two rows show the NSE and RVE values.

		Full period (2008-2013)				Wet season				Dry season	
Parameter	**Unit**	**Initial parameter**	**Gauge**	**Uncorrected CMORPH**	**Bias corrected CMORPH**	**Gauge**	**Uncorrected CMORPH**	**Bias corrected CMORPH**	**Gauge**	**Uncorrected CMORPH**	**Bias corrected CMORPH**
Soil porosity	-	0.5	0.55	0.65 (0.55)	0.6 (0.65)	0.5875	0.62 (0.64)	0.54 (0.57)	0.575	0.55 (0.54)	0.53 (0.57)
Saturated Hydraulic conductivity	m/s	0.005	0.007	0.002 (0.0010)	0.0045 (0.007)	0.00625	0.030 (0.001)	0.005 (0.008)	0.0065	0.003 (0.001)	0.005 (0.007)
Water table depth	m	15	15.5	16 (16.5)	15 (15.4)	16.475	15.6 (16.3)	15 (15.5)	16.15	16 (15.5)	15 (15.6)
At a station depth scaling exponent	---	0.4	0.35	0.60 (0.65)	0.2 (0.35)	0.425	0.50 (0.62)	0.23 (0.37)	0.4	0.55 (0.63)	0.4 (0.37)
Discharge area scaling coefficient	---	2.00E-06	2.00E-05	2^e-6 (2^e-3)	2^e-3 (2^e-4)	0.0000875	2^e-4 (2^e-3)	2^e-3 (2^e-3)	0.000065	2^e-5 (2^e-4)	2^e-6 (2^e-3)
Initial water content	---	0.3	0.35	0.45 (0.46)	0.3 (0.40)	0.425	0.52 (0.58)	0.43 (0.50)	0.4	0.49 (0.50)	0.32 (0.3)
Water content at saturation	---	0.5	0.7	0.45 (0.55)	0.2 (0.5)	0.6625	0.47 (0.63)	0.4 (0.68)	0.675	0.35 (0.37)	0.4 (0.65)
NSE	---			0.59 (0.55)	0.72 (0.72)		0.60 (0.57)	0.73 (0.71)		0.59 (0.53)	0.70 (0.68)
RVE	%			6.2 (5.6)	4.6 (7.4)		8.7 (7.1)	5.2 (6.4)		7.8 (7.0)	5.2 (8.8)

6.5 Conclusions

In this chapter, uncorrected and bias corrected CMORPH satellite rainfall estimates were evaluated for application in the Representative Elementary Watershed (REW) modelling approach in the Kabompo Basin, a headwater catchment of the Zambezi River. Bias correction is performed for six meteorological stations based on point-to-pixel and pixel-to-pixel comparisons. Manual calibration of the REW model was by trial and error in which the model parameters were manually adjusted to optimize model performance for in situ-based rainfall. Manual recalibration was performed when uncorrected and bias corrected SRE was introduced into the model. This study contributes to efforts that aim towards enhancing applicability of SREs in rainfall-runoff modelling. Four conclusions are drawn:

i. Comparison of time series of rain gauge data with uncorrected CMORPH rainfall estimates reveals that results of pixel-to-pixel rainfall comparison are more favourable than for point-to-pixel comparison. *Rel. bias (%)* of uncorrected CMORPH rainfall estimates indicate substantial overestimation (> 20 % point-to-pixel) but also underestimation (< -15 % for pixel-to-pixel) across the 6 stations. The linear multiplicative shift bias correction technique used in this study performed well (20 % bias reduction) to correct the SRE data in terms of the majority of analysed statistics and is most promising. The pixel-to-pixel comparison is more favourable as compared to the point-to-pixel comparison in terms of bias removal as shown by a Taylor diagram and cross-validation approach.

ii. This study targets the applicability of the REW model to assess how SRE bias affects performance of the model to simulate specific streamflow hydrograph characteristics. This has implications on the water balance, if the rainfall model inputs change, then also water storage in the various model flow zones, and thus streamflow may be affected. Not any study on the REW model addressed this issue and investigations in the Kabompo basins are unidentified. In this work, uncorrected as well as bias corrected CMORPH model inputs result in different runoff model performance as assessed by *NSE* and *RVE* metrics.

iii. The study applies parameter sensitivity analysis for low, medium and high flows and also for the wet and dry season. Optimized values of model parameters changed when in situ-based, interpolated rainfall inputs were replaced by bias corrected CMORPH rainfall inputs. In particular, parameters that control the volume of the simulated

hydrograph showed largest change to the different rainfall inputs. Parameters remained all within physically acceptable ranges in the wet season as compared to the dry season. Similar findings were also observed for intermediate as compared to low or high flows.

iv. Overall, it can be concluded that the evaluation and propagation of CMORPH rainfall bias errors into model behavior is indispensable to improve results of rainfall-runoff modeling. This study concludes that bias corrected CMORPH rainfall products have potential value for streamflow simulation in the Kabompo Basin.

Chapter 7: Propagation of CMORPH rainfall errors to REW streamflow simulation mismatch in the Upper Zambezi Basin*

7.1. Introduction

Propagation effects of SRE rainfall bias errors in streamflow simulation commonly are assessed where streamflow results by in situ observed rainfall serve as reference (Fallah *et al.*, 2020; Shin and Kim, 2019). This also is the case for the vastly ungauged Zambezi Basin in southern Africa which supports livelihoods of over 40 million inhabitants (Hughes and Farinosi, 2020). A constraint to streamflow simulation and hydrological assessments of the basin's water balance is the low number of rain gauges that hinder quantitative assessments. To overcome the constraint, satellite rainfall estimates (SREs) can be considered to supplement, or to replace rain gauge data. Satellite rainfall products provide areal coverages and allow construction of time series since observations are consistently repeated over time.

Various studies report on bias error (i.e. systematic error) propagation of SREs that affect specific characteristics of simulated hydrographs such as peak flows (Chen *et al.*, 2020), low and high flows (Dang *et al.*, 2017), as well as the water balance as shown in catchment modelling (Alemu *et al.*, 2020). A study by Jiang *et al.* (2012) in China highlighted SRE bias error propagation by use of the semi-distributed Xinanjiang model and show that relatively small errors of bias-corrected rainfall do not distinctly affect model behavior. Mei *et al.* (2016) showed that larger bias errors propagated to cause significant streamflow mismatch when the Integrated Catchment Hydrological Model (ICHYMOD) was applied in the Upper Adige River Basin, Italy. Pan *et al.* (2010) showed that the Climate Prediction Center-MORPHing (CMORPH) (Joyce *et al.*, 2004) satellite rainfall errors cause mismatches in simulated streamflow volume using the

*__This chapter is based on the paper:__ W. Gumindoga, T.H.M. Rientjes, A.T. Haile, P. Reggiani, H. Makurira. 2021: Propagation of CMORPH rainfall errors to REW streamflow simulation mismatch in the upper Zambezi Basin. *Journal of Hydrology: Regional Studies.* https://doi.org/10.1016/j.ejrh.2021.100966

Variable Infiltration Capacity (VIC) model. Maggioni *et al.* (2013) used a stochastic ensemble-based satellite rainfall error model (SREM2D) in the Tar-Pamlico Basin and showed that CMORPH rainfall bias errors are significantly augmented to cause streamflow mismatch in large basin sizes. Artan *et al.* (2007) showed that in the Mekong River's Nam Ou and Se Done Basins, a slight bias in CMORPH rainfall augmented into simulated streamflow mismatch using the Geospatial Stream Flow Model (GeoSFM).

In hydrological modelling, evaluation of how SRE rainfall errors propagate to cause streamflow mismatch and to affect water balance composition are topics of ongoing interest. Propagation of rainfall error causing streamflow error by hydrological modelling is commonly evaluated by analyzing mismatches between observed streamflow and simulated counterparts subject to respective rainfall input data sources. For that purpose, objective functions may be combined and optimized by use of automated single or multi-objective model calibration algorithms (see De Vos and Rientjes, 2007). Yapo *et al.* (1998) identified a set of optimal solutions (model parameter sets) based on a trade-off between different objective functions. De Vos and Rientjes (2007) showed that not all differences between modelled and observed hydrograph characteristics (e.g., peak flows or low flows) can be expressed adequately by single objective functions and optimized model parameter set. Rientjes *et al.* (2013a), Monteil *et al.* (2020) and Shahed Behrouz *et al.* (2020) show that multi-objective calibration allows the simultaneous evaluation of multiple characteristics of a single output (i.e. streamflow) from the model. These applications have been on knowledge-driven hydrological model approaches and thus, it is likely that aspects of satellite rainfall error propagation can be assessed from such a calibration approach. In this study, multi-objective approaches are tested for SRE error propagation analysis. Assessments target mismatches in streamflow hydrograph shape and volume, specific hydrograph characteristics and composition of the water balance. Effects on parameter optimization for respective rainfall input data sources is shown as well.

In the Kabompo Basin, a number of spatially distributed rainfall-runoff model approaches have been used that relied on use of rain gauge data and SRE's. Omondi (2017) applied the Topographic driven model (TOPMODEL) to assess effectiveness of satellite rainfall estimates for water balance assessment. Ndhlovu and Woyessa (2020) used the Soil and Water Assessment Tool (SWAT) model to determine the impact of climate change on the hydrology of the Kabompo Basin. Matos (2014) successfully used the SWAT model with SREs on a daily

time step to forecast flows for the Zambezi River Basin. In the above studies, no attempts were made to assess effects of SRE errors on streamflow mismatch although there are ample scientific studies that show that SREs are affected by systematic errors (e.g., Gumindoga *et al.*, 2020). This study seeks improved understanding of propagation effects of SRE rainfall errors where the state-of-the-art Representative Elementary Watershed (REW) modelling approach (Reggiani and Hassanizadeh, 2016) is selected and applied at the Kabompo headwater catchment of the Zambezi River. This study demonstrates how SRE bias errors in CMORPH SREs affect streamflow characteristics of a physically based rainfall-runoff model. This study further shows how CMORPH SREs affect actual evapotranspiration *(ET_a)* with emphasis on composition and closure of the water balance. The findings are expected to provide new insights on the hydrologic implications of satellite rainfall error and serves applications in the Zambezi Basin.

7.2. Methodology

In the methodology of chapter 7, only automated REW model parameter sets are used as opposed to Chapter 6 where only manually calibrated parameter sets were used. For Chapter 7 an automatically calibrated reference parameter set is defined that relies on in situ rainfall following *Y* objective function. This set is (further) optimized by rerunning the optimization tool.

7.2.1. Bias correction of CMORPH rainfall estimates

Bias in CMORPH satellite rainfall estimates is corrected using data from six rain gauges and a space and time varying bias correction approach that was successfully applied for the Zambezi Basin (Gumindoga *et al.*, 2019a, 2019b), and the Upper Blue Nile Basin (Bhatti *et al.*, 2016). Bias correction was performed from 1998 to 2012 that matches the period for error propagation assessment. A bias correction procedure by Bhatti *et al.* (2016) and Habib *et al.* (2014) was adopted.

Uncorrected and bias corrected CMORPH rainfall estimates were compared to spatially interpolated gauged rainfall by means of the Inverse Distance approach. By equal projection, pixel-to-pixel comparison at 8 km × 8 km pixel size and at daily time step is performed for pixels that overlay the study area. To assess the match between gauge observations and uncorrected and corrected

CMORPH counterparts, correlation coefficient *(CC)*, root mean squared error *(RMSE)* and mean absolute error *(MAE)* are used as statistical indicators.

7.2.2. ε-NSGAII for multi-objective model calibration

In this study, multi-objective calibration through the Epsilon Dominance Non-dominated Sorting Genetic Algorithm II (ε-NSGAII) algorithm (Yang *et al.*, 2014) was performed for streamflow modelling for optimizing the reference parameter set that target, hydrograph shape and volume, and for combinations of objective functions that target specific hydrograph characteristics. Water balance composition and closure also are assessed for respective cases. The algorithm is an improved version of the NSGAII algorithm proposed by Deb *et al.* (2002). The main purpose of the genetic based search algorithm is optimization of parameter values by fitting simulated streamflow hydrograph characteristics to observed counterparts by multi-objective functions. Important settings of the ε-NSGAII that impact effectiveness of the genetic based search algorithm are simulated binary crossover (SBX) (Deb and Agrawal, 1995) and polynomial mutation (PM) (Deb and Goyal, 1996). Occurrences of the crossover and mutation operations are complementary inputs which are controlled by the crossover rate (Crate). Jung *et al.* (2017) notes that if the Crate is 0.9, the rate of mutation is 0.1. Function of ε-NSGAII algorithm is based on a number of optimization metrics (i.e. quality measures) that assess cardinality, accuracy, and diversity of solutions as demonstrated in Forootan (2018). The quality measures are the Number of Pareto Solutions (NPS), Generation Distance (GD), Spacing (SP), and Maximum Spread (MS).

7.2.3. Representative Elementary Watershed modelling

In this study, the Representative Elementary Watershed (REW) model (Reggiani *et al.*, 1999; Reggiani and Rientjes, 2005) is selected for streamflow simulation. The catchment scale rainfall-runoff model is selected because the semi-distributed model domain reads spatially distributed rainfall as input, as well as by means of its integrated physically based numerical approach, simulates runoff production by Hortonian and saturation excess overland flow, and subsurface runoff contributions for shallow and deeper ground water. This allows to intercompare model outcomes including the water balance, as subject to selected rainfall input data sources in this study. Detailed descriptions on REW flow algorithms are found in Chapter 3, in Reggiani *et al.* (1999) and Reggiani and Rientjes (2005, 2010), whereas recent applications of the model are found in

Reggiani *et al.* (2014), Reggiani and Hassanizadeh (2016), Elgamal *et al.* (2017). Reference is made to Gumindoga *et al.* (2019a) for an application of the REW model to the Kabompo Basin. The model set-up was adopted as it is well suited for water balance closure assessments in this study.

7.2.4. Model calibration

REW model calibration and validation periods were selected for the years Oct 1998 to Sept 2002 and Oct 2002 to Sept 2006 respectively. The selection of calibration and validation periods is based on data availability and completeness. For this study, the reference parameter set with sensitive model parameters (Soil porosity, Saturated hydraulic conductivity and Water content at saturation) was optimized by the ε-NSGAII algorithm using point-to-pixel interpolated in situ observed daily rainfall for the period from Oct 1998 to Sept 2002. The parameter set was validated for the period Oct 2002 to Sept 2006 by also using interpolated in situ observed rainfall. For optimizing the reference parameter set, model performance was assessed through the *Y*-objective function (Akhtar *et al.*, 2009; Rientjes *et al.*, 2013a) that combines Nash-Sutcliffe efficiency *(NSE)* (Nash and Sutcliffe, 1970) and relative volume error *(RVE)* objective functions (Eqs. 6.3 and 6.4 respectively). *Y* becomes 1 when the model estimates perfectly match with observations and becomes 0 when *NSE* is equal to 0. Whereas researchers show that interpreting *Y* values is not straightforward, in modelling practice, models are assumed to perform well for *Y* values > 0.6.

$$Y = \frac{NSE}{1+|RVE|} \qquad [7.1]$$

Combinations of objective functions (Table 7.1) were selected that target high flows, low flows, rising limb and recession limb (de Vos and Rientjes, 2007; 2008a; Tang *et al.*, 2006; Yapo *et al.*, 1998). Indicators *MSE, M4E, RMSE, MSLE* and *RMAEL* vary between 0 and ∞ with a perfect fit of zero (Booij and Krol, 2010). *RMERV* assesses match of high flows (Booij and Krol, 2010) that may vary between –∞ and ∞, but perform best when a value of zero is generated. The recession error constant (r_k) function, is calculated for each point by differentiating ($\frac{dQ}{dt}$) the Dupuit-Boussinesq equation (Blume *et al.*, 2010). The r_k function has best performance of 1.

$$MSE = \frac{1}{n}\sum_{i=1}^{n}\left(Q_{sim,i} - Q_{obs,i}\right)^2 \qquad [7.2]$$

$$M4E = \frac{1}{n}\sum_{i=1}^{n}\left(Q_{sim,i} - Q_{obs,i}\right)^4 \quad [7.3]$$

$$MSLE = \frac{1}{n}\sum_{i=1}^{n}\left(InQ_{sim,i} - lnQ_{obs,i}\right)^2 \quad [7.4]$$

$$MSDE = \frac{1}{n}\sum_{i=1}^{n}\left(\left(Q_{sim,i} - Q_{sim,i-1}\right) - \left(Q_{obs,i} - Q_{obs,i-1}\right)\right)^2 \quad [7.5]$$

$$RMERV = 100 \times \frac{\frac{RV_{sim,i}(y_1) - RV_{obs,i}(y_1)}{RV_{sim,i}(y_1)} + \frac{RV_{sim,i}(y_2) - RV_{obs,i}(y_2)}{RV_{obs,i}(y_2)}}{2} \quad [7.6]$$

$$RMAEL = \frac{\sum_{i=1}^{n}||Q_{sim,i} - Q_{obs,i}||}{\sum_{i=1}^{n} Q_{obs,i}} \quad with\, Q_{obs,i} \leq Q_{f,i} \quad [7.7]$$

$$r_k = -\frac{dQ}{dt}\left(\frac{1}{Q(t)}\right) \quad [7.8]$$

where:

Q_{obs} = *observed streamflow (m^3/s) at a certain day i*

Q_{sim} = *simulated streamflow (m^3/s) at a certain day i*

$Q(t)$ = *discharge (observed/simulated) at time t (m^3/s)*

n = *number of time steps,*

f = *threshold*

y_1 = 10, y_2 = *100*

Table 7.1: Hydrograph characteristics assessed and corresponding objective functions.

Hydrograph characteristic	**Objective functions**	**Reference**
Peak flow (annual peaks for the period 2006-2012)	The Mean Fourth-Power Error (*M4E*), Time to peak (days)	(de Vos and Rientjes, 2007; 2008b;)
High flow	NSE, Relative Mean Error for 10-year and 100-year Return Values (*RMERV*)	(Booij and Krol, 2010; de Vos and Rientjes, 2005; Dhamge *et al.*, 2012)
Low flow	Mean Squared Logarithmic Error (*MSLE*), Relative Mean Absolute Error for Low Flow Assessments (*RMAEL*)	(Booij and Krol, 2010; De Vos and Rientjes, 2007; Demirel and Booij, 2009)

Rising limb	Mean Squared Derivative Error (*MSDE*), Mean Squared Error (*MSE*)	(de Vos and Rientjes, 2008a, 2008b)
Recession limb	Recession Error Constant (r_k)	(Blume *et al.*, 2010)

Findings serve to identify sole effects of a change of rainfall input data source on streamflow mismatch. Changing rainfall input necessitated the rerunning of the ε-NSGAII algorithm so that aspects of error propagation by respective rainfall input data are uniquely identified and not affected by a sub-optimal model parameter set.

7.2.5. Assessments of CMORPH rainfall error propagation

Assessments on rainfall error propagation involves a number of objectives for the assessment period 2006-2012 that is outside periods of calibration and validation.

Streamflow

Similar to error assessments on rainfall input data sources (section 5.3.5), for assessing mismatches on streamflow also correlation coefficient (*R*), root mean squared error (*RMSE*) and mean absolute error (*MAE*) are used as statistical indicators. To indicate effects of error propagation for different rainfall input data sources, ratios of statistical indicators for streamflow (Q_s) and rainfall (P) are calculated by means of R_{Qs}/R_P, MAE_{Qs}/MAE_P, and $RMSE_{Qs}/RMSE_P$. The above ratios are selected because they have different implications: $MAE_{Qs}/MAE_P < 1$ and $RMSE_{Qs}/RMSE_P < 1$ implies error attenuation whereas $R_{Qs}/R_P < 1$ implies augmentation of error. Whereas past studies (e.g. Hong *et al.*, 2006) employed error propagation procedures where objective function values are interpreted, in this study, the magnitude of the ratios was considered to indicate effects of propagation in a relative manner.

Streamflow characteristics

Using the reference parameter set with starting value for further optimization, rerunning of the multi-objective ε-NSGAII algorithm enables a robust evaluation procedure, and assessment for specific hydrograph characteristics given each set of objective functions (Table 7.2) as well as for respective rainfall inputs. Any

difference in objective function values indicate differences in simulated hydrograph characteristics that can be attributed to the rainfall input source.

Water balance

Water balance assessment implies that subject to the rainfall input data source, water balance components will alter with different volumetric values for respective components. The assessment considers the attribution of rainwater to actual evapotranspiration (ET_a) and streamflow (Q_s), and also accounts for rain water storage in the model. For rainfall error propagation analysis, water balance ratios for actual evapotranspiration over rainfall (ET_a/P) (evapotranspiration coefficient) and runoff over rainfall (Q_s/P) (runoff coefficient) are computed from the REW simulation results. Besides ratios, the water balance components, that are subject to the *Y*-objective function, are provided as outcome.

7.3. Results and Discussion

7.3.1. Rainfall error propagation on streamflow

Observed streamflow hydrographs indicate that the Kabompo Basin is a slow responding system as is evident from lack of rapid changes in streamflow over short periods by high rainfall. This is expected considering the large catchment size (67 261 km^2). Results of the REW model calibration (October 1998 - September 2002) and validation (October 2002 - September 2006) by use of interpolated in situ observed daily rainfall are shown in Figure 7.1. For both periods, model underestimation of highest flows and overestimation of low flows are observed. Hydrograph recession periods are slightly underestimated for few years. Though the model shows small underestimation of highest peaks and small overestimation of baseflow, the simulated streamflow successfully resembles the observed streamflow pattern during both the calibration ($Y = 0.77$) and validation period ($Y = 0.71$). These objective function values are appropriate to allow for error propagation analysis on streamflow shape and volume by means of the *Y*-function.

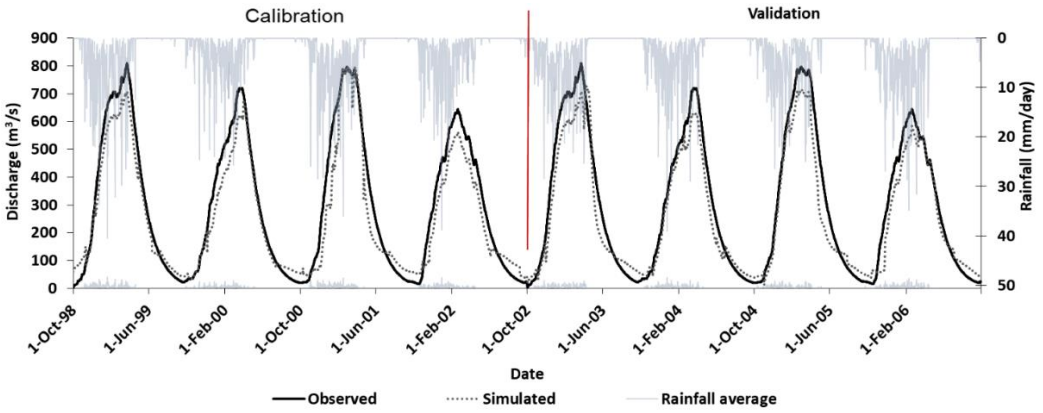

Figure 7.1: REW model calibration (October 1998 –September 2002) and validation (October 2002 – September 2006) by use of the reference parameter set.

For assessments on SRE error propagation on streamflow mismatch, Figure 7.2 shows that for uncorrected CMORPH the ratio R_{Qs}/R_P is 2.0 as compared to a lower ratio for corrected CMORPH (1.2). Any ratio >1 shows attenuation of error and thus a ratio close to 1 is desirable. For *R*, a ratio > 1 shows attenuation of error and thus a ratio close to 1 indicates less propagation effect of rainfall. Also for MAE_{Qs}/MAE_P, and RVE_{Qs}/RVE_P, preferred ratio values are 1, a ratio < 1 implies error attenuation, whereas a ratio > 1 shows error augmentation. The ratio MAE_{Qs}/MAE_P for uncorrected CMORPH was 1.3 and indicates error augmentation whereas for bias corrected CMORPH the ratio was 0.2 indicating error attenuation. While there is no substantial difference between uncorrected and corrected CMORPH for the RVE_{Qs}/RVE_P ratio, uncorrected CMORPH shows error augmentation (1.2) whereas bias corrected CMORPH shows error attenuation (0.9). The error in uncorrected satellite rainfall is shown to amplify in streamflow simulations by the REW model. When corrected CMORPH is introduced, there is attenuation of error. In the context of error propagation, findings indicate that attenuation is more evident for *MAE* followed by *R* and less evident for *RVE*. Overall, but subject to the use of the reference parameter set in this analysis, the ratios provide insights about the extent of error propagation from rainfall to streamflow mismatch. Substantial error is introduced by uncorrected CMORPH whereas a small error is introduced by corrected CMORPH. The linear bias correction scheme indicates satisfying results in error reduction and is recommended for similar studies.

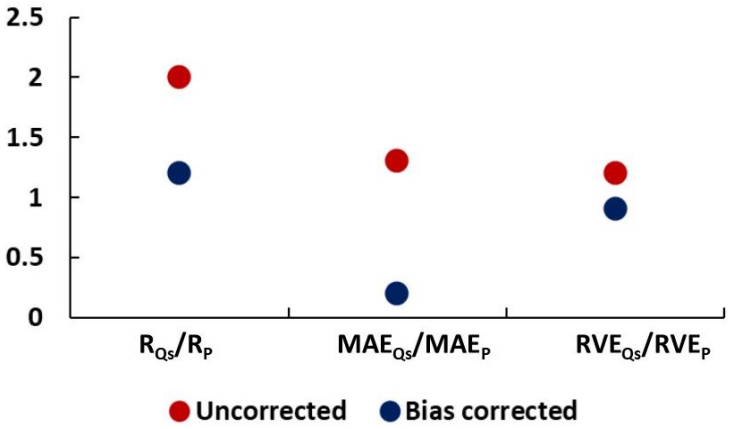

Figure 7.2: Ratios R_{Qs}/R_P, MAE_{Qs}/MAE_P, and $RMSE_{Qs}/RMSE_P$ for uncorrected and bias corrected CMORPH for the 2006-2012 period that coinicides with the bias correction period. Note that the reference parameter set was used.

7.3.2. Streamflow for respective rainfall data sources

Figure 7.3. shows the rainfall error propagation simulated hydrograph for the period (2006–2012). Except for baseflow, all hydrograph characteristics show fair match between observed streamflow and the CMORPH simulated streamflow. Time to peak of hydrograph shows that the best hydrograph simulation is indicated for rain gauge-based simulation, that is followed by bias corrected CMORPH and uncorrected CMORPH based streamflow simulation results. There is consistent underestimation of baseflow.

There is smooth transition from recession limb to baseflow for the observed hydrograph and model simulations. A drop at the start of baseflow is noted for bias corrected and uncorrected CMORPH based simulations.

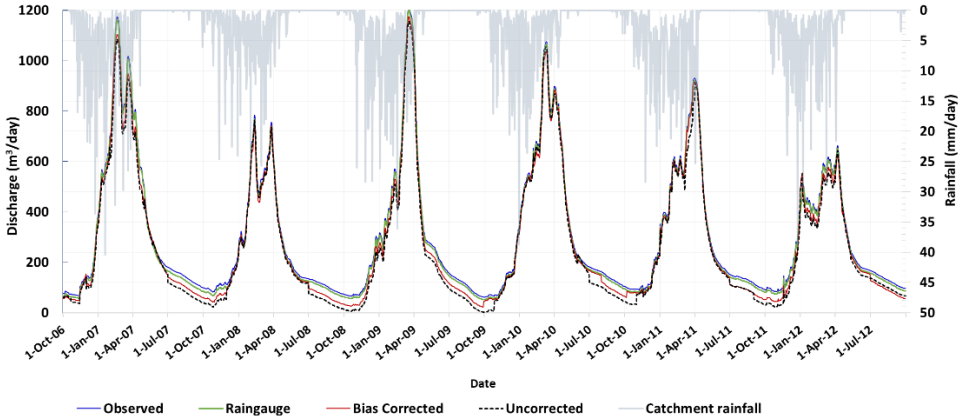

Figure 7.3: Simulated hydrographs for respective rainfall data sources after-running ε-NSGAII algorithm for Y-function for the period 2006-2012. The catchment rainfall is also shown on secondary axis. Note that the reference parameter set was used.

7.3.3. Streamflow hydrograph characteristics for respective rainfall data sources

Table 7.2 shows objective function values used to assess model performance by pairing of objective functions (e.g., the use of *NSE* and *RMERV* for high flows). The approach involved selection of the reference parameter set for further optimization by rerunning the ε-NSGAII algorithm. This applies for respective rainfall sources and for all cases in Table 7.2.

Table 7.2: Results of hydrograph characteristic and associated objective functions for respective rainfall data sources for the period 2006-2012. Perfect fit is given as NSE=1, MSE= 0, M4E= 0, MSLE=0, MSDE=0, RMSE=0, RAMAEL=0, RMERV=0, r_k=1. Bold=best performance noted for satellite rainfall CMORPH.

Hydrograph Characteristic	Uncorrected	Bias Corrected	Rain gauge	Uncorrected	Bias Corrected	Rain gauge
	NSE			*RMERV (%)*		
High flow	0.64	**0.69**	0.72	4.32	**1.64**	1.60
	MSLE (m^3/s)			*RMAEL* (m^3/s)		
Low flow	7.1 e^{-5}	**4.9 e^{-7}**	0.5 e^{-7}	0.62	**0.34**	0.20
	MSE (m^3/s)			*MSDE* (m^3/s)		
	0.0095	**0.0018**	0.00097	6.3 e^{-5}	**4.5 e^{-7}**	6.8 e^{-8}

Shape of rising limb						
	M4E (m^3/s)			Time to peak (days)		
Peak flow	0.015	0.020	0.013	6	**3**	2
Shape of recession limb	r_k			*MSDE* (m^3/s)		
	2.3	1.2	1.1	**5.5 e^{-6}**	4.3 e^{-7}	4.9 e^{-8}

Peak flow

Though physical inspection of hydrographs seemingly indicate that all graphs coincide for the highest peaks in each year, hydrographs for uncorrected CMORPH rainfall generally are poor on the timing of the peak flows (in days). This is based on 'Time to peak' objective function that only is applied to highest peak flow for each year for the period 2006-2012. Bias corrected rainfall shows better matching with observed streamflow peaks as compared to uncorrected CMORPH. For all three rainfall sources, results of this study show improved *M4E* and penalization for overestimation of peak flows. There is a trade-off in having good overall fit and having accurate timing to the peak flow, as ε-NSGAII already provides optimum solutions. De Vos and Rientjes (2005) note that *M4E* may fail to show effects of a time shift in the streamflow series.

High flows

High flows are defined as flows above the threshold of 500 m^3/s that coincides with the 75th percentile value range of all observations. Table 7.2 shows that the *NSE* values for both corrected and uncorrected CMORPH are in the same order of magnitude for high flows (all in range of 0.64-0.69). The multi-objective parameter assessment by the ε-NSGAII has preference towards improving hydrograph shape (high *NSE*) and good agreement of high flows (low *RMERV*). The combination of *NSE* and *RMERV* gives satisfactory results for bias corrected CMORPH rainfall simulations. Uncorrected CMORPH indicated poor results for both *NSE* and *RMERV* objective functions.

Low flows

Low flows are below the threshold of 95 m^3/s that coincides with the 25^{th} percentile value range of all observations. Figure 7.3. shows that there is match of high flows, rising and falling limbs at the costs of matching low flows. Simulation results possibly are affected by the automatically calibrated reference parameter that relies on in situ rainfall following *Y* objective function, which caused that low flows were over-estimated throughout the entire calibration period (see Fig 7.3). Table 7.2 shows relatively poor objective function values for *RMAEL* and *MSLE*. Results on magnitude of the low flows indicates satisfying results for bias corrected CMORPH as compared to uncorrected CMORPH. The model simulation with uncorrected CMORPH was successful only for flow values below 25 m^3/s. In Table 7.2, a large increase in the value of *RMAEL* is observed for uncorrected CMORPH compared to corrected CMORPH. Furthermore, *RMAEL* seems to be more appropriate for model calibration than *MSLE*, although *MSLE* is used more often (Demirel and Booij, 2009; Madsen, 2000).

Recession limb

Simulation results in Figure 7.3 with uncorrected CMORPH show that the shapes of annual recession curves are not adequately matched as compared to streamflow simulated by in situ rainfall. This is because of poor rainfall representation by CMORPH in the dry season (see Gumindoga *et al.*, 2019c). Table 7.2 shows that use of bias corrected CMORPH rainfall input resulted in improved simulation of the recession limb. This is evidenced by *rk* of 2.3 for uncorrected CMORPH compared to *rk* = 1.4 for bias corrected CMORPH. An *rk* closer to 1 is preferred.

Shape of rising limb

Figure 7.3. shows that yearly rising limbs are well simulated as compared to other hydrograph characteristics except for the recession limb. There is improved *MSE* of 0.0018 m^3/s for bias corrected CMORPH as compared to *MSE* of 0.0095 m^3/s for uncorrected CMORPH as shown in Table 2. Similarly, *MSDE* of 6.3 e-5 m^3/s is achieved for uncorrected CMORPH as compared to an improved value of 4.5 e-7 m^3/s for bias corrected CMORPH. Overall, there is closeness of fit between simulated and observed rising and falling limbs when bias corrected CMORPH rainfall is used.

7.3.4. Effect of rainfall data source on the water balance

The percentage ratios for water balance coefficients ET_a/P (evapotranspiration coefficient) and Q_s/P (runoff coefficient) are shown in Figure 7.4. Ratios are calculated for all three rainfall data input sources for the period 2006-2012 (assessment period) as well as comparison with observed streamflow. Highest ET_a/P is shown for rain gauge (70 %) followed by bias corrected CMORPH (66 %) and uncorrected CMORPH (64 %). Changes in ET_a/P for the same assessment period are not equal to changes in Q_s/P in the model indicating model responses to actual water storage by rainfall. The results show that rainfall input source affects the model simulated water balance as the above-mentioned differences are more evident for uncorrected than for corrected CMORPH. Results also show that for uncorrected CMORPH, approximately 36 % of rainfall received attributes to runoff for the period 2006-2012. However, the observed streamflow runoff coefficient computed with raingauge rainfall shows that significantly lower percentage (25 %) of rainfall received attributes to runoff.

The evapotranspiration coefficient shows different values for rain gauge, uncorrected and bias corrected CMORPH based simulations. However, the runoff coefficient values do not significantly change when changing the rainfall input data source.

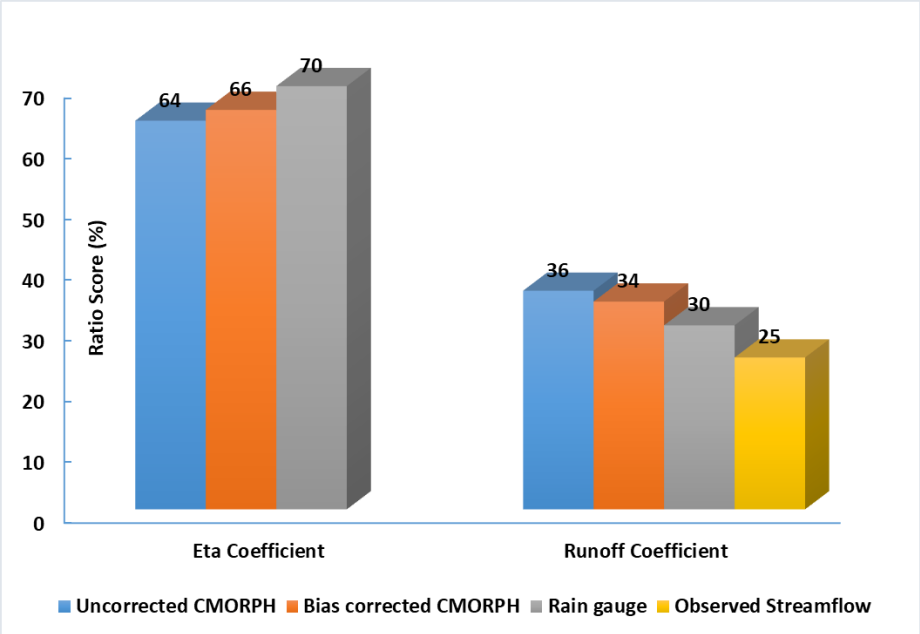

Figure 7.4: Percentage ratio scores for water balance coefficients (Runoff and ETa) for the period 2006-2012 for respective rainfall data sources as well as for observed streamflow.

7.3.5. Water balance components and parameter optimization

Table 7.3 shows a comparison of water balance components subject to optimized parameter sets for respective rainfall inputs by rerunning the ε-NSGAII algorithm for the reference parameter set. The *Y*-function was selected as objective function (Eq. 7.1). The table also shows results of water balance closure analysis and the different water balance terms that result from the model because of the change of rainfall input source. Water balance closure represents the water balance equation residual term that is expressed as percentage of rainfall. A residual (1.4 %) is shown for rain gauge-based rainfall input compared to 2.7 % for bias corrected satellite rainfall estimates and 15.9 % for uncorrected CMORPH. Improved closure for corrected CMORPH is also indicated by the higher *Y*-objective function after model calibration.

Table 7.3: Water balance components and closure for the 2006-2012 period. Bold= best performance for analysis with satellite rainfall.

Water balance Component (mm) and Objective function	Rain gauge	Bias corrected	Uncorrected
Rainfall	3621	**3635**	4300
ET_a	2850	2827	**2866**
Streamflow	718.8	**710.8**	750
Residual/rain (%)	1.4	**2.7**	15.9
Y	0.76	**0.72**	0.55

The study also assessed how optimized model parameter values (Lee *et al.,* 2005; Reggiani and Rientjes, 2005; Varado *et al.,* 2006) are affected by error in the rainfall inputs after bias correction is applied (Table 7.4). Each rainfall distribution (in situ, uncorrected and bias corrected CMORPH) represents its own amount of rain water that serves model forcing. As such, the REW model responds to the amount of water that it receives. Soil porosity, saturated hydraulic conductivity and water content at saturation have values within the allowable value ranges. Even after bias correction, sensitive parameters that control the volume of the simulated hydrograph show large changes compared to the

parameters using rain gauge input. Factors that control groundwater table depth and eventually baseflows, are less affected.

Table 7.4: Optimized parameter values (2006-2012). Bold= best performance for analysis with satellite rainfall.

Parameter	Rain gauge	Bias correcte	Uncorrected
Soil Porosity []	0.50	0.55	**0.54**
Saturated Hydraulic Conductivity [m^3/s]	0.006	**0.0058**	0.0005
Water Content at Saturation []	0.6	**0.55**	0.50

7.3.6. Pareto distributions

Figures 7.5a-l shows Pareto distributions for selected parameters that are Water content at saturation, Soil porosity and At a station depth scaling exponent. Optimization of parameter values by running the ε-NSGAII algorithm for respective rainfall input sources resulted in different trade-offs in the *Y*-objective function (Eq. 7.1). Results are presented for low flows, high flows and overall shape. For the same forcing data and objective functions (Table 7.2), a range of optimum model parameter values result that all perform equally well subject to ε -NSGAII parameter optimization.

The curve shape of the output is the actual Pareto front that shows the trade-off in criterion 1 (x-axis) and 2 (y-axis) for example, if the value of water content at saturation represents the catchment conditions, then for soil porosity it deteriorates (and vice-versa), but any combination shows an equally optimal solution. All the Pareto plots (Figures 7.5a-d) show that multi-objective parameter optimization results in fair spread indicating consistent optimization. The Pareto-based approach in this study also served to compare merits of how SRE bias correction affects results of parameter optimization. A shift of the Pareto front toward the origin of the axes subject to the same calibration record indicates in a relative sense error attenuation by the selected bias correction scheme. Such an approach provides a useful guidance for model improvement.

Visual inspection of Fig 7.5. and analysis of the quality measures of ε-NSGAII algorithm for calibrating the REW model based on the Y-objective function (Eq.

7.1) reveal an improved performance for bias corrected CMORPH rainfall input compared to uncorrected CMORPH as well as various degree of performance for low flows and high flows.

For the ε-NSGAII algorithm, a greater NPS number indicates that the algorithm is better suited to provide a greater number of Pareto solutions whereas a better optimization algorithm provides lower GD. An algorithm with a smaller SP indicates that the solutions are distributed (nearly) uniformly, making it a good measure to evaluate diversity. Larger maximum spread values (MS) indicate a good performance of the algorithm as demonstrated in Forootan (2018). Best performing quality measures are shown for corrected CMORPH.

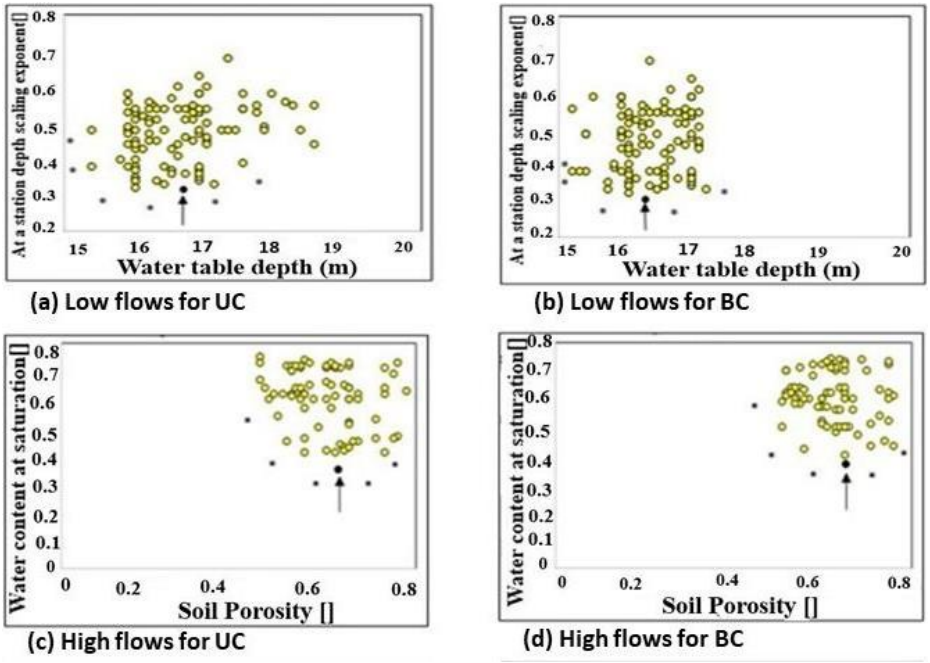

Figure 7.5a-l: Trade-off along the Pareto front for uncorrected (panels a,c) and bias corrected (panels b,d) CMORPH for the period 2006-2012. The plots were generated using 100 trials for the ε -NSGAII algorithm. The shape of the Pareto front is indicated by the black dots.

7.4. Conclusions

This study successfully assessed effects of SRE error propagation on hydrological modelling by the REW rainfall-runoff model. Parameters of the model were automatically optimized using the ε-NSGAII algorithm for in situ rainfall to obtain a reference parameter set which was subsequently used for the

corrected and uncorrected rainfall-based simulations. Assessments on error propagation targeted streamflow modelling for hydrograph shape and volume, specific hydrograph characteristics, and water balance composition. From this study, 4 conclusions are drawn:

i. Model calibration and validation

The REW model successfully simulated runoff in the Kabompo Basin using interpolated in situ observed rainfall for the calibration and validation period, although some underestimation of highest flows and overestimation of low flows is shown. Sources of uncertainty and error that could contribute to the mismatch are rainfall representation, inaccurate representation of catchment characteristics such as land cover, and stage-discharge relationship.

ii. Streamflow hydrograph mismatch by rainfall error propagation

Ratio indicators that show streamflow error by *SRE* error streamflow indicate that attenuation is more evident for mean absolute error (*MAE)* followed by correlation coefficient *(R)* and less substantial for relative volume error (*RVE)* functions. Ratios of MAE_{Qs}/MAE_P for uncorrected and corrected CMORPH are 1.3 and 0.2; Ratios of R_{Qs}/R_P for uncorrected and corrected CMORPH are 2.0 and 1.2; and Ratios of RVE_{Qs}/RVE_P for uncorrected and corrected CMORPH are 1.2 and 0.9. This approach showed improved evaluation of CMORPH error propagation as compared to previous studies in the Kabompo Basin, and other catchment basins of the Zambezi River. The use of a reference parameter set for corrected and uncorrected rainfall input proved to be effective to identify how SRE errors propagate to effect REW simulations.

iii. Mismatch of hydrograph characteristics by CMORPH rainfall

Multi-objective parameter optimization enables a reliable and robust evaluation procedure, and assessment for specific hydrograph characteristics. Though physical inspection of hydrographs seemingly indicates that streamflow hydrographs for respective rainfall inputs coincide for the highest peaks in each year, for uncorrected CMORPH rainfall the hydrograph generally is poor on representing specific characteristics. For example, by use of the bias corrected CMORPH rainfall, streamflow hydrograph shows an improved recession limb (*rk* of 2.3 for uncorrected CMORPH compared to r_k = 1.4 for bias corrected CMORPH). There is also closeness of fit between simulated and observed rising and falling limbs when bias corrected CMORPH rainfall is used. Matching of streamflow hydrograph for the 2006-2012 period shows best overall fit for rain

gauge-based simulation, that is followed by bias corrected CMORPH and uncorrected CMORPH based streamflow simulation results. Objective function values indicate that use of bias corrected CMORPH rainfall results in attenuation of CMORPH rainfall bias error.

iv. Effect of error propagation on the water balance

Percentage ratios for water balance coefficients *ETa/P* (evapotranspiration coefficient) and Q_s/P (runoff coefficient) also obtained from the reference parameter show improved water balance closure for bias corrected CMORPH as compared to uncorrected CMORPH with reference to rain gauge-based simulation results. This study shows that analysis for water balance composition has great potential to improve application of satellite precipitation products in water management and decision making in the Zambezi basin. An important observation is that the use of raingauge data alone results in improved water balance estimation, but still limitations exist in the Zambezi Basin because of incomplete raingauge records and at times shorter time series of these records. The use of bias corrected satellite rainfall bridges the gap and is thus recommended to either fill in missing values or to extend short raingauge time series with the overall intension of improving water balance assessments in data poor catchments.

Chapter 8: Conclusions and recommendations

Understanding the water balance of the Zambezi Basin is of great importance for water resources management within a data limited environment. By the application of bias corrected satellite rainfall estimates and bias error propagation assessment through hydrological modelling, this thesis contributes to a better quantification of rainfall characteristics for water resources management. This concluding chapter starts with reflecting on the objective of this thesis and answering the research questions (Section 8.1). Subsequently, directions for further research are recommended (Section 8.2).

8.1 Conclusions

The Zambezi Basin was selected as the case study because of its great importance to Southern Africa's water resources. The Zambezi River is central for securing sustainable livelihoods for more than 250 million people in Southern Africa (Hoel, 2015), and enhancing economic opportunities. This support system provided by the river much depends on accurate rainfall estimation. Dependable rainfall estimation techniques are critical for water balance assessment. Improved water resource management could have substantial benefits for Southern Africa's energy security, agricultural production, tourism and job creation. Thus, this study proposed satellite rainfall estimation techniques to improve rainfall estimation in the basin. Given increasing development pressures on the basin's resources and the impacts of climate change, the need to ensure a suitable satellite rainfall bias correction technique and a well calibrated operational hydrological model is more critical than ever.

In the text below, the findings from these chapters are summarized:

***i**: What is the performance of CMOPRH satellite rainfall in the Zambezi basin of large extent?*

Chapter 4 addresses this question. SREs embody an important source of rainfall information since estimates are timely and spatially coherent. Across the sub-basins, CMORPH in the Zambezi Basin predicts 60 % of the rainfall occurrences with better rainfall detection in the wet season than the dry season. Rainfall detection is best for the rainfall rates smaller than 2.5 mm/day. Findings on error decomposition revealed major sources of Hit, Missed and False rainfall

bias. Best performance in terms of rainfall rate, occurrence and volume of CMORPH at sub-basin scale in this study is shown when daily estimates are accumulated to weekly estimates. Findings in the Zambezi Basin suggest that errors in CMORPH rainfall should be corrected before the product can serve water resources applications such as hydrological modelling. The study supports ongoing literature on SREs that are considered only representations of reality with specific spatial (i.e., the pixel footprint size) and temporal resolutions (revisit time) and thus findings are only unique for CMORPH rainfall product and the study area. Statements and reports in literature which assert that SREs can be used directly in water resources applications are invalidated and deposed by this study.

Detection results in this study, confirm the generalities previously validated in literature that SREs demonstrate a seasonal dependence and display better performance during the wet season, performance during the dry season is considered low (Kim et al., 2016). For example, studies conducted in China, South America and Mozambique indicate that SREs show better detection in the rainy seasons when precipitation is warm and convective (Miao *et al.* 2015; Pereira Filho *et al.* 2010; Toté *et al.* 2015). Ebert *et al.* (2007) highlights the tendency by SREs to wrongly detect rainfall in dry arid conditions in the United States, Australia, and northwestern Europe.

ii: *What is the performance of bias correction schemes for CMORPH rainfall estimates in the Zambezi River Basin?*

This question was addressed in Chapter 5. The study assesses the effectiveness of five linear/non-linear and time-space variant/invariant bias correction schemes to remove bias in the Climate Prediction Center-MORPHing (CMORPH) rainfall estimates in the Lower, Middle and Upper Zambezi. Overall, rainfall bias removal is more effective for the Spatio-temporal bias and Elevation zone bias schemes compared to other bias correction schemes (Power transform, Distribution transformation and Quantile mapping based on an empirical distribution). Taylor Diagrams and rigorous statistical tests further show that bias is effectively reduced for very low to moderate rainfall rates (< 2.5 and 5.0-10.0 mm/day) than the high to very high rainfall rates (10.0-20.0 mm/day and > 20.0 mm/day). For this basin, SRE bias is more effectively removed for the wet season than for the dry season. The study also tested, yet on a very small rain gauge sample, the influence of elevation and distance from large water bodies on bias. Analysis using Taylor diagrams on gauge and CMORPH rainfall estimates

suggest that performance increases for areas at higher elevation (> 950 m) in the Zambezi Basin and that CMORPH has largest mismatch at low elevation. The match between gauge and CMORPH estimates improved at increasing distance to large scale open water bodies. Results in this study are useful to satellite rainfall algorithm developers so as to application of SREs in water resources management.

iii: *What is the performance of bias corrected CMORPH rainfall estimates as error propagation serves to assess performance evaluation*

Chapter 6 discusses hydrologic evaluation of bias corrected CMORPH rainfall estimates at the headwater catchment of the Zambezi River. Comparison of rain gauge observations to CMORPH estimates was at point to pixel scale, as well as pixel to pixel scale in the Kabompo River Basin. The REW model was calibrated for rain gauge rainfall as input where parameter optimization was manually by trial and error to optimize model performance. The model was further manually recalibrated for each case when bias corrected and uncorrected rainfall SREs serves as rainfall forcing. Results show significant biases (> 20 %) in the uncorrected satellite rainfall estimates, which were effectively removed by the Spatio-temporal bias correction scheme. Bias correction at the point-to-pixel scale performs better than the pixel-to-pixel scale. The bias in uncorrected CMORPH causes large mismatch between simulated and observed streamflow. After bias correction, there is substantial reduction in mismatch. Results showed that REW parameters during manual calibration changed significantly (> 50 %) when using gauge-based rainfall estimates, uncorrected, and bias corrected CMORPH estimates, though parameters remained within physically acceptable range. It was found that bias correction of precipitation is critical and can yield to substantial improvement in capturing both streamflow pattern and magnitude for effective water resources management.

iv: *How do errors in satellite rainfall propagate to cause mismatch in streamflow characteristics in a headwater catchment of the Zambezi River Basin?*

This question is addressed in Chapter 7 where the focus is on the error propagation of the CMORPH rainfall product on simulated streamflow and the application of an automated multi-objective calibration approach (2006–2012). Unlike manual calibration in Chapter 6, the ε-NSGAII algorithm was used to optimize the model parameters in Chapter 7. Assessments on error propagation targeted streamflow modelling for hydrograph shape and volume, specific

hydrograph characteristics, and water balance composition. Parameters of the model were first optimized for rain gauge rainfall using the ε-NSGAII algorithm to obtain a reference parameter set. That reference parameter set was applied for multi-objective assessments with SRE rainfall sources by rerunning the ε-NSGAII algorithm. By the use of multi-objective functions, uncorrected CMORPH results in substantial augmentation of rainfall error to streamflow simulation mismatch whereas bias corrected estimates result in attenuation of error. This study shows that ratios of model based actual evapotranspiration over rainfall (ET_a/P) and streamflow over rainfall (Q_s/P) (runoff coefficient) as well as model water storage (ΔS) change subject to selected rainfall input data source. Findings provided new hydrological insights on propagation effects of satellite-based rainfall errors in streamflow modelling. Analysis for water balance composition has great potential to improve application of satellite precipitation products in water management and decision making in the Zambezi basin.

8.2 Recommendations for future work

For this study, time series data of only 60 meteorological stations were available for the vast Zambezi River basin (area of 1.39 million km^2) that as such must be considered a poorly gauged basin. It seems relevant to use more rain gauge stations in future studies, so that the spatial patterns of rainfall using satellite products can be investigated, and a pixel-to-pixel analysis can be applied to conduct in-depth analysis.

Findings in this study apply for the CMORPH rainfall product and the study area. Use of other satellite rainfall products to the study area may result in different study outcomes. To enhance applicability of SRE to serve hydrological applications, it is recommended to explore multi-satellite blended precipitation products. Satellite rainfall blending techniques involve high-resolution satellite products being blended using simple statistical or advanced machine learning based techniques to come up with an improved gridded rainfall product based on the strengths of the respective data sources. To achieve the desired outcomes, the blending of the selected satellite products requires in situ-based rainfall to train the algorithms. Data scarce areas with complex topography such as the Zambezi Basin could benefit from such research initiatives.

Further research for the Zambezi Basin should aim to develop bias correction schemes that can be applied to correct for onset and end of rainfall season. The

further use of SREs to differentiate rainfall types will be a welcome research area which is important for management of floods and drought in the Basin.

This study successfully assessed effects of SRE error propagation on hydrological modelling by the REW rainfall-runoff model. Parameters of the model were optimized using the ε-NSGAII algorithm for in situ-based rainfall to obtain a reference parameter set. Future studies should further quantify and advise on sources of uncertainty and error that could contribute to streamflow mismatch such as rainfall representation, inaccurate representation of catchment characteristics such as land cover, and stage-discharge relation.

Still in multi-objective optimization, future studies should also consider techniques that combine all the multi-objective functions into one scalar, composite or weighted objective function. In this approach, the original multi-objective optimization problem will be transformed into a single-objective optimization problem to result in the solution methods for solving single-objective problems employable.

The above applications require regulators and river basin managers to develop experimental observation networks that are capable of monitoring the variability in meteorological and hydrological processes that control runoff generation processes relevant for water resources management. The hydrometeorological network in the Zambezi basin and its quality are slowly deteriorating. Putting resources by governments in southern Africa on a good monitoring network is essential for satellite rainfall error assessment as well as to assurance reliable hydrological modelling.

Bibliography

Abbott, M.B., Bathurst, J.C., Cunge, J.A., O'Connell, P.E., Rasmussen, J., 1986. An introduction to the European Hydrological System — Systeme Hydrologique Europeen, "SHE", 1: History and philosophy of a physically-based, distributed modelling system. J. Hydrol. 87, 45–59. https://doi.org/https://doi.org/10.1016/0022-1694(86)90114-9.

Akhtar, M., Ahmad, N., Booij, M.J., 2009. Use of regional climate model simulations as input for hydrological models for the Hindukush-Karakorum-Himalaya region. Hydrol. Earth Syst. Sci. 13, 1075–1089. https://doi.org/10.5194/hess-13-1075-2009.

Allen, R.G., Pereira, L.S., Raes, D., Smith, M., 1998. Crop evapotranspiration-Guidelines for computing crop water requirements. FAO Irrigation and Drainage Paper 56, FAO, ISBN 92-5-104219-5. Rome, Italy.

Artan, G., Gadain, H., Smith, J., Asante, K., Bandaragoda, C.J., Verdin, J., 2007. Adequacy of satellite derived rainfall data for streamflow modeling. Nat Haz 43, 167–185.

Alazzy, A.A., Lü, H., Chen, R., Ali, A.B., Zhu, Y., Su, J., 2017. Evaluation of Satellite Precipitation Products and Their Potential Influence on Hydrological Modeling over the Ganzi River Basin of the Tibetan Plateau. Adv. Meteorol. 2017, 23. https://doi.org/10.1155/2017/3695285.

Alemu, M.L., Worqlul, A.W., Zimale, F.A., Tilahun, S.A., Steenhuis, T.S., 2020. Water Balance for a Tropical Lake in the Volcanic Highlands: Lake Tana, Ethiopia. Water . https://doi.org/10.3390/w12102737.

Asadullah, A., Mcintyre, N., Kigobe, M.A.X., Asadullah, A., Mcintyre, N., Kigobe, M.A.X., 2010. Evaluation of five satellite products for estimation of rainfall over Uganda. Hydrol. Sci. J. 6667. https://doi.org/10.1623/hysj.53.6.1137.

Adeyewa, Z. D., and K. Nakamura, 2003: Validation of TRMM Radar Rainfall Data over Major Climatic Regions in Africa. Journal of Applied Meteorology, 42, 331-347.

AghaKouchak, A., A. Mehran, H. Norouzi, and A. Behrangi, 2012: Systematic and random error components in satellite precipitation data sets. Geophysical Research Letters, 39, L09406.

Ahmed Suliman, A. H., W. Gumindoga, A. Katimon, and I. Z. M. Darus, 2014: Semi-distributed rainfall-runoff modeling utilizing ASTER DEM in Pinang catchment of Malaysia. Sains Malaysiana, 43, 1379-1388.

Alazzy, A. A., H. Lü, R. Chen, A. B. Ali, Y. Zhu, and J. Su, 2017: Evaluation of Satellite Precipitation Products and Their Potential Influence on

Hydrological Modeling over the Ganzi River Basin of the Tibetan Plateau. Advances in Meteorology, 2017, 23.

Allen, R. G., L. S. Pereira, D. Raes, and M. Smith, 1998: Crop evapotranspiration-Guidelines for computing crop water requirements. FAO Irrigation and Drainage Paper 56, FAO, ISBN 92-5-104219-5.

Artan, G., H. Gadain, J. Smith, K. Asante, C. J. Bandaragoda, and J. Verdin, 2007: Adequacy of satellite derived rainfall data for streamflow modeling. Nat Haz, 43, 167-185.

Awange, J.L., Ferreira, V.G., Forootan, E., Khandu, N.O., Andam-Akorful, S.A., Agutu, N.O., He, X.F., 2016. Uncertainties in remotely sensed precipitation data over Africa. Int. J. Climatol. 36, 303–323. https://doi.org/10.1002/joc.4346.

Baker, N.C., Taylor, P.C., 2016. A Framework for Evaluating Climate Model Performance Metrics. J. Clim. 29, 1773–1782. https://doi.org/10.1175/jcli-d-15-0114.1

Bajracharya, S. R., M. S. Shrestha, and A. B. Shrestha, 2014: Assessment of high-resolution satellite rainfall estimation products in a streamflow model for flood prediction in the Bagmati basin, Nepal. Journal of Flood Risk Management, 10 (1). https://doi.org/10.1111/jfr3.12133

Beck, L., and T. Bernauer, 2011: How will combined changes in water demand and climate affect water availability in the Zambezi river basin? Global Environ. Change. 21 (3), 1061-1072.

Behrangi, A., B. Khakbaz, T. C. Jaw, A. AghaKouchak, K. Hsu, and S. Sorooshian, 2011: Hydrologic evaluation of satellite precipitation products over a mid-size basin. Journal of Hydrology, 397, 225-237.

Beilfuss, R., 2012: A Risky Climate for Southern African Hydro: Assessing hydrological risks and consequences for Zambezi River Basin dams. International Rivers Network (IRN). DOI: 10.13140/RG.2.2.30193.48486

Beilfuss, R., P. Dutton, and D. Moore, 2000: Landcover and Landuse change in the Zambezi Delta. Zambezi Basin Wetlands Volume III Landuse Change and Human impacts, Chapter 2, Biodiversity Foundation for Africa, 31-105.

Beniston, M., 2012: Impacts of climatic change on water and associated economic activities in the Swiss Alps. Journal of Hydrology, 412–413, 291-296.

Beven, K., 2012: Down to Basics: Runoff Processes and the Modelling Process. Rainfall-Runoff Modelling, John Wiley & Sons, Ltd, 1-23.

Beven, K. J., 1997: Distributed hydrological modelling: Applications of the TOPMODEL concept. . John Wiley and Sons Ltd.

Beven, K. J., 2001: Rainfall-Runoff Modelling: The Primer. John Wiley & Sons.

Beyer, M., M. Wallner, L. Bahlmann, V. Thiemig, J. Dietrich, and M. Billib, 2014: Rainfall characteristics and their implications for rain-fed agriculture: a case study in the Upper Zambezi River Basin. Hydrological Sciences Journal, null-null.

Bhatti, H., T. Rientjes, A. Haile, E. Habib, and W. Verhoef, 2016: Evaluation of Bias Correction Method for Satellite-Based Rainfall Data. Sensors, 16, 884.

Biftu, G. F., and T. Y. Gan, 2004: A semi-distributed, physics-based hydrologic model using remotely sensed and Digital Terrain Elevation Data for semi-arid catchments. International Journal of Remote Sensing, 25, 4351-4379.

Bisselink, B., Zambrano-Bigiarini, M., Burek, P., de Roo, A., 2016. Assessing the role of uncertain precipitation estimates on the robustness of hydrological model parameters under highly variable climate conditions. J. Hydrol. Reg. Stud. 8, 112–129. https://doi.org/https://doi.org/10.1016/j.ejrh.2016.09.003.

Bitew, M. M., and M. Gebremichael, 2011: Evaluation of satellite rainfall products through hydrologic simulation in a fully distributed hydrologic model. Water Resources Research, 47.

Bitew, M. M., M. Gebremichael, L. T. Ghebremichael, and Y. A. Bayissa, 2011: Evaluation of High-Resolution Satellite Rainfall Products through Streamflow Simulation in a Hydrological Modeling of a Small Mountainous Watershed in Ethiopia. Journal of Hydrometeorology, 13, 338-350.

Blume, T., Zehe, E., Bronstert, A., Blume, T., Zehe, E., Bronstert, A., 2010. Rainfall — runoff response , event-based runoff coefficients and hydrograph separation 6667. https://doi.org/10.1623/hysj.52.5.843.

Booij, M.J., Krol, M.S., 2010. Balance between calibration objectives in a conceptual hydrological model. Hydrol. Sci. J. 55, 1017–1032. https://doi.org/10.1080/02626667.2010.505892

Botter, G., A. Porporato, I. Rodriguez-Iturbe, and A. Rinaldo, 2007: Basin-scale soil moisture dynamics and the probabilistic characterization of carrier hydrologic flows: Slow, leaching-prone components of the hydrologic response. Water Resources Research, 43, n/a-n/a.

Bouwer, L. M., J. C. J. H. Aerts, G. M. Van de Coterlet, N. Van de Giessen, A. Gieske, and C. Manaerts, 2004: Evaluating downscaling methods for preparing Global Circulation Model (GCM) data for hydrological impact modelling. Chapter 2, in Aerts, J.C.J.H. & Droogers, P.

(Eds.), Climate Change in Contrasting River Basins: Adaptation Strategies for Water, Food and Environment. (pp. 25-47). Wallingford, UK: Cabi Press.

Breidenbach, J. P., and J. S. Bradberry, 2001: Multisensor Precipitation Estimates Produced by National Weather Service River Forecast Centers for Hydrologic Applications. Poceedings of the 2001 Georgia Water Resources Conference, April 26 and 27, 2001, Athens, Georgia.

Brocca, L., L. Ciabatta, C. Massari, S. Camici, and A. Tarpanelli, 2017: Soil Moisture for Hydrological Applications: Open Questions and New Opportunities. Water, 9, 140.

Cattani, E., A. Merino, and V. Levizzani, 2016: Evaluation of Monthly Satellite-Derived Precipitation Products over East Africa. Journal of Hydrometeorology, 17, 2555-2573.

Cecinati, F., Rico-Ramirez, M.A., Heuvelink, G.B.M., Han, D., 2017. Representing radar rainfall uncertainty with ensembles based on a time-variant geostatistical error modelling approach. J. Hydrol. 548, 391–405. https://doi.org/http://dx.doi.org/10.1016/j.jhydrol.2017.02.053

Chacon-Hurtado, J.C., Alfonso, L., Solomatine, D.P., 2017. Rainfall and streamflow sensor network design: a review of applications, classification, and a proposed framework. Hydrol. Earth Syst. Sci. 21, 3071–3091. https://doi.org/10.5194/hess-21-3071-2017.

Chai, T., Draxler, R.R., Prediction, C., 2014. Root mean square error (RMSE) or mean absolute error (MAE)? – Arguments against avoiding RMSE in the literature 1247–1250. https://doi.org/10.5194/gmd-7-1247-2014.

Chavula, G., P. Brezonik, and M. Bauer, 2011: Land Use and Land Cover Change (LULC) in the Lake Malawi Drainage Basin , 1982-2005 International Journal of Geosciences 2, 172-178.

Chen, S., Hong, Y., Cao, Q., Kirstetter, P.-E., Gourley, J.J., Qi, Y., Zhang, J., Howard, K., Hu, J., Wang, J., 2012. Performance evaluation of radar and satellite rainfalls for Typhoon Morakot over Taiwan: Are remote-sensing products ready for gauge denial scenario of extreme events? J. Hydrol. https://doi.org/http://dx.doi.org/10.1016/j.jhydrol.2012.12.026

Chen, F., Yuan, H., Sun, R., Yang, C., 2020. Streamflow simulations using error correction ensembles of satellite rainfall products over the Huaihe river basin. J. Hydrol. 589, 125179. https://doi.org/https://doi.org/10.1016/j.jhydrol.2020.125179

Chisanga, C.B., Mubanga, K.H., Sichigabula, H., Banda, K., Muchanga, M., Ncube, L., van Niekerk, H.J., Zhao, B., Mkonde, A.A., Rasmeni, S.K., 2022. Modelling climatic trends for the Zambezi and Orange River Basins:

implications on water security. J. Water Clim. Chang. 13, 1275–1296. https://doi.org/10.2166/wcc.2022.308.

Choi, H., 2013: Parameterization of High Resolution Vegetation Characteristics using Remote Sensing Products for the Nakdong River Watershed, Korea. Remote Sensing, 5, 473-490.

Chrysoulakis, N., M. Abrams, H. Feidas, and Velianitis. D, 2004: Analysis of ASTER multispectral stereo imagery to produce DEM and land cover databases for Greek Islands: the REALDEMS project. EU-LAT Workshop on e-Environment, Brussels, Belgium 13-17 December.

Chu, T., and K.-E. Lindenschmidt, 2017: Comparison and Validation of Digital Elevation Models Derived from InSAR for a Flat Inland Delta in the High Latitudes of Northern Canada. Canadian Journal of Remote Sensing, 43, 109-123.

Cohen Liechti, T., Matos, J.P., Boillat, J.L., Schleiss, A.J., 2012. Comparison and evaluation of satellite derived precipitation products for hydrological modeling of the Zambezi River Basin. Hydrol. Earth Syst. Sci. 16, 489–500.

Ciach, G.J., Krajewski, W.F., 2006. Analysis and modeling of spatial correlation structure in small-scale rainfall in Central Oklahoma. Adv. Water Resour. 29, 1450–1463. https://doi.org/https://doi.org/10.1016/j.advwatres.2005.11.003

Cuvelier, C., and Coauthors, 2007: CityDelta: A model intercomparison study to explore the impact of emission reductions in European cities in 2010. Atmospheric Environment, 41, 189-207.

Dang, Q.T., Laux, P., Kunstmann, H., 2017. Future high- and low-flow estimations for Central Vietnam: a hydro-meteorological modelling chain approach. Hydrol. Sci. J. 62, 1867–1889. https://doi.org/10.1080/02626667.2017.1353696.

de Vos, N.J., Rientjes, T.H.M., 2008a. Correction of Timing Errors of Artificial Neural Network Rainfall-Runoff Models, in: Abrahart, R.J., See, L.M., Solomatine, D.P. (Eds.), Practical Hydroinformatics: Computational Intelligence and Technological Developments in Water Applications. Springer Berlin Heidelberg, Berlin, Heidelberg, pp. 101–112. https://doi.org/10.1007/978-3-540-79881-1_8 LB - de Vos2008.

de Vos, N.J., Rientjes, T.H.M., 2008b. Multiobjective training of artificial neural networks for rainfall-runoff modeling. Water Resour. Res. 44, n/a-n/a. https://doi.org/10.1029/2007WR006734.

de Vos, N.J., Rientjes, T.H.M., 2005. Constraints of artificial neural networks for

rainfall-runoff modelling: trade-offs in hydrological state representation and model evaluation. Hydrol. Earth Syst. Sci. 9, 111–126. https://doi.org/10.5194/hess-9-111-2005.

De Vos, N.J., Rientjes, T.H.M., 2007. Multi-objective performance comparison of an artificial neural network and a conceptual rainfall—runoff model. Hydrol. Sci. J. 52, 397–413. https://doi.org/10.1623/hysj.52.3.397.

Deb, K., Goyal, M., 1996. A Combined Genetic Adaptive Search (GeneAS) for Engineering Design 1 Introduction 2 Genetic Adaptive Search. Comput. Sci. Inf. 1–20.

Deb, K., Agrawal, R.., 1995. Simulated Binary Crossover for Continuous Search Space. Complex Syst. 9, 115–148.

Deb, K., Pratap, A., Agarwal, S., Meyarivan, T., 2002. A fast and elitist multiobjective genetic algorithm: NSGA-II. IEEE Trans. Evol. Comput. 6, 182–197. https://doi.org/10.1109/4235.996017.

Deckers, D. E. H., M. Booij, T. M. Rientjes, and M. Krol, 2010: Catchment Variability and Parameter Estimation in Multi-Objective Regionalisation of a Rainfall–Runoff Model. Water Resources Management, 24, 3961-3985.

Delrieu, G., and Coauthors, 2009: Weather radar and hydrology. Advances in Water Resources, 32, 969-974.

Demirel, M.C., Booij, M.J., 2009. Identification of an appropriate low flow forecast model for the Meuse River 296–303.

Dezfuli, A.K., Ichoku, C.M., Mohr, K.I., Huffman, G.J., 2017. Precipitation Characteristics in West and East Africa from Satellite and in Situ Observations. J. Hydrometeorol. 18, 1799–1805. https://doi.org/10.1175/jhm-d-17-0068.1

Dembélé, M., and S. J. Zwart, 2016: Evaluation and comparison of satellite-based rainfall products in Burkina Faso, West Africa. International Journal of Remote Sensing, 37, 3995-4014.

Dennis, R., and Coauthors, 2010: A framework for evaluating regional-scale numerical photochemical modeling systems. Environmental Fluid Mechanics, 10, 471-489.

Devia, G. K., B. P. Ganasri, and G. S. Dwarakish, 2015: A Review on Hydrological Models. Aquatic Procedia, 4, 1001-1007.

Dhamge, N.R., Atmapoojya, S.L., Kadu, M.S., 2012. Genetic Algorithm Driven ANN Model for Runoff Estimation. Procedia Technol. 6, 501–508. https://doi.org/https://doi.org/10.1016/j.protcy.2012.10.060.

Dinku, T., S. Connor, and P. Ceccato, 2010b: Comparison of CMORPH and TRMM-3B42 over Mountainous Regions of Africa and South America. Satellite Rainfall Applications for Surface Hydrology, M. Gebremichael, and F. Hossain, Eds., Springer Netherlands, 193-204.

Dinku, T., Chidzambwa, S., Ceccato, P., Connor, S.J., Ropelewski, C.F., 2008. Validation of high-resolution satellite rainfall products over complex terrain. Int. J. Remote Sens. 29, 4097–4110. https://doi.org/10.1080/01431160701772526.

Dinku, T., P. Ceccato, E. Groverâ€• Kopec, M. Lemma, S. J. Connor, and C. F. Ropelewski, 2007: Validation of satellite rainfall products over East Africa's complex topography. International Journal of Remote Sensing, 28, 1503-1526.

Du, J., Qian, L., Rui, H., Zuo, T., Zheng, D., Xu, Y., Xu, C.Y., 2012. Assessing the effects of urbanization on annual runoff and flood events using an integrated hydrological modeling system for Qinhuai River basin, China. J. Hydrol. 464–465, 127–139. https://doi.org/http://dx.doi.org/10.1016/j.jhydrol.2012.06.057

Ebert, E. E., J. E. Janowiak, and C. Kidd, 2007: Comparison of Near-Real-Time Precipitation Estimates from Satellite Observations and Numerical Models. Bulletin of the American Meteorological Society, 88, 47-64.

Elgamal, A., Reggiani, P., Jonoski, A., 2017. Impact analysis of satellite rainfall products on flow simulations in the Magdalena River Basin, Colombia. J. Hydrol. Reg. Stud. 9, 85–103. https://doi.org/http://dx.doi.org/10.1016/j.ejrh.2016.09.001.

Falck, A.S., Maggioni, V., Tomasella, J., Vila, D.A., Diniz, F.L.R., 2015. Propagation of satellite precipitation uncertainties through a distributed hydrologic model: A case study in the Tocantins–Araguaia basin in Brazil. J. Hydrol. 527, 943–957. https://doi.org/https://doi.org/10.1016/j.jhydrol.2015.05.042.

Fallah, A., O, S., Orth, R., 2020. Climate-dependent propagation of precipitation uncertainty into the water cycle. Hydrol. Earth Syst. Sci. 24, 3725–3735. https://doi.org/10.5194/hess-24-3725-2020

Fang, G.H., Yang, J., Chen, Y.N., Zammit, C., 2015a. Comparing bias correction methods in downscaling meteorological variables for a hydrologic impact study in an arid area in China. Hydrol. Earth Syst. Sci. 19, 2547–2559. https://doi.org/10.5194/hess-19-2547-2015

FAO/IIASA/ISRIC/ISS-CAS/JRC, 2009. Harmonized World Soil Database (version 1.1). FAO, Rome, Italy and IIASA, Laxenburg, Austria.

Forootan, A.M.E., 2018. Comparing multi-objective optimization techniques to calibrate a conceptual hydrological model using in situ runoff and daily GRACE data. Computational Geosciences, 22, 789–814.

Franchito, S. H., V. B. Rao, A. C. Vasques, C. M. E. Santo, and J. C. Conforte, 2009: Validation of TRMM precipitation radar monthly rainfall estimates over Brazil. Journal of Geophysical Research: Atmospheres, 114, D02105.

Fylstra, D., L. Lasdon, J. Watson, and A. Waren, 1998: Design and Use of the Microsoft Excel Solver. Interfaces, 28, 29-55.

Garrison, S., 2017. Soil Classification. Encycl. Br. inc. URL https://www.britannica.com/science/soil/Soil-classification. Accessed 11 December 2022.

Gao, Y. C., and M. F. Liu, 2013: Evaluation of high-resolution satellite precipitation products using rain gauge observations over the Tibetan Plateau. Hydrol. Earth Syst. Sci., 17, 837-849.

Gebregiorgis, A. S., and F. Hossain, 2013: Understanding the Dependence of Satellite Rainfall Uncertainty on Topography and Climate for Hydrologic Model Simulation. Geoscience and Remote Sensing, IEEE Transactions on, 51, 704-718.

Gebregiorgis, A. S., Y. Tian, C. D. Peters-Lidard, and F. Hossain, 2012: Tracing hydrologic model simulation error as a function of satellite rainfall estimation bias components and land use and land cover conditions. Water Resources Research, 48, n/a-n/a.

Gosset, M., J. Viarre, G. Quantin, and M. Alcoba, 2013: Evaluation of several rainfall products used for hydrological applications over West Africa using two high-resolution gauge networks. Quarterly Journal of the Royal Meteorological Society, 139, 923-940.

Gumindoga, W., D. T. Rwasoka, and A. Murwira, 2011: Simulation of streamflow using TOPMODEL in the Upper Save River catchment of Zimbabwe. Physics and Chemistry of the Earth, Parts A/B/C, 36, 806-813.

Gumindoga, W., T. H. M. Rientjes, A. T. Haile, and T. Dube, 2014: Predicting streamflow for land cover changes in the Upper Gilgel Abay River Basin, Ethiopia: A TOPMODEL based approach. Physics and Chemistry of the Earth, Parts A/B/C, 76–78, 3-15.

Gumindoga, W., Rientjes, T., Shekede, M.D., Rwasoka, D.T., Nhapi, I., Haile, A.T., 2014. Hydrological impacts of urbanization of two catchments in Harare, Zimbabwe. Remote Sens. 6. https://doi.org/10.3390/rs61212544

Gumindoga, W., T. H. M. Rientjes, A. T. Haile, H. Makurira, and P. Reggiani, 2016: Bias correction Gumindoga, W., Rientjes, T.H.M., Haile, A.T., Makurira, H., Reggiani, P., 2017. Performance of bias correction schemes for CMORPH rainfall estimates in the Zambezi River Basin. Hydrol. Earth Syst. Sci. Discuss. 2017, 1–27. https://doi.org/10.5194/hess-2017-385.

Gumindoga, W., Rientjes, T.H.M., Haile, A.T., Makurira, H., Reggiani, P., 2019a. Performance evaluation of CMORPH satellite precipitation product in the Zambezi Basin. Int. J. Remote Sens. 40, 1–20. https://doi.org/10.1080/01431161.2019.1602791.

Gumindoga, W., Rientjes, T.H.M., Haile, A.T., Makurira, H., Reggiani, P., 2019b. Performance of bias-correction schemes for CMORPH rainfall estimates in the Zambezi River basin. Hydrol. Earth Syst. Sci. 23, 2915–2938. https://doi.org/10.5194/hess-23-2915-2019.

Gumindoga, W., Rientjes, T.H.M., Reggiani, P., Makurira H, A.T., A, H., 2020. Hydrologic evaluation of bias corrected CMORPH rainfall estimates at the headwater catchment of the Zambezi River. Phys. Chem. Earth 115. https://doi.org/10.1016/j.pce.2019.11.004.

Grillakis, M.G., Koutroulis, A.G., Daliakopoulos, I.N., Tsanis, I.K., 2017. A method to preserve trends in quantile mapping bias correction of climate modeled temperature. Earth Syst. Dynam. Discuss. 2017, 1–26. https://doi.org/10.5194/esd-2017-53.

Gutjahr, O., Heinemann, G., 2013. Comparing precipitation bias correction methods for high-resolution regional climate simulations using COSMO-CLM. Theor. Appl. Climatol. 114, 511–529. https://doi.org/10.1007/s00704-013-0834-z.

Guo, H., Chen, S., Bao, A., Hu, J., Gebregiorgis, A., Xue, X., Zhang, X., 2015. Inter-Comparison of High-Resolution Satellite Precipitation Products over Central Asia. Remote Sens. 7, 7181.

Habib, E., B. F. Larson, and J. Graschel, 2009: Validation of NEXRAD multisensor precipitation estimates using an experimental dense rain gauge network in south Louisiana. Journal of Hydrology, 373, 463-478.

Habib, E., M. ElSaadani, and A. T. Haile, 2012a: Climatology-Focused Evaluation of CMORPH and TMPA Satellite Rainfall Products over the Nile Basin. Journal of Applied Meteorology and Climatology, 51, 2105-2121.

Habib, E., A. T. Haile, Y. Tian, and R. J. Joyce, 2012b: Evaluation of the High-Resolution CMORPH Satellite Rainfall Product Using Dense Rain Gauge

Observations and Radar-Based Estimates. Journal of Hydrometeorology, 13, 1784-1798. https://doi.org/10.1175/jhm-d-12-017.1

Habib, E., Haile, A., Sazib, N., Zhang, Y., Rientjes, T., 2014. Effect of Bias Correction of Satellite-Rainfall Estimates on Runoff Simulations at the Source of the Upper Blue Nile. Remote Sens. 6, 6688–6708.

Haile, A. T., T. Rientjes, A. Gieske, and M. Gebremichael, 2009: Rainfall Variability over Mountainous and Adjacent Lake Areas: The Case of Lake Tana Basin at the Source of the Blue Nile River. Journal of Applied Meteorology and Climatology, 48, 1696-1717.

Haile, A. T., E. Habib, and T. H. M. Rientjes, 2013a: Evaluation of the climate prediction center CPC morphing technique CMORPH rainfall product on hourly time scales over the source of the Blue Nile river. Hydrological processes, 27, 1829-1839.

Haile, A. T., E. Habib, M. Elsaadani, and T. Rientjes, 2013b: Inter-comparison of satellite rainfall products for representing rainfall diurnal cycle over the Nile basin. International Journal of Applied Earth Observation and Geoinformation, 21, 230-240.

Haile, A.T., Yan, F., Habib, E., 2014. Accuracy of the CMORPH satellite-rainfall product over Lake Tana Basin in Eastern Africa. Atmos. Res. Press. Accept. Manuscr. https://doi.org/http://dx.doi.org/10.1016/j.atmosres.2014.11.011.

Heidinger, H., Yarlequé, C., Posadas, A., Quiroz, R., 2012. TRMM rainfall correction over the Andean Plateau using wavelet multi-resolution analysis. Int. J. Remote Sens. 33, 4583–4602. https://doi.org/10.1080/01431161.2011.652315.

Hempel, S., Frieler, K., Warszawski, L., Schewe, J., Piontek, F., 2013. A trend-preserving bias correction - the ISI-MIP approach. Earth Syst. Dynam. 4, 219–236. https://doi.org/10.5194/esd-4-219-2013.

Hernandez, M., S. Miller, D. Goodrich, B. Goff, W. Kepner, C. Edmonds, and K. Bruce Jones, 2000: Modeling Runoff Response To Land Cover And Rainfall Spatial Variability In Semi-Arid Watersheds. Monitoring Ecological Condition in the Western United States, S. Sandhu, B. Melzian, E. Long, W. Whitford, and B. Walton, Eds., Springer Netherlands, 285-298.

Hirpa, F. A., M. Gebremichael, and T. Hopson, 2010: Evaluation of High-Resolution Satellite Precipitation Products over Very Complex Terrain in Ethiopia. Journal of Applied Meteorology and Climatology, 49, 1044-1051.

Hoel, A., 2015. Collaborative Management of the Zambezi River Basin Ensures Greater Economic Resilience. World Bank Group Online Report. Accessed

11 December 2022.

Hong, Y., Hsu, K., Moradkhani, H., Sorooshian, S., 2006. Uncertainty quantification of satellite precipitation estimation and Monte Carlo assessment of the error propagation into hydrologic response. Water Resour. Res. 42, W08421. https://doi.org/10.1029/2005WR004398.

Hughes, D. A., 2006: Comparison of satellite rainfall data with observations from gauging station networks. Journal of Hydrology, 327, 399-410.

Hughes, D.A., Farinosi, F., 2020. Assessing development and climate variability impacts on water resources in the Zambezi River basin. Simulating future scenarios of climate and development. J. Hydrol. Reg. Stud. 32, 100763. https://doi.org/https://doi.org/10.1016/j.ejrh.2020.100763.

Immerzeel, W. W., 2010: Bias Correction for Satellite Precipitation Estimation used by the MRC Mekong Flood Forecasting System. Mekong River Commission-Mission report -March 2010.

Ines, A. V. M., and J. W. Hansen, 2006: Bias correction of daily GCM rainfall for crop simulation studies. Agricultural and Forest Meteorology, 138, 44-53.

Jamandre, C. A., and G. T. Narisma, 2013: Spatio-temporal validation of satellite-based rainfall estimates in the Philippines. Atmospheric Research, 122, 599-608.

Janssen, P. H. M., and P. S. C. Heuberger, 1995: Calibration of process-oriented models. Ecological Modelling, 83, 55-66.

Jiang, S., Zhou, M., Ren, L., Cheng, X., Zhang, P., 2016. Evaluation of latest TMPA and CMORPH satellite precipitation products over Yellow River Basin. Water Sci. Eng. 9, 87–96. https://doi.org/http://dx.doi.org/10.1016/j.wse.2016.06.002.

Johnsen, K.-P., Mengelkamp, H.-T., Huneke, S., 2005. Multi-objective calibration of the land surface scheme TERRA/LM using LITFASS-2003 data. Hydrol. Earth Syst. Sci. 9, 586–596. https://doi.org/10.5194/hess-9-586-2005.

Jothityangkoon, C., C. Hirunteeyakul, K. Boonrawd, and M. Sivapalan, 2013: Assessing the impact of climate and land use changes on extreme floods in a large tropical catchment. Journal of Hydrology.

Joyce, R. J., J. E. Janowiak, P. A. Arkin, and P. Xie, 2004: CMORPH: A method that produces global precipitation estimates from passive microwave and infrared data at high spatial and temporal resolution. J. Hydromet., 5, 487-503.

Jury, M.R., 2017. Spatial gradients in climatic trends across the southeastern Antilles 1980–2014. Int. J. Climatol. 37, 5181–5191. https://doi.org/10.1002/joc.5156.

Jung, D., Choi, Y.H., Kim, J.H., 2017. Multiobjective Automatic Parameter Calibration of a Hydrological Model. https://doi.org/10.3390/w9030187

Karbalaee, N., K. Hsu, S. Sorooshian, and D. Braithwaite, 2017: Bias adjustment of infrared-based rainfall estimation using Passive Microwave satellite rainfall data. Journal of Geophysical Research: Atmospheres, 122, 3859-3876.

Kashaigili, J. J., and A. M. Majaliwa, 2013: Implications of Land Use and Land Cover Changes on Hydrological Regimes of the Malagarasi River, Tanzania. Journal of Agricultural Science and Applications, 2, 45-50.

Katiraie-Boroujerdy, P., N. Nasrollahi, K. Hsu, and S. Sorooshian, 2013: Evaluation of satellite-based precipitation estimation over Iran. Vol. 97, Elsevier, 15 pp.

Kersten, M. S., 1949: Thermal properties of soils. Bulletin 28, 227 pp.

Khan, S. I., Y. Hong, J. J. Gourley, M. U. K. Khattak, B. Yong, and H. J. Vergara, 2014: Evaluation of three high-resolution satellite precipitation estimates: Potential for monsoon monitoring over Pakistan. Advances in Space Research, 54, 670-684.

Kim, J., Jung, I., Park, K., Yoon, S., Lee, D., 2016. Hydrological Utility and Uncertainty of Multi-Satellite Precipitation Products in the Mountainous Region of South Korea. Remote Sens. 8, 608.

Kimani, M., Hoedjes, J., Su, Z., 2017. An Assessment of Satellite-Derived Rainfall Products Relative to Ground Observations over East Africa. Remote Sens. 9, 430.

Kite, G. W., and A. Pietroniro, 1996: Remote sensing application in hydrological modeling. Hydrological Sciences Journal - des Sciences Hydrologiques, 41, 563-591.

Kling, H., P. Stanzel, and M. Preishuber, 2014: Impact modelling of water resources development and climate scenarios on Zambezi River discharge. Journal of Hydrology: Regional Studies, 1, 17-43.

Kollat, J.B., Reed, P.M., 2006. Comparing state-of-the-art evolutionary multi-objective algorithms for long-term groundwater monitoring design. Adv. Water Resour. 29, 792–807. https://doi.org/10.1016/j.advwatres.2005.07.010.

Koutsouris, A.J., Chen, D., Lyon, S.W., 2016. Comparing global precipitation data sets in eastern Africa: a case study of Kilombero Valley, Tanzania. Int. J. Climatol. 36, 2000–2014. https://doi.org/10.1002/joc.4476.

Krampe, F., 2012: Zambezi River Basin: A risk zone of climate change and economic vulnerabilitymore. Life & Peace Institute, March 2012, Volume 17.

Lafon, T., S. Dadson, G. Buys, and C. Prudhomme, 2013: Bias correction of daily precipitation simulated by a regional climate model: a comparison of methods. Int. J. Climatol., 33, 1367-1381.

Lee, H., M. Sivapalan, and E. Zehe, 2005: Representative Elementary Watershed (REW) approach, a new blueprint for distributed hydrologic modelling at the catchment scale: Numerical implementation. In: Physically Based models of river runoff and their application to ungauged basins, Proceedings, NATO Advanced Research Workshop, P.E. O'Connell and L. Kuchment (Editors).

Lekula, M., Lubczynski, M.W., Shemang, E.M., Verhoef, W., 2018. Validation of satellite-based rainfall in Kalahari. Phys. Chem. Earth, Parts A/B/C 105, 84–97. https://doi.org/https://doi.org/10.1016/j.pce.2018.02.010.

Lenderink, G., A. Buishand, and W. van Deursen, 2007: Estimates of future discharges of the river Rhine using two scenario methodologies: direct versus delta approach. Hydrol. Earth Syst. Sci., 11, 1145-1159.

Li, J., Heap, A.D., 2011. A review of comparative studies of spatial interpolation methods in environmental sciences: Performance and impact factors. Ecol. Inform. 6, 228–241. https://doi.org/http://dx.doi.org/10.1016/j.ecoinf.2010.12.003.

Li, X., Q. Zhang, and C.-Y. Xu, 2013: Assessing the performance of satellite-based precipitation products and its dependence on topography over Poyang Lake basin. Theor Appl Climatol, 115, 713-729.

Likasa, H. G., 2013: Remote Sensing and Regionalization for Integrated Water Resources Modeling In Upper and Middle Awash River Basin, Ethiopia, Faculty ITC, University of Twente, Twente, 88 pp.

Liu, X., F. M. Liu, X. X. Wang, X. D. Li, Y. Y. Fan, S. X. Cai, and T. Q. Ao, 2017: Combining rainfall data from rain gauges and TRMM in hydrological modelling of Laotian data-sparse basins. Applied Water Science, 7, 1487-1496.

Luo, Y., W. Qian, R. Zhang, and D.-L. Zhang, 2013: Gridded Hourly Precipitation Analysis from High-Density Rain Gauge Network over the

Yangtze–Huai Rivers Basin during the 2007 Mei-Yu Season and Comparison with CMORPH. Journal of Hydrometeorology, 14, 1243-1258.

Madsen, H., 2000. Automatic calibration of a conceptual rainfall–runoff model using multiple objectives. J. Hydrol. 235, 276–288. https://doi.org/https://doi.org/10.1016/S0022-1694(00)00279-1

Maggioni, V., Massari, C., 2018. On the performance of satellite precipitation products in riverine flood modeling: A review. J. Hydrol. 558, 214–224. https://doi.org/https://doi.org/10.1016/j.jhydrol.2018.01.039

Maggioni, V., Vergara, H.J., Anagnostou, E.N., Gourley, J.J., Hong, Y., Stampoulis, D., 2013. Investigating the Applicability of Error Correction Ensembles of Satellite Rainfall Products in River Flow Simulations. J. Hydrometeorol. 14, 1194–1211. https://doi.org/10.1175/JHM-D-12-074.1

Maidment, R.I., Grimes, D., Black, E., Tarnavsky, E., Young, M., Greatrex, H., Allan, R.P., Stein, T., Nkonde, E., Senkunda, S., Alcántara, E.M.U., 2017. A new, long-term daily satellite-based rainfall dataset for operational monitoring in Africa 4, 170063. https://doi.org/10.1038/sdata.2017.63.

Manz, B., Buytaert, W., Zulkafli, Z., Lavado, W., Willems, B., Robles, L.A., Rodríguez-Sánchez, J.-P., 2016. High-resolution satellite-gauge merged precipitation climatologies of the Tropical Andes. J. Geophys. Res. Atmos. 121, 1190–1207. https://doi.org/10.1002/2015JD023788.

Maraun, D., 2016. Bias Correcting Climate Change Simulations - a Critical Review. Curr. Clim. Chang. Reports 2, 211–220. https://doi.org/10.1007/s40641-016-0050-x.

Mashingia, F., F. Mtalo, and M. Bruen, 2014: Validation of remotely sensed rainfall over major climatic regions in Northeast Tanzania. Physics and Chemistry of the Earth, Parts A/B/C, 67–69, 55-63.

Matos, J.P., 2014. Hydraulic-hydrologic model for the Zambezi River using satellite data and artificial intelligence techniques, Communication (Laboratoire de constructions hydrauliques, Ecole polytechnique fédérale de Lausanne). EPFL - LCH. https://doi.org/10.5075/epfl-lchcomm-60.

Matos, J. P., T. Cohen Liechti, D. Juízo, M. M. Portela, and A. J. Schleiss, 2013: Can satellite based pattern-oriented memory improve the interpolation of sparse historical rainfall records? Journal of Hydrology, 492, 102-116.

McCabe, M. F., and Coauthors, 2017: The future of Earth observation in hydrology. Hydrol. Earth Syst. Sci., 21, 3879-3914.

Mei, Y., Nikolopoulos, E.I., Anagnostou, E.N., Zoccatelli, D., Borga, M., 2016. Error Analysis of Satellite Precipitation-Driven Modeling of Flood Events

in Complex Alpine Terrain. Remote Sens. 8, 293.

Meier, P., A. Frömelt, and W. Kinzelbach, 2011: Hydrological real-time modelling in the Zambezi river basin using satellite-based soil moisture and rainfall data. Hydrol. Earth Syst. Sci., 15, 999-1008.

Meyer, H., Drönner, J., Nauss, T., 2017. Satellite-based high-resolution mapping of rainfall over southern Africa. Atmos. Meas. Tech. 10, 2009–2019. https://doi.org/10.5194/amt-10-2009-2017

Miao, C., H. Ashouri, K.-L. Hsu, S. Sorooshian, and Q. Duan, 2015: Evaluation of the PERSIANN-CDR Daily Rainfall Estimates in Capturing the Behavior of Extreme Precipitation Events over China. Journal of Hydrometeorology, 16, 1387-1396.

Moazami, S., S. Golian, M. R. Kavianpour, and Y. Hong, 2013: Comparison of PERSIANN and V7 TRMM Multi-satellite Precipitation Analysis (TMPA) products with rain gauge data over Iran. International Journal of Remote Sensing, 34, 8156-8171.

Moazami, S., Golian, S., Kavianpour, M.R., Hong, Y., 2014. Uncertainty analysis of bias from satellite rainfall estimates using copula method. Atmos. Res. 137, 145–166. https://doi.org/http://dx.doi.org/10.1016/j.atmosres.2013.08.016.

Moore, R.D., Trubilowicz, J.W., Buttle, J.M., 2012. Prediction of Streamflow Regime and Annual Runoff for Ungauged Basins Using a Distributed Monthly Water Balance Model. J. Am. Water Resour. Assoc. 48, 32–42. https://doi.org/10.1111/j.1752-1688.2011.00595.x

Monteil, C., Zaoui, F., Le Moine, N., Hendrickx, F., 2020. Multi-objective calibration by combination of stochastic and gradient-like parameter generation rules – the caRamel algorithm. Hydrol. Earth Syst. Sci. 24, 3189–3209. https://doi.org/10.5194/hess-24-3189-2020.

Muhammed, A. H., 2012: Satellite based Evapotranspiration and Runoff Simulation: A TOPMODEL application to the Gilgel Abbay Catchment, Ethiopia.

Müller, M. F., and S. E. Thompson, 2013: Bias adjustment of satellite rainfall data through stochastic modeling: Methods development and application to Nepal. Advances in Water Resources, 60, 121-134.

Muzumara, M., 2010: Application of remote sensing using a GIS based soil water assessment tool(SWAT)to estimate river discharge in the Kabompo river basin-Zambia, MSc Thesis, University of Zambia, Lusaka, Zambia, 167 pp.

Mwale, F. D., A. J. Adeloye, and R. Rustum, 2012: Infilling of missing rainfall and streamflow data in the Shire River basin, Malawi – A self organizing map approach. Physics and Chemistry of the Earth, Parts A/B/C, 50–52, 34-43.

Mwansa, P., 2018. Investigating the impact of fire on the natural regeneration of woody species in dry and wet Miombo woodland. MSc Thesis, 1–187. Faculty of AgriSciences, Stellenbosch University, Stellenbosch, South Africa.

Najmaddin, P. M., M. J. Whelan, and H. Balzter, 2017: Application of Satellite-Based Precipitation Estimates to Rainfall-Runoff Modelling in a Data-Scarce Semi-Arid Catchment. Climate, 5, 32.

Nash, J. E., and J. V. Sutcliffe, 1970: River flow forecasting through conceptual models. Part I: a discussion of principles. J. Hydrol., 10, 282-290.

Ndhlovu, G.Z., Woyessa, Y.E., 2020. Modelling impact of climate change on catchment water balance, Kabompo River in Zambezi River Basin. J. Hydrol. Reg. Stud. 27, 100650. https://doi.org/https://doi.org/10.1016/j.ejrh.2019.100650.

Nicholson, S.E., 2013. The West African Sahel: A Review of Recent Studies on the Rainfall Regime and Its Interannual Variability. ISRN Meteorol. 2013, 32. https://doi.org/10.1155/2013/453521.

Nikolopoulos, E. I., E. N. Anagnostou, and M. Borga, 2012: Using High-Resolution Satellite Rainfall Products to Simulate a Major Flash Flood Event in Northern Italy. Journal of Hydrometeorology, 14, 171-185.

Nash, J.E., Sutcliffe, J. V, 1970. River flow forecasting through conceptual models. Part I: a discussion of principles. J. Hydrol. 10, 282–290.

Nazaripour, H., Mansouri Daneshvar, M.R., 2016. Rain gauge network evaluation and optimal design using spatial correlation approach in arid and semi-arid regions of Iran. Theor. Appl. Climatol. https://doi.org/10.1007/s00704-016-1853-3 LB - Nazaripour2016.

Nugroho, P., D. Marsono, P. Sudira, and H. Suryatmojo, 2013: Impact of Land-use Changes on Water Balance. Procedia Environmental Sciences, 17, 256-262.

Omondi, C.K., 2017. Assessment of bias corrected satellite rainfall products for streamflow simulation : A TOPMODEL application in the Kabompo River Basin , Zambia. MSc Thesis, Enschede, The Netherlands.

Paparrizos, S., and F. Maris, 2017: Hydrological simulation of Sperchios River basin in Central Greece using the MIKE SHE model and geographic information systems. Applied Water Science, 7, 591-599.

Pan, M., Li, H., Wood, E., 2010. Assessing the skill of satellite-based precipitation estimates in hydrologic applications. Water Resour. Res. 46. https://doi.org/10.1029/2009WR008290.

Parida, B., S. Behera, O. Bakimchandra, A. Pandey, and N. Singh, 2017: Evaluation of Satellite-Derived Rainfall Estimates for an Extreme Rainfall Event over Uttarakhand, Western Himalayas. Hydrology, 4, 22.

Pereira Filho, A. J., R. E. Carbone, J. E. Janowiak, P. Arkin, R. Joyce, R. Hallak, and C. G. M. Ramos, 2010: Satellite Rainfall Estimates Over South America – Possible Applicability to the Water Management of Large Watersheds1. JAWRA Journal of the American Water Resources Association, 46, 344-360.

Petersen-Perlman, J. D., 2016: Water Conflict/Cooperation Case Study: Zambezi River Basin☆. Reference Module in Earth Systems and Environmental Sciences, Elsevier.

Piniewski, M., M. Szcześniak, and I. Kardel, 2017: CHASE-PL—Future Hydrology Data Set: Projections of Water Balance and Streamflow for the Vistula and Odra Basins, Poland. Data, 2, 14.

Pombo, S., R. P. de Oliveira, and A. Mendes, 2014: Validation of remote-sensing precipitation products for Angola. Meteorological Applications, 22 (3), 395-409.

Prakash, S., V. Sathiyamoorthy, C. Mahesh, and R. M. Gairola, 2014: An evaluation of high-resolution multisatellite rainfall products over the Indian monsoon region. International Journal of Remote Sensing, 35, 3018-3035.

Pullan, S.P., Whelan, M.J., Rettino, J., Filby, K., Eyre, S., Holman, I.P., 2016. Development and application of a catchment scale pesticide fate and transport model for use in drinking water risk assessment. Sci. Total Environ. 563–564, 434–447. https://doi.org/https://doi.org/10.1016/j.scitotenv.2016.04.135

Qin, C., Y. Jia, Z. Su, Z. Zhou, Y. Qiu, and S. Suhui, 2008: Integrating Remote Sensing Information Into A Distributed Hydrological Model for Improving Water Budget Predictions in Large-scale Basins through Data Assimilation. Sensors, 8, 4441-4465.

Reichert, P., Schuwirth, N., 2012. Linking statistical bias description to multiobjective model calibration. Water Resources Research, 48, 1–20. https://doi.org/10.1029/2011WR011391

Reggiani, P., and J. Schellekens, 2003 Modelling of hydrological responses: the representative elementary watershed approach as an alternative blueprint for watershed modelling. . Hydrol. Process, 17, 3785-3789.

Reggiani, P., and T. H. M. Rientjes, 2005: Flux parameterization in the Representative Elementary Watershed (REW) approach: Application to a natural basin. Water Resour. Res, 41 W04013, doi:10.1029/2004WR003693.

Reggiani, P., and T. H. M. Rientjes, 2010: Closing horizontal groundwater fluxes with pipe network analysis: An application of the REW approach to an aquifer. Environmental Modelling & Software, 25, 1702-1712.

Reggiani, P., and S. Majid Hassanizadeh, 2016: Megascale thermodynamics in the presence of a conservative field: The watershed case. Advances in Water Resources, 97, 73-86.

Reggiani, P., M. Sivapalan, and S. M. Hassanizadeh, 1998: A unifying framework for watershed thermodynamics: balance equations for mass, momentum, energy and entropy and the second law of thermodynamics. . Adv. in Water Resourc, 22, 367-398.

Reggiani, P., M. Sivapalan, and S. M. Hassanizadeh, 2000: Conservation equations governing hillslope responses: exploring the physical basis for water balance. Water Resour. Res, 36.

Reggiani, P., E. Todini, and D. Meißner, 2014: A conservative flow routing formulation: Déjà vu and the variable-parameter Muskingum method revisited. Journal of Hydrology, 519, 1506-1515.

Reggiani, P., S. M. Hassanizadeh, M. Sivapalan, and W. G. Gray, 1999: A unifying framework for watershed thermodynamics: constitutive relationships. Adv. in Water Resourc, 23, 15-39.

Reusser, D.E., Blume, T., Schaefli, B., Zehe, E., 2009. Analysing the temporal dynamics of model performance for hydrological models. Hydrol. Earth Syst. Sci., 13, 999–1018, 2009. https://doi.org/10.5194/hess-13-999-2009.

Rientjes, T.H.M., 2007. Modeling in Hydrology. Lecture Notes. ITC, Enschede, The Netherlands.

Rientjes, T.H.M., Perera, B.U.J., Haile, A.T., Reggiani, P., Muthuwatta, L.P., 2011. Regionalisation for lake level simulation – the case of Lake Tana in the Upper Blue Nile, Ethiopia. Hydrol. Earth Syst. Sci. 15, 1167–1183.

Rientjes, T.H.M., Muthuwatta, L.P., Bos, M.G., Booij, M.J., Bhatti, H.A., 2013a. Multi-variable calibration of a semi-distributed hydrological model using streamflow data and satellite-based evapotranspiration. J. Hydrol. 505, 276–290. https://doi.org/http://dx.doi.org/10.1016/j.jhydrol.2013.10.006.

Rientjes, T., A. T. Haile, and A. A. Fenta, 2013b: Diurnal rainfall variability over the Upper Blue Nile Basin: A remote sensing based approach. International Journal of Applied Earth Observation and Geoinformation, 21, 311-325.

Ringard, J., M. Becker, F. Seyler, and L. Linguet, 2015: Temporal and Spatial Assessment of Four Satellite Rainfall Estimates over French Guiana and North Brazil. Remote Sensing, 7, 15831.

Romano, F., Cimini, D., Nilo, S., Di Paola, F., Ricciardelli, E., Ripepi, E., Viggiano, M., 2017. The Role of Emissivity in the Detection of Arctic Night Clouds. Remote Sens. 9, 406.

Romilly, T. G., and M. Gebremichael, 2011: Evaluation of satellite rainfall estimates over Ethiopian river basins. Hydrol. Earth Syst. Sci., 15, 1505-1514.

Saber, M., and K. Yilmaz, 2016: Bias Correction of Satellite-Based Rainfall Estimates for Modeling Flash Floods in Semi-Arid regions: Application to Karpuz River, Turkey. Nat. Hazards Earth Syst. Sci. Discuss., 2016, 1-35.

Santillan, J., E. Paringit, R. Ramos, R. Mendoza, N. Espanola, and J. Alconis, 2012: Near real-time flood flood extent monitoring in Marikina River, Philippines: Model parameterization using remotely-sensed data and field measurements. In Proceedings of the 33rd Asian Conference on Remote Sensing, ACRS 2012 – Aiming Smart Space Sensing, November 26-30, 2012, Ambassador City Jomtien Hotel, Pattaya, Thailand. .

Schlosser, C. A., and K. Strzepek, 2015: Regional climate change of the greater Zambezi River Basin: a hybrid assessment. Climatic Change, 130, 9-19.

Schmugge, T. J., W. P. Kustas, J. C. Ritchie, T. J. Jackson, and A. A. Rango, 2002: Remote sensing in hydrology. Adv. Water Resources, 25, 1367-1385.

Sedano, F., P. Gong, and M. Ferra, 2005: Land cover assessment with MODIS imagery in southern African Miombo ecosystems. Remote Sensing of Environment 98, 429 - 441.

Shahed Behrouz, M., Zhu, Z., Matott, L.S., Rabideau, A.J., 2020. A new tool for automatic calibration of the Storm Water Management Model (SWMM). J. Hydrol. 581, 124436. https://doi.org/https://doi.org/10.1016/j.jhydrol.2019.124436.

Shin, M.-J., Kim, C.-S., 2019. Analysis of the Effect of Uncertainty in Rainfall-Runoff Models on Simulation Results Using a Simple Uncertainty-Screening Method. Water 11, 1361.

Seo, D. J., J. P. Breidenbach, and E. R. Johnson, 1999: Real-time estimation of mean field bias in radar rainfall data. Journal of Hydrology, 223, 131-147.

Serrat-Capdevila, A., Merino, M., Valdes, J., Durcik, M., 2016. Evaluation of the Performance of Three Satellite Precipitation Products over Africa. Remote Sens. 8, 836.

Schaefli, B., Gupta, H. V, 2007. Do Nash values have value? Hydrol. Process. 21, 2075–2080. https://doi.org/10.1002/hyp.6825.

Shepard, D., 1968. A Two-dimensional Interpolation Function for Irregularly-spaced Data, in: Proceedings of the 1968 23rd ACM National Conference. ACM, New York, NY, USA, pp. 517–524. https://doi.org/citeulike-article-id:3733066 doi: 10.1145/800186.810616.

Sevruk, B., and V. Nespor, 1998: Empirical and theoretical assessment of the wind induced error of rain measurement. Water Science and Technology, 37, 171-178.

Shahed Behrouz, M., Zhu, Z., Matott, L.S., Rabideau, A.J., 2020. A new tool for automatic calibration of the Storm Water Management Model (SWMM). J. Hydrol. 581, 124436. https://doi.org/https://doi.org/10.1016/j.jhydrol.2019.124436.

Shanhu, J., Liliang, R.E.N., Bin, Y., Yang, H., Xiaoli, Y., Fei, Y., 2016. Evaluation of Latest TMPA and CMORPH Precipitation Products with Independent Rain Gauge Observation Networks over High-latitude and Low-latitude Basins in China 26, 439–455. https://doi.org/10.1007/s11769-016-0818-x.

Sheffield, J., Ferguson, C.R., Troy, T.J., Wood, E.F., McCabe, M.F., 2009. Closing the terrestrial water budget from satellite remote sensing. Geophys. Res. Lett. 36. https://doi.org/10.1029/2009gl037338.

Shen, P., A. Xiong, Y. Wang, and P. Xie, 2010: Performance of high-resolution satellite precipitation products over China. Journal of Geographical Research, 115.

Shen, Y., P. Zhao, Y. Pan, and J. Yu, 2014: A high spatiotemporal gauge-satellite merged precipitation analysis over China. Journal of Geophysical Research: Atmospheres, 119, 2013JD020686.

Shrestha, M. S., 2011: Bias-adjustment of satellite-based rainfall estimates over the central Himalayas of Nepal for flood prediction. PhD thesis, Kyoto University.

Shrestha, M. S., G. A. Artan, S. R. Bajracharya, and R. R. Sharma, 2008: Using satellite-based rainfall estimates for streamflow modelling: Bagmati Basin J Flood Risk Management 1, 89-99.

Silvestro, F., S. Gabellani, F. Delogu, R. Rudari, and G. Boni, 2013: Exploiting remote sensing land surface temperature in distributed hydrological modelling: the example of the Continuum model Hydrol. Earth Syst. Sci., 17, 39-62.

Smiatek, G., H. Kunstmann, and A. Senatore, 2016: EURO-CORDEX regional climate model analysis for the Greater Alpine Region: Performance and expected future change. Journal of Geophysical Research: Atmospheres, 121, 7710-7728.

Smith, T. M., P. A. Arkin, J. J. Bates, and G. J. Huffman, 2006: Estimating Bias of Satellite-Based Precipitation Estimates. Journal of Hydrometeorology, 7, 841-856.

Sorooshian, S., and Coauthors, 2011: Advanced Concepts on Remote Sensing of Precipitation at Multiple Scales. Bulletin of the American Meteorological Society, 92, 1353-1357.

Song, Y., Park, Y., Lee, J., Park, M., 2019. Flood Forecasting and Warning System Structures : Procedure and Application to a Small Urban Stream in South Korea.

Spalding-Fecher, R., B. Joyce, and H. Winkler, 2017: Climate change and hydropower in the Southern African Power Pool and Zambezi River Basin: System-wide impacts and policy implications. Energy Policy, 103, 84-97.

Spalding-Fecher, R., and Coauthors, 2016: The vulnerability of hydropower production in the Zambezi River Basin to the impacts of climate change and irrigation development. Mitig Adapt Strateg Glob Change, 21, 721-742.

Srivastava, P. K., T. Islam, M. Gupta, G. Petropoulos, and Q. Dai, 2015: WRF Dynamical Downscaling and Bias Correction Schemes for NCEP Estimated Hydro-Meteorological Variables. Water Resources Management, 29, 2267-2284.

Stisen, S., and I. Sandholt, 2010: Evaluation of remote-sensing-based rainfall products through predictive capability in hydrological runoff modelling. Hydrological Processes, 24, 879-891.

Switanek, M.B., Troch, P.A., Castro, C.L., Leuprecht, A., Chang, H.I., Mukherjee, R., Demaria, E.M.C., 2017. Scaled distribution mapping: a bias correction method that preserves raw climate model projected changes. Hydrol. Earth Syst. Sci. 21, 2649–2666. https://doi.org/10.5194/hess-21-2649-2017.

Takeuchi, K., Ao, T., Ishidaira, H., 1999. Introduction of block-wise use of TOPMODEL and Muskingum-Cunge method for the hydroenvironmental

simulation of a large ungauged basin. Hydrol. Sci. J. 44, 633–646. https://doi.org/10.1080/02626669909492258.

Talib, A., and T. O. Randhir, 2017: Climate change and land use impacts on hydrologic processes of watershed systems. Journal of Water and Climate Change.

Tang, Y., Reed, P., Wagener, T., 2006. How effective and efficient are multiobjective evolutionary algorithms at hydrologic model calibration? Hydrol. Earth Syst. Sci. 10, 289–307. https://doi.org/10.5194/hess-10-289-2006.

Tarboton, D. G., 1997: A new method for the determination of flow directions and upslope areas in grid digital elevation models. Water Resources Research, 33, 309-319.

Taylor, K. E., 2001: Summarizing multiple aspects of model performance in a single diagram. Journal of Geophysical Research: Atmospheres, 106, 7183-7192. https://doi.org/10.1029/2000JD900719

Tesfagiorgis, K., S. E. Mahani, N. Y. Krakauer, and R. Khanbilvardi, 2011: Bias correction of satellite rainfall estimates using a radar-gauge product – a case study in Oklahoma (USA). Hydrol. Earth Syst. Sci., 15, 2631-2647.

Teutschbein, C., and J. Seibert, 2013: Is bias correction of regional climate model (RCM) simulations possible for non-stationary conditions? Hydrol. Earth Syst. Sci., 17, 5061-5077.

Thakur, J. K., S. K. Singh, and V. S. Ekanthalu, 2017: Integrating remote sensing, geographic information systems and global positioning system techniques with hydrological modeling. Applied Water Science, 7, 1595-1608.

Themeßl, M. J., A. Gobiet, and A. Leuprecht, 2010: Empirical-statistical downscaling and error correction of daily precipitation from regional climate models. Int. J. Climatol., 31, 1530-1544.

Themeßl, M. J., A. Gobiet, and G. Heinrich, 2012: Empirical-statistical downscaling and error correction of regional climate models and its impact on the climate change signal. Clim. Change, 112, 449–468.

Thiemig, V., R. Rojas, M. Zambrano-Bigiarini, and A. De Roo, 2013: Hydrological evaluation of satellite-based rainfall estimates over the Volta and Baro-Akobo Basin. Journal of Hydrology, 499, 324-338.

Thiemig, V., R. Rojas, M. Zambrano-Bigiarini, V. Levizzani, and A. De Roo, 2012: Validation of Satellite-Based Precipitation Products over Sparsely Gauged African River Basins. Journal of Hydrometeorology, 13, 1760-1783. https://doi.org/10.1016/j.jhydrol.2013.07.012.

Thom Vu, T., N. Khoi Dao, and Q. Linh Do, 2017: Using gridded rainfall products in simulating streamflow in a tropical catchment – A case study of the Srepok River Catchment, Vietnam. Journal of Hydrology and Hydromechanics, 18.

Thorne, V., P. Coakeley, D. Grimes, and G. Dugdale, 2001: Comparison of TAMSAT and CPC rainfall estimates with rain gauges, for southern Africa. International Journal of Remote Sensing, 22, 1951-1974.

Tian, X., A. Dai, D. Yang, and Z. Xie, 2007: Effects of precipitation-bias corrections on surface hydrology over northern latitudes. Journal of Geophysical Research: Atmospheres, 112, n/a-n/a.

Tian, Y., and C. D. Peters-Lidard, 2007: Systematic anomalies over inland water bodies in satellite-based precipitation estimates. Geophysical Research Letters, 34.

Tian, Y., C. D. Peters-Lidard, and J. B. Eylander, 2010: Real-Time Bias Reduction for Satellite-Based Precipitation Estimates. Journal of Hydrometeorology, 11, 1275-1285.

Tian, Y., and Coauthors, 2009: Component analysis of errors in satellite-based precipitation estimates. Journal of Geophysical Research: Atmospheres, 114, D24101.

Tobin, Kenneth J, Bennett, M.E., 2010. Adjusting Satellite Precipitation Data to Facilitate Hydrologic Modeling. J. Hydrometeorol. 11, 966–978. https://doi.org/doi:10.1175/2010JHM1206.1

Tong, K., F. Su, D. Yang, and Z. Hao, 2014: Evaluation of satellite precipitation retrievals and their potential utilities in hydrologic modeling over the Tibetan Plateau. Journal of Hydrology, 519, Part A, 423-437.

Toté, C., D. Patricio, H. Boogaard, R. van der Wijngaart, E. Tarnavsky, and C. Funk, 2015: Evaluation of Satellite Rainfall Estimates for Drought and Flood Monitoring in Mozambique. Remote Sensing, 7, 1758.

Tsidu, G.M., 2012. High-Resolution Monthly Rainfall Database for Ethiopia: Homogenization, Reconstruction, and Gridding. J. Clim. 25, 8422–8443. https://doi.org/10.1175/JCLI-D-12-00027.1

Tumbare, M. J., 2000: Management of River Basins and Dams: The Zambezi River Basin. Taylor & Francis, 318 pp.

——, 2005: The Management of the Zambezi River Basin and Kariba Dam. Bookworld Publishers.

Valdés-Pineda, R., Demaría, E.M.C., Valdés, J.B., Wi, S., Serrat-Capdevilla, A., 2016. Bias correction of daily satellite-based rainfall estimates for hydrologic forecasting in the Upper Zambezi, Africa. Hydrol. Earth Syst.

Sci. Discuss. 2016, 1–28. https://doi.org/10.5194/hess-2016-473.

Varado, N., I. Braud, S. Galle, M. Le Lay, L. Seguis, B. Kamagate, and C. Depraetere, 2006: Multi-criteria assessment of the Representative Elementary Watershed approach on the Donga catchment (Benin) using a downward approach of model complexity. Hydrol. Earth Syst. Sci., 10, 427-442.

Verdin, J., Klaver, R., 2002. Grid cell based crop water accounting for the famine early warning system. Hydrol Process 16, 1617-1630.

Vernimmen, R. R. E., A. Hooijer, Mamenun, E. Aldrian, and A. I. J. M. van Dijk, 2012: Evaluation and bias correction of satellite rainfall data for drought monitoring in Indonesia. Hydrol. Earth Syst. Sci., 16, 133-146.

Villarini, G., Mandapaka, P. V, Krajewski, W.F., Moore, R.J., 2008. Rainfall and sampling uncertainties: A rain gauge perspective. J. Geophys. Res. Atmos. 113, n/a-n/a. https://doi.org/10.1029/2007jd00921

Vu, T.T., Li, L., Jun, S.K., 2018. Evaluation of Multi-Satellite Precipitation Products for Streamflow Simulations: A Case Study for the Han River Basin in the Korean Peninsula, East Asia. Water . https://doi.org/10.3390/w10050642

Wang, W., X. Yang, and T. Yao, 2012: Evaluation of ASTER GDEM and SRTM and their suitability in hydraulic modelling of a glacial lake outburst flood in southeast Tibet. Hydrological Processes, 26, 213-225.

Wehbe, Y., Ghebreyesus, D., Temimi, M., Milewski, A., Al Mandous, A., 2017. Assessment of the consistency among global precipitation products over the United Arab Emirates. J. Hydrol. Reg. Stud. 12, 122–135. https://doi.org/http://dx.doi.org/10.1016/j.ejrh.2017.05.002.

Weissling, B. P., and H. Xie, 2008: Proximal watershed validation of a remote sensingbased streamflow estimation model Journal of Applied Remote Sensing, 2.

Welde, K., and B. Gebremariam, 2017: Effect of land use land cover dynamics on hydrological response of watershed: Case study of Tekeze Dam watershed, northern Ethiopia. International Soil and Water Conservation Research, 5, 1-16.

Wolters, E. L. A., B. J. J. M. van den Hurk, and R. A. Roebeling, 2011: Evaluation of rainfall retrievals from SEVIRI reflectances over West Africa using TRMM-PR and CMORPH. Hydrol. Earth Syst. Sci., 15, 437-451.

Woody, J., R. Lund, and M. Gebremichael, 2014: Tuning Extreme NEXRAD and CMORPH Precipitation Estimates. Journal of Hydrometeorology, 15, 1070-1077.

World Bank, 2010a: The Zambezi River Basin: A Multi-Sector Investment Opportunities Analysis, Volume 2 Basin Development Scenarios.

——, 2010b: The Zambezi River Basin : A Multi-Sector Investment Opportunities Analysis - Summary Report. World Bank. © World Bank. https://openknowledge.worldbank.org/handle/10986/2958 License: Creative Commons Attribution CC BY 3.0.

Worqlul, A. W., B. Maathuis, A. A. Adem, S. S. Demissie, S. Langan, and T. S. Steenhuis, 2014: Comparison of rainfall estimations by TRMM 3B42, MPEG and CFSR with ground-observed data for the Lake Tana basin in Ethiopia. Hydrol. Earth Syst. Sci., 18, 4871-4881.

Wu, L., and P. Zhai, 2012: Validation of daily precipitation from two high-resolution satellite precipitation datasets over the Tibetan Plateau and the regions to its east. Acta Meteorol Sin, 26, 735-745.

Xu, S., Shen, Y., Du, Z., 2016. Tracing the Source of the Errors in Hourly IMERG Using a Decomposition Evaluation Scheme. Atmosphere (Basel). 7, 161.

Yang, L., X. Meng, and X. Zhang, 2011: SRTM DEM and its application advances. International Journal of Remote Sensing, 32, 3875-3896.

Yang, J., Castelli, F., Chen, Y., 2014. Multiobjective sensitivity analysis and optimization of distributed hydrologic model MOBIDIC 4101–4112. https://doi.org/10.5194/hess-18-4101-2014

Yapo, P.O., Gupta, H.V., Sorooshian, S., 1998. Multi-objective global optimization for hydrologic models. J. Hydrol. 204, 83–97. https://doi.org/https://doi.org/10.1016/S0022-1694(97)00107-8.

Yin, Z.Y., Zhang, X., Liu, X., Colella, M., Chen, X., 2008. An assessment of the biases of satellite rainfall estimates over the tibetan plateau and correction methods based on topographic analysis. J. Hydrometeorol. 9, 301.

Yong, B., Chen, B., Tian, Y., Yu, Z., Hong, Y., 2016. Error-Component Analysis of TRMM-Based Multi-Satellite Precipitation Estimates over Mainland China. Remote Sens. 8, 440.

Yoo, C., Park, C., Yoon, J., Kim, J., 2014. Interpretation of mean-field bias correction of radar rain rate using the concept of linear regression. Hydrol. Process. 28, 5081–5092. https://doi.org/10.1002/hyp.9972.

Young, M. P., C. J. R. Williams, J. C. Chiu, R. I. Maidment, and S.-H. Chen, 2014: Investigation of Discrepancies in Satellite Rainfall Estimates over Ethiopia. Journal of Hydrometeorology, 15, 2347-2369.

Zambrano-Bigiarini, M., Nauditt, A., Birkel, C., Verbist, K., Ribbe, L., 2017. Temporal and spatial evaluation of satellite-based rainfall estimates across the complex topographical and climatic gradients of Chile. Hydrol. Earth Syst. Sci. 21, 1295–1320. https://doi.org/10.5194/hess-21-1295-2017.

ZAMCOM/SADC/SARDC, 2015: Zambezi Environment Outlook 2015. Harare, Gaborone.

Zeweldi, D. A., M. Gebremichael, and C. W. Downer, 2011: On CMORPH Rainfall for Streamflow Simulation in a Small, Hortonian Watershed. Journal of Hydrometeorology, 12, 456-466.

Zhang, G. P., and H. H. G. Savenije, 2005: Rainfall-runoff modelling in a catchment with a complex groundwater flow system: application of the Representative Elementary Watershed (REW) approach. Hydrol. Earth Sys. Sci. Discuss., 2, 639-690.

Zhang, G. P., H. H. G. Savenije, F. Fenicia, and L. Pfister, 2006: Modelling subsurface storm flow with the Representative Elementary Watershed (REW) approach: application to the Alzette River Basin. Hydrol. Earth Syst. Sci., 10, 937-955.

Zhou, Y., Zhou, C., Deng, F., Dongchen, E., Liu, H., Wen, Y., n.d. No Title. 2015 162, 112.

Zhuo, L., and D. Han, 2017: Hydrological Evaluation of Satellite Soil Moisture Data in Two Basins of Different Climate and Vegetation Density Conditions. Advances in Meteorology, 2017, 15.

Zulkafli, Z., W. Buytaert, C. Onof, B. Manz, E. Tarnavsky, W. Lavado, and J.-L. Guyot, 2014: A Comparative Performance Analysis of TRMM 3B42 (TMPA) Versions 6 and 7 for Hydrological Applications over Andean–Amazon River Basins. Journal of Hydrometeorology, 15, 581-592.

Curriculum Vitae

Webster Gumindoga was born on 4 March 1984 in Gutu, Zimbabwe. He did his Secondary and High School Education at Gutu High School in south eastern Zimbabwe. He went on to study for BSc (Hons) and MSc at the University of Zimbabwe.

In 2008, Webster joined the International Institute for Geoinformation Science and Earth Observation (ITC) of the University of Twente in the Netherlands where he graduated with an MSc in Geoinformation Science for Earth Observation in Water Resources and Environmental Management. The title of his thesis was *Hydrological impacts of Landuse and Landcover change in the Blue Nile Basin.*

In 2013, Webster rejoined ITC as an extramural PhD student where he was researching in the areas of development of bias correction schemes for satellite rainfall estimation in the Zambezi Basin, hydrological modelling and water balance estimation.

He is currently a lecturer at the University of Zimbabwe in Harare. With the application of GIS and Remote Sensing, Webster's research interests are in the areas of spatial and quantitative hydrology, water balance assessment and monitoring, hydrological modelling, quantification of water cycle components, use of Unmanned Aerial Vehicles (UAVS) for water resources assessments, as well as development of computer programs for civil engineering data processing/modeling.

List of publications

Papers in peer-reviewed journals

1. **Gumindoga, W.,** Rientjes T., Haile A., Reggiani P and Makurira H, 2021. Propagation of CMORPH rainfall errors to REW streamflow simulation mismatch in the Upper Zambezi Basin. Journal of Hydrology Regional Studies. https://doi.org/10.1016/j.ejrh.2021.10096

2. **Gumindoga, W.,** Rientjes T., Reggiani, P., Makurira, H. and Haile A.2019. Hydrologic evaluation of bias corrected CMORPH rainfall estimates at the headwater catchment of the Zambezi River. Physics and Chemistry of the Earth. https://doi.org/10.1016/j.pce.2019.11.004

3. **Gumindoga, W.,** Rientjes T., Haile A., Makurira, H. and Reggiani, P. 2019. Bias Correction Schemes for CMORPH satellite rainfall estimates in the Zambezi Basin. Hydrological Earth System Sciences (HESS). https://www.hydrol-earth-syst-sci-discuss.net/hess-2017-385/

4. **Gumindoga, W.,** Rientjes T., Haile A., Makurira, H. and Reggiani, P., 2019. Performance evaluation of CMORPH satellite precipitation product in the Zambezi Basin. International Journal of Remote Sensing. In Press. https://doi.org/10.1080/01431161.2019.1602791

Full Conference papers (with peer review) and awards

1. **Gumindoga, W.,** Rientjes T., Reggiani, P., Makurira, H. and Haile A.2017. Observing Zambezi Basin from Space: Setbacks and Strengths in the Zambezi Basin. Paper presented at the 18th WaterNet/WARFSA/GWPSA Symposium in Namibia.

   Presentation selected for best oral presentation award: Surface, Groundwater and Urbanisation category

2. **Gumindoga, W.,** Rientjes T., Haile A., Makurira, H. and Reggiani, P. 2016. Performance of Bias Correction Schemes for CMORPH satellite rainfall estimates in the Zambezi Basin. Paper presented at *17th WaterNet/WARFSA/GWPSA Symposium in Gaborone, Botswana*

   Presentation selected for best oral presentation award: Hydrology category

3. **Gumindoga, W.,** Rientjes T., Haile A., Makurira, H. and Reggiani, P., 2015. Performance evaluation of CMORPH satellite precipitation product in the Zambezi Basin. International Journal of Remote Sensing**.** Paper presented at 16th WaterNet/WARFSA/GWPSA Symposium in Mauritius

   Presentation selected for best oral presentation award: Hydrology category

Coverpage

Understanding patterns, intensity and distribution of rainfall is important for hydrological modelling and water balance assessment in the Zambezi Basin. Satellite rainfall are preferable in the data scarce Zambezi Basin. This research comes up with a space time variant bias correction scheme for the satellite rainfall. Analysis serves to improve the reliability of SRE applications in hydrological analysis and water resource applications in the Zambezi basin such as in drought analysis, flood prediction, weather forecasting, and rainfall–runoff modelling.

This research is carried out in Southern Africa's Zambezi basin, an example of many world regions that can benefit from satellite-based rainfall products for resource assessments and monitoring. With over 47 million inhabitants and serving 8 countries, this Basin is suitable for carrying out the study objectives. The Kabompo River Basin, with an area of 72,140 km^2 and situated in the North-western part of Zambia is selected for REW model hydrologic simulations. Kabompo River originates in North-Western Province of Zambia along the watershed between the Zambezi and Congo River Basins.

This book is structured across 4 research topics: i) satellite rainfall performance assessment ii) development of bias correction schemes for satellite rainfall iii) hydrologic evaluation of bias corrected satellite rainfall iv) error propagation to streamflow mismatch

The study concludes that satellite rainfall contains substantial bias errors that must be corrected before errors propagate to cause streamflow mismatch and water balance simulation errors. The evaluation of the bias error associated with CMORPH rainfall estimates into model behavior is indispensable for improving rainfall-runoff modelling. By use of multiple objective functions, this study shows that uncorrected CMORPH results in substantial augmentation of rainfall error to streamflow simulation mismatch whereas bias corrected estimates result in attenuation of error. Analysis for water balance composition has great potential to improve application of satellite precipitation products in water management and decision making in the Zambezi basin.